X-Ray Astronomy to Resonant Theranostics for Cancer Treatment

Sultana N. Nahar

Abstract

Atomic spectroscopy is fundamental to study of astronomical objects for their formation, evolution, composition, physical conditions etc. Information are extracted from the spectral analysis of the electromagnetic radiation emitted by these objects. This article will focus on the study of X-ray radiation which is used as a powerful diagnostic for astrophysical plasmas, particularly those surrounding black holes. There are space observatories, such as Chandra, XMM-Newton, dedicated in measuring the X-ray emissions in astronomical objects. The knowledge of X- ray astronomy is very similar to that used in cancer treatment in medical facilities. Using this connection, we have formulated a new method, Resonant Nano-Plasma Theranostics or RNPT, which gives indication for one most efficient way for destruction of malignant cells.

Introduction

The brightness and width of spectral lines from the plasmas of an astronomical object or environment carry important information on elemental composition, physical and chemical processes, abundances of various ionic states, plasma temperature, density etc. The detection itself of various broad and narrow band radiation provide considerable knowledge of the object.

Astronomical objects can be studied in a few ways, such as, imaging, photometry, and spectroscopy. Images of an astronomical object can be formed either by broad-band spectrometer or by superposition of low resolution pictures of various emissions. It gives general information on the high-low temperature regions, shapes and sizes, and location of the object. Figure 1 is an example of an image of galaxy Centauras A with a black hole in the center. The falling particles spiral around the black hole, move faster close to it and release energy in the form of radiation, mainly X-rays. The highly energetic super hot atoms near the black hole are in a plasma state and emit bright Kα (1s-2p transitions) X-rays. One main evidence of presence of a black hole is large amount of high energy X- rays, especially hard X-rays (wavelength range less than 100 ˚) emission. A black often gives out jets of particles, formed by the conservation of energy and angular momentum of the falling particles, on the opposite sides.

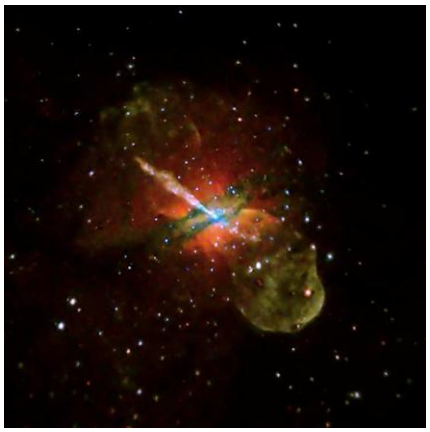

Figure 1: *Image of galaxy Centaurus A showing the presence of a black hole and its jets at the center (Observed by X-ray space observatory Chandra). In the image: red indicates low-energy X-rays. Toward the center, the green represents intermediate- energy X-rays, and blue that of the highest energy X-rays. The dark green and blue bands are dust lanes that absorb X-rays. A jet of a billion solar-masses extending to 13,000 light years is seen being blasted out from the black hole.*

Photometry gives some more information on the elemental composition that can be used to categorize the astronomical object, such as, a carbon star which produces dominant carbon lines. Figure 2 shows the

photometric image of the supernova remnant Cassiopia A created from observations by three space observatories, Spitzer, Hubble, and Chandra.

Various colors indicate production of various types emissions, infrared, visible, and X-rays from the remnant. They provide information on activities in various regions of the remnant. Supernova explosions introduce elements heavier than iron or nickel in space. In a star, nuclear fusions create elements from helium to iron and nickel. In the universe the most abundant element, up to 90% is hydrogen. Helium is the next with 7%. The rest of the elements which combined together is called the metals, consist mainly of Li, Be, B, C, N, O, F, Ne, Na, Mg, Al, Si, S, Ar, Ca, Ti, Cr, Fe, is about 3%. The existence of heavier elements in our solar system indicates that the system was created from the debris of supernova explosions.

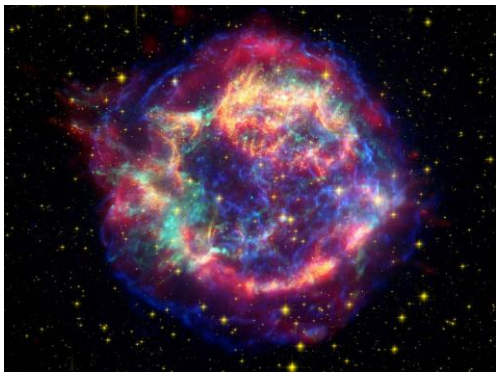

Figure 2: *Photometric image of supernova remnant Cassiopia A observed by three space observatories, Spitzer shows infrared (red) emission, Hubble shows visible (yellow), and Chandra shows X-ray (green and blue) emissions of the remnants. While the star elements are from H though Fe, some Ni, the heavy elements, beyond Iron, are created through nuclear fusion during supernova explosions and are scattered into interstellar medium.*

Spectroscopy of an astronomical object gives the most detailed information on physical conditions of temperature, density, abundances, etc. and the chemical composition. The brightness of the line indicates abundance of the element and width of the spectral lines indicate other effects such plasma broadening due to collisions, Stark effects etc. Figure 3 shows the well-known Kα (1s-2p) transition array lines of iron near a black hole in Seyfert I galaxy MCG-6-30-15 6 observed by Advanced Satellite for Cosmology and Astrophysics (ASCA) and Chandra. The maximum energy for a 1s-2p transition in iron is 5.4 keV. However, the large extension of the lines toward low energy means that the escaped photons have lost energies in the black hole. X-rays are powerful diagnostics and there are space observatories dedicated in measuring X- ray emissions.

Radioative Atomic Processes

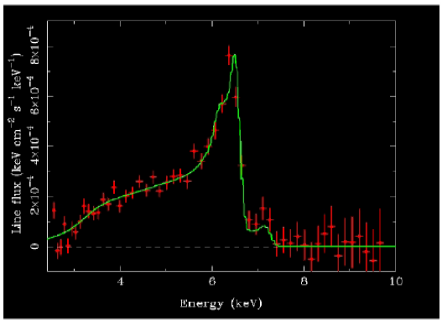

Figure 3: *The Kα (1s-2p) transition array lines of iron around 6.4 keV observed by ASCA and Chandra. The asymmetric stretching toward lower energy to about 5 keV indicates presence of a black hole nearby. The Kα photons lose energy due to gravitational potential of the black hole.*

Several atomic parameters relevant to the atomic processes emitting or absorbing the photons are needed to study the astronomical objects. Interaction between an atomic species X+z of charge z and a X-ray photon or any other photon usually lead to two processes, photo-excitation (inverse is de-excitation) and photoionization (inverse is electron-ion recombination). In photoexcitation an electron absorbs the photon and jumps to a higher excited level,

$$X^{+z} + h\nu \rightarrow X^{+z*}$$

but remains bound to the ion. The asterisk (*) denotes an excited state. Its strength is determined by the oscillator strength (f). The atomic parameter for de-excitation is the radiative decay rate or Einstein's A- coefficient.

In photoionization/ photo-dissociation/ photo-electric effect an electron absorbs a photon and exits to continuum or a free state:

$$X^{+z} + h\nu \longrightarrow X^{+z+1} + e$$

This direct ionization gives the background feature of the process. Photoionization often occurs via an intermediate state, the doubly excited autoionizing state, as shown below.

$$e + X^{+z} \rightleftharpoons (X^{+z-1})^{**} \rightleftharpoons \begin{cases} e + X^{+z} & \text{AI} \\ X^{+z-1} + h\nu & \text{DR} \end{cases}$$

An electron collides with the ion and goes to the doubly excited autoionizing state. The state leads either to autoionization (AI) when the electron goes free or dielectronic recombination (DR) when a photon is emitted. The inverse of DR is photoionization. The photoionization cross section σ_{PI} give the measure of ionization probability.

Theoretical Treatment

The atomic parameters (f, A, σ_{PI}) can be obtained from atomic structure calculations or the R-matrix method. In relativistic Breit-Pauli approximation the Hamiltonian is written as (e.g. [1])

$$H^{\rm BP} = H^{NR} + H^{\rm mass} + H^{\rm Dar} + H^{\rm so} + \frac{1}{2}\sum_{i\neq j}^{N}[g_{ij}(so + so') + g_{ij}(ss') + g_{ij}(css') + g_{ij}(d) + g_{ij}(oo')] \quad (1)$$

where H^{NR} is the nonrelativistic Hamiltonian

$$H^{NR} = \sum_{i=1}^{N}\left\{-\nabla_i^2 - \frac{2Z}{r_i} + \sum_{j>i}^{N}\frac{2}{r_{ij}}\right\} \quad (2)$$

and relativistic one-body terms are,

the mass correction $H^{mass} = -\frac{\alpha^2}{4}\sum_i p_i^4$

the Darwin term $H^{Dar} = \frac{\alpha^2}{4}\sum_i \nabla^2\left(\frac{Z}{r_i}\right)$

and the spin- orbit interaction

$$H^{so} = \left[\frac{Ze^2\hbar^2}{2m^2c^2r^3}\right]\mathbf{L}.\mathbf{S}.$$

The rest of the terms are weak interaction two-body terms.

The wave functions and energies of the atomic system are obtained by solving $H^{BP}\Psi = E\Psi$. The solutions are bound states with $E < 0$ and continuum states with $E > 0$. They are used to calculate the transition matrix elements with photon interaction, $< \Psi_f \|D\|\Psi_i >$ where the dipole operator $D = \sum_i r_i$ and the sum is over all electrons, and the corresponding line stregnth S.. The oscillator strength (f_{ij}), radiative decay rate (A_{ji}), and photoionization cross section (σ_{PI}) are then obtained from the line strength as

$$f_{ij} = \left[\frac{E_{ji}}{3g_i}\right]S, \quad A_{ji}(sec^{-1}) = \left[0.8032\times 10^{10}\frac{E_{ji}^3}{3g_j}\right]S \quad (3)$$

$$\sigma_{PI}(K\alpha,\nu) = \frac{4\pi^2 a_o^2\alpha}{3}\frac{E_{ij}}{g_k}S \quad (4)$$

The useful quantity mass attenuation coefficient for a photon absorption by an atomic species with atomic weight WA is same as σ_{PI} except by a constant factor,

$$\kappa(\nu; K\alpha) = \frac{\sigma_{PI}(\nu; K\alpha)}{uW_A} \quad (5)$$

where u is 1 amu=1.66054e^{-24} g.

Resonant Nano-Plasma Theranostics for Cancer Treatment

The physics of X-ray spectroscopy for a black hole is very similar to that of X-ray sources in medical facilities, especially for cancer treatment. The main difference is in the atomic species. Medical facilities typically use heavier elements because of their characteristic absorption or emission of high energy X-rays. The absorption or emission occurs largely through the inner shell transitions. These transitions can be used as the source of radiation or electrons productions in biomedical applications. Using these facts we have developed a new method called Resonant Nano-Plasma Theranostics [2, 3, 4] (RNPT) or in short Resonant Theranostics. Theranostics stands for the two words, therapy and diagnostics (imaging). Through RNPT we show how monochromatic X-rays, targeted at resonant energies, can be used for most efficient treatment of cancer with elimination or grossly reducing the harmful side effects due to overexposure in irradiation. The objective has to deal with several factors which are described below.

Cancer Treatment with Nanoparticles

Experiments on mice have shown that a cancerous tumor can be treated more effectively with gold nanoparticles embedded in the tumor and then irradiated with X-rays rather than X-ray irradiation alone [5]. Figure 4 has 3 pictures from Heinfeld et al [5]. Gold nanoparticles were injected in to the hind leg tumor of the mice (top left figure). Thirty days experiment shows that with only gold (no treatment) tumor increased, with X-rays the growth was reduced. However, with gold and X-ray reduced the tumor by 80%. The lower right figure shows mice survival with these three treatments. The topmost line (triangles) showed 85% survival over a year with higher gold concentrations and X-ray irradiation. In addition to more effective treatment, the experiment showed that with gold nanoparticles less intense radiation was needed for the malignant cell destruction.

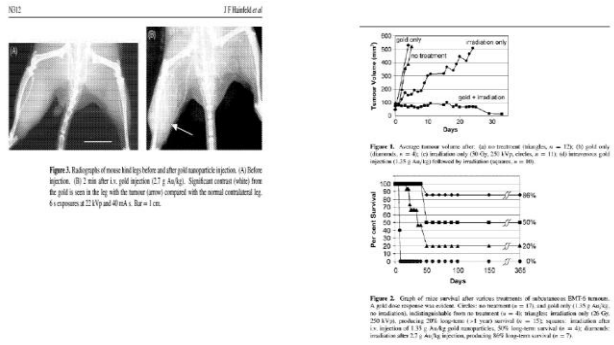

Figure 4: *Cancer treatment with gold nanoparticles and X-rays [5].*
Top left: radiograph of mouse hind leg before and after injection of gold nanoparticles (1.35g Au/kg) in the tumor.
Top right: tumor growth reduction in 30 days with only gold, only radiation, and with gold and radiation (30 Gy).
Bottom right: Mice survival treating with only gold, only radiation, radiation and two concentrations of gold.

Studies are being carried out with many different nanoparticles as gold is expensive. There are a few criteria to meet by the nanoparticles. Toxicity is one most important issue to resolve since most of the nanoparticles become toxic in vivo. The other issue is radiation absorption. Nanoparticles should be high-Z heavy particles. These can absorb high energy X-rays that are non-interactive to biogenic elements, such as, H, O, C, K, Fe etc. Gold has been the most studied in nanoparticles as it absorbs high energy X-rays and it is nontoxic to body cell. The other elements of interest are platinum, iodine, bromine, gadolinium etc. In a nanoparticle compound, only the high Z element is able to interact with the radiating high energy X-rays since the other constituent lighter elements of the compound will be transparent to the high energy photons.

Photoionization and Low Energy Electron Productions

During irradiation, the gold nanoparticles absorb X-ray photons and produce low energy electrons through photoionization. These ejected electrons attach themselves to the surrounding cells leading to breakdown of the DNA. Research investigations have been carried out in an effort to increase the production of ejected electrons. The focus has been on the K-shell ionization energy of the atom or ion. It is known that photoionization rises at the ionization thresholds of various shells as illustrated in Figure 5. It shows the rises in the background photoionization cross section (blue curve) at M-, L-, and K-shell ionization thresholds of gold [6]. The rise at K-edge is assumed to produce more electrons through photoionization of by absorption of X-rays. However, experiments have not been able to detect any such increment. RNPT predicts that the energy for enhanced electron production will occur due to resonances below the K-shell ionization energy.

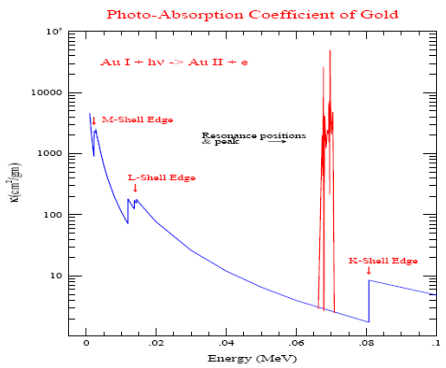

Figure 5: *Photoabsorption coefficient κ of gold. The blue curve represents the background with rises at M-, L-, K-edges. The high resonances (red) lie below the K-edge and peak orders of magnitude higher than that at K-edge.*

RNPT prediction is based on the atomic properties of high-Z elements. These properties for heavy elements are largely unknown. Through atomic structure calculations, we can predict resonances and the resonant energies. They correspond to 1s-np transitions. We concentrate on 1s-2p Kα transitions as they are the strongest ones ([7, 8]). The energy for the 1s-2p transitions varies some with the ionic state of the element and gives a narrow band resonant energy for the element. The strength of the process depends on the oscillator strength of the transitions. The Kα transitions introduce resonances in photoionization cross sections that are orders of magnitude higher than that around the K-edge. Hence, although there is a rise, the magnitude of the K-edge rise is considerably insignificant to low energy cross sections and resonances. These resonances for gold are illustrated in Figure 5. The figure shows sum of all resonances due to 1s-2p transitions in all ionization stages, from F- to H-like gold. The purpose of the sum is to show the resultant effect of Auger transitions as gold is being ionized through cascading as explained below.

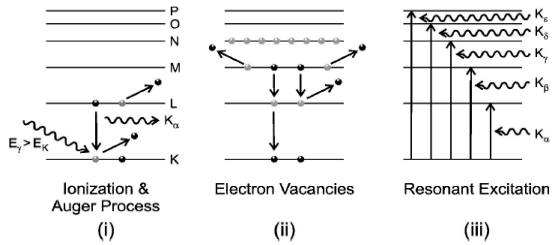

Figure 6: *i) Auger process, ii) Koster-Kronig cascade, iii) inverse of Auger process for gold*

Auger Process and RNPT

K-shell ionization of a high-Z element by a X-ray photon ejects an electron and introduce a hole or vacancy. This leads to Auger process where an upper L-shell electron drops down to fill the vacancy and emits a photon of excess energy which in turn can eject another L-shell electron. The vacancies in the L-shell will be filled out by droppings of M-shell electrons. Such process can lead to Koster-Kronig cascade giving out a number of photons and electrons as the element goes through various ionic states and the vacancies move to the outermost shell. The first two diagrams of Figure 6 illustrate the process in gold for which the energy levels go

up to P. The resonances in Figure 5 shows that such cascading has the maximum probability at the resonant energy range and such cascade is are highly desirable in radiation therapy application.

The 1s-2p transitions can occur for nine ionic states, from hydrogen to fluorine like ions. The 2p subshell is filled beyond fluorine. The number of 1s-2p transitions in each ionic state is different because of different number of 2p electrons. Atomic calculations [7] show that there are 2, 2, 6, 2, 14, 35, 35, 14 and 2 transitions in H-, He-, Li-, Be-, B-, C-, N-, O-, and F-like ions respectively. Hence in the event of breaking of gold to its various the ionic states due to Auger process can have a total of 112 Kα transitions for the element. For gold, the resonant energy range corresponding to all these transitions is 67 - 71 keV. The right most diagram in Figure 7 shows the inverse of Auger process. By an external X-ray source, the K-shell electron can be excited to a vacancy in L-shell and thus introducing another hole in K-shell. This will in turn multiply the electron productions.

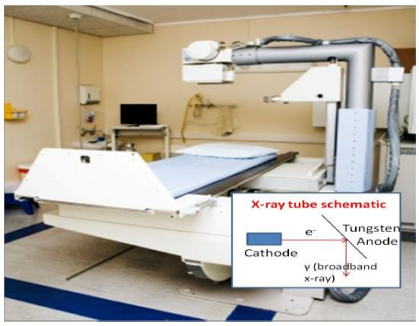

Figure 7: *Typical set-up of a X-ray source in a medical facility. Inset: diagram of radiation*

X-Ray Sources in Medical Facilities

The X-ray sources used for therapy and diagnostics in medical facilities implement the Roentgen X-ray tube which is still very much the same as the original set-up. A beam of electrons is accelerated across the potential difference between the cathode and the anode, striking a high-Z target such as tungsten (Z=74), producing characteristic radiation, known as the bremsstrahlung, as they decelerate as shown in the inset of Figure 7. The emitted radiation ranges all energies from zero to the peak value, denoted as KVp for peak voltage in KeV, of the machine potential. The typical X-ray sources are high energy linear accelerators or LINACs of up to 10-15 MVp, or lower energy machines such as CAT Scanners of up to 100-250 KVp.

The low energy X-rays interact with biogenic elements and cause considerable damage to cells. Hence the exposure by low energy radiation is reduced by a filter, typically of aluminum. Figure 8 shows the bremsstrahlung (curve with squares) of tungsten (W) with low energy radiation filtered out an Al filter. The resultant bremsstrahlung is an energy distribution starting with low intensity X-rays which peaks around 1/3 of the peak voltage of the machine. However, the patient is still exposed to indiscriminate radiation of relatively large energy band where the high energy X-rays pass through the body without any significant attenuation. Therefore, for both the low and the high energy X-ray sources it becomes necessary to increase radiation dosage to high levels as well as high energy intense beam in order to penetrate the body tissue to reach the cancer site.

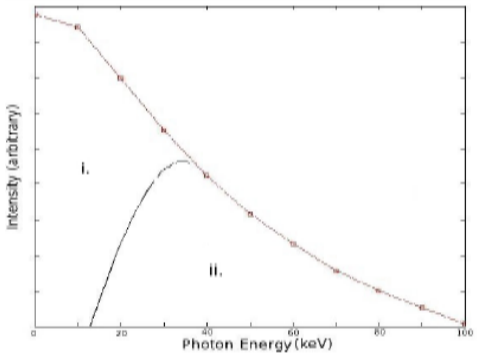

Figure 8: *X-ray bremsstrahlung radiation by W (squares) with low energy X-rays are filtered out by an Al filter (dotted curve) giving a resultant radiation distribution with a peak around 35 keV.*

Producing Monochromatic X-Rays

To avoid the radiation damages, RNPT aims to create monochromatic X- rays targeted to the resonant energy. One particular technique to generate the targeted radiation is based on partial conversion of bremsstahlung radiation into monochromatic Kα energy. We were able to create preliminary monochromatic Kα X-rays from the bremsstrahlung radiation of a X-source at a medical facility by using a zirconium plate. The X- rays were absorbed by Zr for inner K-shell ionization which was followed by radiative decays by the upper shell electrons. The fluorescence in Zr produced the monochromatic X-rays shown in Figure 9 (the high peak Kα emission). It may be assumed, to a good approximation that each K-shell ionization leads to the production of a Kα photon. The method should be more effective with high Z-elements, such as for Pt or Au, since the K-fluorescence yield, ωK is close to 1, estimated from the branching ratio:

$$\omega_{\mathbf{K}} = \frac{\mathbf{A_r(L-K)}}{[\mathbf{A_r(L-K)} + \mathbf{A_a(L)}]} \qquad (6)$$

where A_r is radiative decay rate, A_a is autoionization rate. It also means that X-ray photons, from threshold energy of the filter plate to the peak voltage of the bremsstrahlung, could be used to produce the monochromatic beam with high efficiency. The work is under process for an enhanced intensity of the monochromatic beam with a high Z plate [9].

The advantage of monochromatic over bremsstrahlung radiation is that the former can be controlled and targeted at specific features in X-ray photoionization cross sections for maximal radiation absorption. Such spectroscopic radiation should be far more efficient with reduced exposure. In addition, in contrast to broadband imaging, spectroscopy gives more detailed microscopic and accurate information.

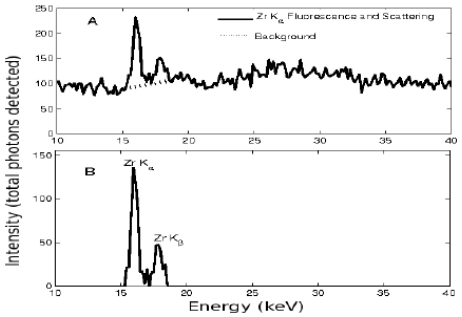

Figure 9: *Monochromatic X-rays (the high peak) from Kα transitions in Zr created from bremsstrahlung radiation of a typical X-ray machine in a medical facility.*
Top: measured X-ray emission.
Bottom: filtered over the background noise.

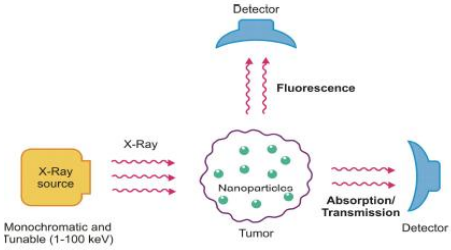

Figure 10: *RNPT: Monochromatic Kα X-rays irradiate the tumor doped with high Z nanoparticles. Auger process leads to cascade and ejections of electrons for cell destruction while emitted radiations are detected for imaging and to observe attenuation effect.*

RNPT and Monte Carlo Simulation

Combining all elements together RNPT scheme can be described in Figure 10. A targeted monochromatic X-ray beam, at resonant energy of the nanoparticles embedded in the tumor, irradiates the tumor. The radiation is absorbed and Auger process is initiated followed by enhanced emission of electrons and photons from inner shells. While ejected Auger electrons destroy the surrounding malignant cells, attenuation of incident X-rays and emitted fluorescent photons for imaging are detected.

With the gold atomic data with resonances, we carried out Monte Carlo simulations of RNPT using the Geant4 computational package [8]. The simulation showed that the RNPTT scheme would enhance the rate of Auger processes via Coster-Kronig and Super-Coster-Kronig branching transitions [1], and result in significant number of electron and photon emission. The geometry of the experiment is given in Figure 11 where a water phantom (15 × 5 × 5 cm) models body tissue (density 1.02 g/cc in contrast to 1.00 g/cc of water) with a tumor of thickness 2 cm at the depth of 10 cm below the skin. The tumor is embedded with gold nanoparticles of thickness 2 cm at 5 mg/ml.

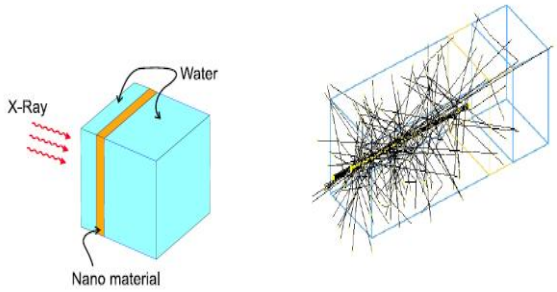

Figure 11: *RNPT simulation:*
(Left) A water phantom with a gold layer models a tumor of thickness 2 cm embedded with gold nanoparticles 10 cm from the skim.
(Right) Snapshot of 68 keV X-rays transmitting through the water where considerable number of the photons are lost by Compton scattering before reaching the tumor.

The simulation experiment was carried out with three different monochromatic X-ray beams, 68 keV (the resonant energy for gold for enhanced photoabsorption as predicted in RNPT), 82 keV (K-shell ionization energy that most experiment have focused on), and 2 MeV (voltage at highest intensity in a 6 MeV LINAC at medical facilities). The simulation results are presented in the following two plots, Figures 12 and 13. Even with significant loss of photons by Compton scatterings, the 68 keV beam reaching the tumor had the maximum effects. Figure 12 presents counts of electron productions at the three X-rays irradiation. The red curve represents the electrons produced with gold nanoparticles in the tumor while the blue curve represents the production without them. The electron count is over 3 at 68 keV in contrast to 0.03 at 82 keV and about 0.7 at 2 MeV. A considerably large number of electrons, by more than an order of magnitude, were produced by 68 keV X-rays compared to those by 82 keV and 2 MeV.

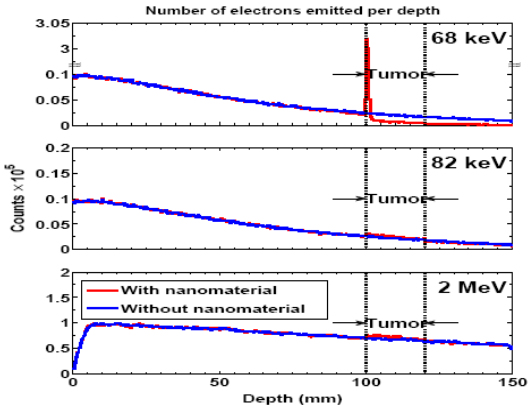

Figure 12: *Number of Auger electrons produced with depth following X-ray absorptions: Red curve - tumor embedded with gold nanoparticles at 5 mg/ml in region 100 to 120 mm, Blue curve - only water. Top: X-ray at 68 keV - averaged Kα resonant energy, Middle: 82 keV - just above K-edge ionization energy, Bottom: 2 MeV - high energy X-rays commonly used in clinics.*

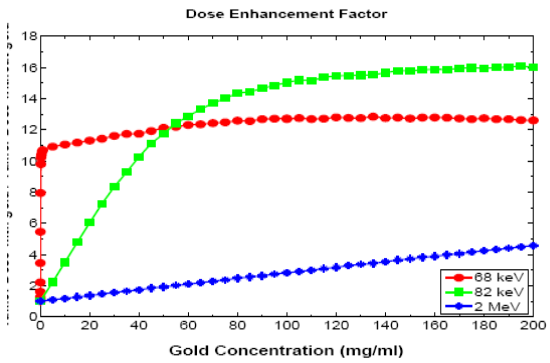

Figure 13: *Dose enhancement factor (DEF) with 3 X-ray beams, resonant 68 keV (red), K-shell ionization energy 82 keV (green), and clinically common beam of 2 MeV (blue). The resonant beam gives the most effect DEF at the lowest concentration of gold nanoparticles [8].*

DEF (dose ehnacement factor) of X-ray absorptions is an important factor in cancer treatment. It is the ratio of the average radiation dose absorbed by the tumor when it is loaded with a contrast medium or agent, such as with nanoparticles, to the dose absorbed without that agent. Figure 13 shows DEF of the three X-ray beams at various gold concentrations from 0 to 200 mg/ml [8]. The curves show that the energy deposition is most effective with 68 keV (red) where the deposition reaches its maximum with the lowest concentration. With 82 keV (green), the DEF increaes with higher concentration before becoming a plateau at about 80 mg/ml. The 2 MeV (blue) beam has the least effect, slow increase in DEF with higher concentrations. The DEFs obtained for the resonant X-ray beam of 68 keV are one order of magnitude greater than those calculated at lower concentration.

These results indicate that RNPT offers a highly effective radiation therapy and diagnostics for cancer. Research is under progress for experimental verifications and clinical tests.

Acknowledgment

Partially supported by DOE-NNSA and NSF. Computations were carried out at the Ohio Supercomputer Center.

References

[1]. Anil K. Pradhan and Sultana N. Nahar, Atomic Astrophysics and Spectroscopy (Cambridge University Press, 2011)
[2]. A.K. Pradhan, Y. Yu, S.N. Nahar, E. Silver, R. Pitzer, The Radiotherapy Dynamics (XVth Int. Conf. Use of Comput. in Radiat. Ther.) Vol. 2, 89 (2007)
[3]. E. Silver, A.K. Pradhan,Y. Yu, RT Image 21, 30 (2008)
[4]. A.K. Pradhan, S.N. Nahar, M. Montenegro et al., J. Phys. Chem. A 113, 12356, (2009)
[5]. Hainfeld, D. Slatkin, Smilowitz 2004), Phys. Med. Biol. 2004;49:N309-N315
[6]. NIST website: http://physics.nist.gov/PhysRefData/Xcom
[7]. S.N. Nahar, A.K. Pradhan, C. Sur, J. Quant. Spec. Rad. Transfer 109 19512008
[8]. M. Montenegro, S.N. Nahar, A.K. Pradhan et al., J. Phys. Chem. A 113 123642009
[9]. Pradhan et al, 2012 (in preparation)

QCD studies with anti-proton at FAIR: Development of SiPM based Scintillation Detector

Bidyut Jyoti Roy

Physics Goals

Understanding the strong nuclear force in terms of quarks and gluons is one of the outstanding questions in nuclear physics. The Quantum Chromo dynamics (QCD) is the basic theory of strong interactions and the study of QCD will be one of the highlights of the programme at future international facility FAIR (Facility for Anti Proton and Ion Research), Darmstadt, Germany. The central part of FAIR, which will be an upgraded facility of the existing GSI accelerator complex, is a synchrotron complex consisting of two separate synchrotron accelerator rings of same circumference and housed in same tunnel. One of the major goals of the accelerator complex is to provide intense pulsed proton beams at about 29 GeV which will be then used to produce antiproton beams. The antiproton beams will be accumulated and transferred to the High Energy Storage Ring (HESR) where the antiprotons can be accelerated between 1 and 15 GeV/c thus the maximum centre of mass energy in antiproton - proton collision will be approximately 5.5 GeV. A versatile detector PANDA (antiProton ANnihilation at DArmstadt) will be installed in the HESR storage ring where internal target experiments (with frozen hydrogen target in the form of pellet as well as nuclear targets) can be performed. The collaboration, known as PANDA collaboration, has proposed a rich experimental programme [1, 2] that aims study of fundamental questions of hadrons and nuclear physics, carry out precision tests of the strong interaction, investigation of in-medium modifications of hadron mass as they interact with nuclear matter, spectroscopy of single and double hyper-nuclei and study of electromagnetic process to measure nucleon form factor.

The one of the main topics at PANDA is the study of charmonium (ccbar meson: c=charm quark, cbar=anti-charm quark) spectroscopy and search for gluballs and hybrids in the charmonium mass region. Gluballs are excited state of pure gluons whereas hybrids are resonances consisting of a quark, an antiquark and excited gluons. These gluballs and hybrids, in contrast to normal mesons and other fermion–antifermion systems, can have spin-exotic quantum numbers as the gluons carry additional degrees of freedom. Lattice QCD calculations predict a whole spectrum of bound gluon states and hybrids, whereas experimental information is scarce. Bound gluonic systems offer a unique way to study one of the long standing problems in hadron physics- the origin of mass of strongly interacting particles. As we know, the Higgs mechanism might be responsible for creation of mass of elementary particles. But for proton, the Higgs mechanism accounts for only a few percentage of its mass while rest of its mass, as believed to be, created by the strong interaction. The gluons which are massless carry color charge i.e., charges of strong interaction and thereby interact strongly between themselves. This mutual gluon attraction may allow formation of meson-like bound states of gluons even if no quarks are present. Thus gluballs acquire mass which arises solely from the strong interaction. At PANDA it should be possible to search all glueballs and hybrids upto mass 5.5 GeV and make a high precision study by detecting both hadronic and electromagnetic decay modes revealing their true nature.

For the charmonium spectroscopy (both hidden and open charm), the goal at PANDA is to make a comprehensive measurement of spectroscopy of charmonium systems and hence to provide a detailed experimental information

of the QCD confining forces in the charm region to complement theoretical investigation. It should be highlighted that most of the charmonium states have very narrow width and low production cross section, only in experiments like panda with its phase space cooled antiproton beam and high luminosity it is possible to measure their mass, width and a systematic investigation of decay modes.

Investigation of medium modification of hadron mass in nuclear matter is another interesting topic that has been planned at PANDA. These studies, so far, have focused in the light quark sector eg., pion and kaon mesons due to the limitation in available energy. The in-medium pion mass is observed to shift as compared to its vacuum value and pion-nucleus potential has been deduced from experimental studies of deeply bound pionic atoms at GSI[3]. For kaons, repulsive mass shifts for K+ and attractive mass shifts for negative kaons are observed experimentally [4 and references therein]. At PANDA, the medium modification of hadron mass studies can be extended to the charm sector (with both hidden and open charm). For example, experiments are being planned to study sub-threshold production of D-Dbar mesons in antiproton – nucleus collision. If the D meson mass gets reduced in the nuclear environment, the in-medium DDbar threshold would be lowered resulting in an enhancement of production cross section at sub-threshold energies.

The PANDA collaboration has an extensive program on single and double hypernuclear physics. Such studies will provide us information on hyperon-nucleus and hyperon-hyperon interaction, the present knowledge of which is very limited. So far only few double hypernuclear events have been observed. Hypernuclei are nuclear systems in which one or more nucleons are replaced by hyperons. A hyperon in a nucleus is not bound by the Pauli Exclusion Principle, unlike a neutron or proton do. As a result it can populate all possible nuclear states which are not accessible otherwise. Certainly hypernuclei studies will provide a sensitive probe to the nuclear structure. It is to mention that JPARC accelerator in Japan has a programme on hypernuclear studies. However, at JPARC hypernuclei are produced with kaon beams that make certain limitation. The PANDA experiment plans to take a totally different and unique approach to hypernuclear physics in antiproton – p annihilation process thereby allowing a rich programme on hypernuclear physics. More details on the physics programme with PANDA can be found in refs.[1, 2].

The SciTil hodoscope detector

The PANDA detector is a complex detector designed to achieve 4π acceptance, high resolution for tracking, particle identification, calorimetry, and high rate capabilities (about 2 x10^7 annihilations / s). The details of the PANDA detector is described elsewhere [1, 2]. The Indian group has taken responsibility in construction of some components of the PANDA detector, namely, Luminisity monitor (based on silicon microstrip detector) and silicon photomultiplier (SiPM) based fast scintillation detector (known as SciTil hodoscope). The present article reports the design details and initial R&D studies with SciTil/SiPM in which the physics department, AMU, Aligarh, has taken interest to contribute in this development together with the Nuclear Physics Division, BARC, Mumbai and Gauhati university, Guwahati from the Indian collaboration side.

The detector, SciTil, will serve for precision time measurements for triggering and determination of time-of-flight. The detector, in the present design, consists of about 5700 scintillator tiles readout by Silicon Photomultipliers (SiPM) and will be mounted in

the space between the electromagnetic calorimeter (EMC) and DIRC Cherenkov detector (DIRC stands for Detection of Internally Reflected Cherenkov light, it is a Cherenkov detector for particle identification of high energy charged particles like pion, kaon, proton etc.). The concept of SciTil provides the use of minimum material (so that not to deteriorate performance of other surrounding detectors) and a good spatial resolution due to its granularity. The timing detector concept is based on 3 × 3 × 0.5 cm^3 scintillator tiles matching the front face of the calorimeter crystals. The scintillation photons produced in the scintillator tiles due to passage of charged particles will be collected and readout by SiPMs. The number and size of the SiPMs and position of SiPM that will be coupled to the tile will be optimized based on a detailed simulation and R&D studies. In addition to timing and position information, the hodoscope will allow clean detection of gamma-conversions in front of the EMC in particular within the region of DIRC. In addition, it is best suited for discrimination between charged and neutral particles. The conceptual design [5] of the SciTil is shown in the Figs. 1-2.

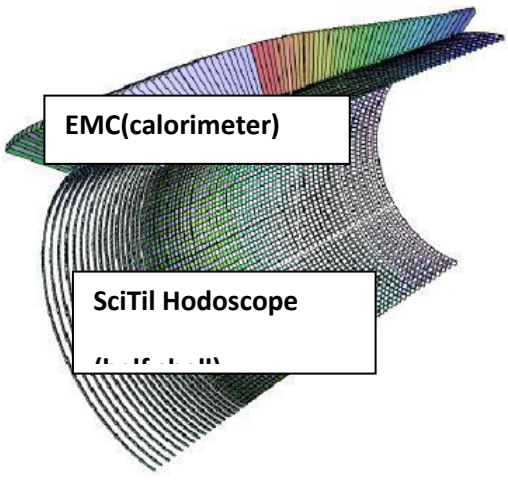

Fig.1: *A conceptual design of half shell of the SciTIl is shown along with the EMC crystal.*

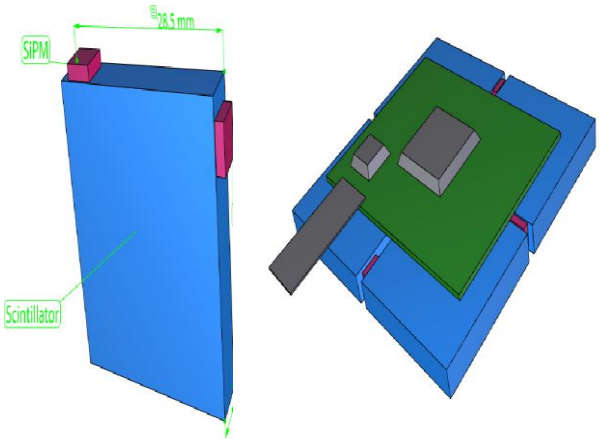

Fig. 2: *(Left) Design view of a single scintillator tile with SiPM attached. (Right) a quad SciTil module with planned PCB readout.*

R&D studies with Silicon Photomultiplier

Silicon photomultipliers (SiPMs) are very new type of photon counting devices that show great promise to be used as detection device in combination with scintillators/Cherenkov radiators. SiPM is essentially an avalanche photo-diode operated in limited Geiger mode. The SiPM module is a photon counting device capable of low light level detection. It is essentially an opto-semiconductor device with excellent photon counting capability and possesses great advantages over the conventional PMTs because of low voltage operation and insensitivity to magnetic fields. In many of the high energy physics experiments, the photon sensors are required to operate in high magnetic fields precluding the use of conventional PMTs. This problem can be overcome with the use of SiPMs. SiPM operating in Geiger mode, a very large gain (~ 10^6), magnitude of which is determined by the internal diode capacitance and applied over-bias voltage, comparable to that of PMTs can be achieved. A SiPM consists of matrix of micro cells (known as pixels), typically between 100 and 10000 per mm^2. Each micro cell acts as digital device where the output signal is independent of the number of

photons absorbed. When all the cells are connected in parallel, the SiPM becomes an analog device thereby allowing the number of incident photons to be counted. Detailed R&D studies with SiPM are needed for the use of this device to PANDA experiment. With this motivation in mind, we have developed a SiPM test facility and have tested several commercially available SiPM for their performance study[6,7,8,9] and comparison with other photon counting devices. Different types of SiPM manufactured by Hamamatsu and Zecotek with different sizes of pixels and active area have been tested. A list of the SiPMs used in the present study is given in Table 1. Studies are also being done with Hamamatsu make MPPC of size 3 x 3 mm^2, an array of 2 x 2 with total active area 6 x 6 mm^2.

Table 1: *SiPM details used in our present study. MPPC1 and MPPC2 are Hamamatsu make while MAPD3N is from Zecotek.*

Device	Active area (mm^2)	Pixel size (μm)	Pixel ensity ($1/mm^2$)
MPPC1	1x1	100	100
MPPC2	1 x 1	25	1600
MAPD3N	3 x 3	7	15000

During the measurement, all devices were mounted in a light tight box and were illuminated by a pico-second pulsed diode laser (make Pico-Quant) of 660 nm wavelength as well as LED with λ = 460 nm. In order to be able to distinguish between single and multi-photon peaks, the laser intensity was controlled. The voltage and current on the SiPM were measured by high precision multimeter and I-V characteristic of the photo-diode was studied. The preamplifier used was "Photonique SA" make two varieties: one with high gain(20x – 60x) but relatively slow rise time(~5ns) and the other one with lower gain(10x – 20x) but having faster rise time (~700ps). We have also measured the particle detection efficiency (PDE) as a function of wavelength of the incident photons. For this, a monochromator that spans wavelength from 200 to 800 nm was used. Different intensity filters were used for light intensity attenuation. The photo-sensitivity of different SiPMs was normalized with a PIN diode which itself was calibrated by the producer. The dark count of the MPPCs were measured at 0.5thr and 1.5thr and found to be in agreement with the specifications provided by the supplier. Fig.3 shows a typical SiMP spectrum for low intensity laser light, showing up to eight individual peaks corresponding to different number pixels fired.

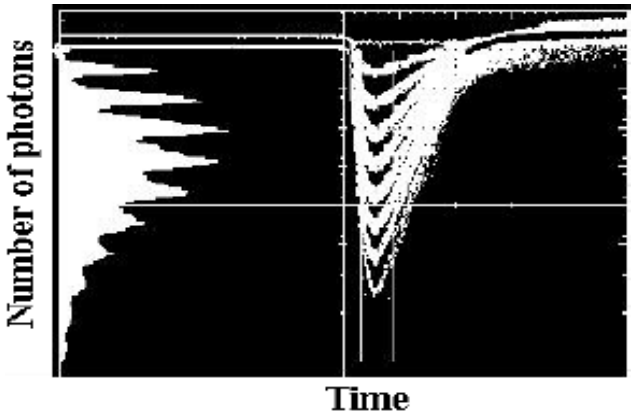

Fig.3: *A typical SiPM spectrum from Hamamatsu MPPC triggered by laser light. Different peaks correspond to different photo peaks, hence, the number of pixels fired. In this case up to eight photon peaks are seen (photograph taken from digital oscilloscope with histogram mode on).*

In fig.4, we plot the photon detection efficiency (PDE) distribution as a function of the wavelength λ for Zecotek make MAPD3N and Hamamatsu make MPPC. For MAPD3N, the distribution has been normalized with PDE=24.5% at λ = 450 nm[10] and for MPPC, PDE=32.4% at λ = 450 nm[11]. It is to be noted that the present data for MPPC shows much broader distribution extended over larger wavelength range as compared to the report of Hamamatsu.

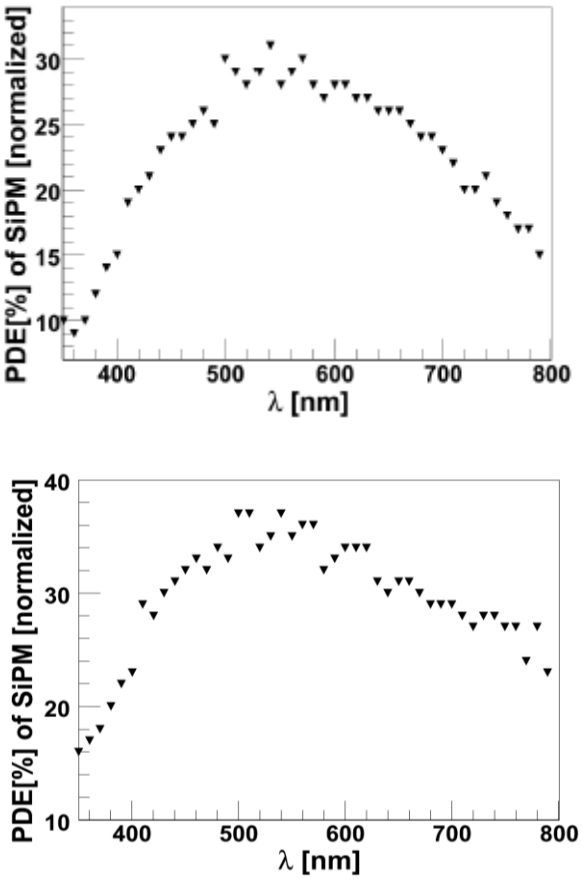

Fig.4: *(Left part) Photon detection efficiency distribution of MAPD3N as a function of wave length normalized with data from ref.[10] at λ = 450 nm.*
(Right part) Photon detection efficiency distribution of MPPC normalized with data from ref.[11] at λ = 450 nm.

For the SciTil hodoscope, in order to optimize the geometry of SiPM and light collection efficiency, simulations are being performed with a Monte Carlo simulation program SLitrani. SLitrani stands for light transmission in anisotropic media, with 'S' having the meaning of super. It is a general purpose Monte Carlo program that simulates light propagation in isotropic media (it can also be used for anisotropic media) and is built upon ROOT. The one of the main emphasis of this hodoscope detector is to provide a very fast timing (sub nanosecond timing), detailed simulation studies and prototype development for which are in progress [12].

Summary

The facility for antiproton and ion research (FAIR) will be a unique facility for the investigation of hadron structure and QCD in the charm sector. The Indian hadron physics community has taken strong initiative to be a part of this exiting physics programme and to contribute in the detector construction, simulation & software development and physics case studies. The Aligarh Muslim University has shown interest to be a part of the SiPM / SciTil hodoscope development work. Initial R&D studies with SiPM show a great promise of this device to be used as photon counter and a great potential to replace the conventional PMTs.

Acknowledgements

We thank the whole India-PANDA collaboration team and especially Dr. S.kailas, BARC and Prof. R.Varma, IIT-Bombay for their effort and continued interest in this work. The work reported here has been carried out in close collaboration with the HAD-1 group, GSI, Germany. We thank the GSI group (Prof. K.Peters, Dr. H.Orth, Dr. C.Schwarz, Dr. Lars Smith and Dr. A.Wilms) for their support and interest.

References

1. PANDA collaboration- physics performance report, arXiv:0903.3905 and PANDA technical progress report, Gold version, 2005.
2. QCD studies with anti-protons at FAIR: Indian participation in PANDA, *S.Kailas, B.J.Roy, D.Dutta. V.Jha, R.Varma,* Current Science, Vol. 100, No.5 (2011) and references therein.

3. Geissel H et al, Phys. Rev. Lett. 88, 122301(2002), Phys. Lett.B., 549 (2002) 64 and references therein.
4. Nekipelov M. et al, Phys. Lett. B, 540 (2002) 207, Rudy Z. et al, Euro. Phys. J A15 (2002) 303.
5. Proposal for a Scintillation Tile Hodoscope for PANDA, K.Goetzen, H.Orth, G.Schepers, C.Schwarz, A.Wilms (private communication).
6. SiPM as photon counter for Cherenkov detectors, *B.J.Roy, H.orth, C.Schwarz, A.Wilms, K.Peters,* DAE Symp. Nucl. Phys. Vol. 54, 666 (2009).
7. Study of the spectral sensitivity of G-APDs in the wavelength range from 250 to 800 nm, *B.J.Roy et al*, 12th Vienna Conf. on Instrumentation, Feb. 2010, Vienna.
8. In-beam test of a DIRC Cherenkov radiator with SiPM, *B.Kroeck, A.Hayrapetyan, K.Foehl, O.Merle, M.Duren, B.J.Roy, K.Peters,* DAE Symp. Nucl. Phys. Vol. 54, 668 (2009).
9. Development of SiPM based scintillation detector for fast timing application in the PANDA experiment, H.Kumawat, B.J.Roy, V. Jha, U.K.Pal, A.Chatterjee and S.Kailas, DAE symp. Nucl. Phys, (2011).
10. D. Renker, PSI (private communication).
11. N.Anfimov, Dubna (private communication).
12. Simulations of SiPM based scintillation detector for PANDA, U.K.Pal, B.J.Roy, V.Jha, H.Kumawat, A.Chatterjee and S.Kailas, DAE symp. Nucl. Phys, (2011).

Wong *vs.* Dynamical Cluster-decay Model for Heavy Ion Reactions

Manie Bansal, Sahila Chopra and Raj K. Gupta[*]

Introduction

Heavy-ion reactions at low-energies (<15 MeV/A) give rise to compound nuclear systems that are excited, carry angular momentum ℓ, and decay by emitting multiple light particles (LPs: n, p, α) and γ-rays (constituting the evaporation residue ER), fusion-fission ff (consisting of the, so-called, intermediate mass fragments IMFs of masses $5 \leq A \leq 20$ and charges $2<Z<10$, and the near-symmetric and symmetric fission fragments nSF and SF of masses $A/2 \pm 20$), and many a times by a non-compound, quasi-fission qf or, equivalently, capture process. Such a compound nucleus (CN) decay cross-section is termed as the CN production cross-section, or simply as the (total) fusion cross-section σ_{fus}, given as

$$\sigma_{fus} = \sigma_{ER} + \sigma_{ff} + \sigma_{qf}. \quad (1)$$

Different compound nucleus reactions measure different combinations of these three processes (ER, ff and qf or capture) or any one of them as a dominant mode.

Wong [1] gave a model for the (total) fusion cross-section σ_{fus} in terms of the penetration probability P of the *barrier for the incoming channel*, which has been applied to σ_{fus} consisting alone of dominant ER, fission or capture cross-section. Actually, Wong worked out a simplified formula for σ_{fus} in terms the $\ell=0$ barrier properties (position, height and curvature), referred to here as the $\ell=0$ barrier-based Wong formula, which has recently been shown to be inadequate by Gupta and collaborators [2]. These authors showed that Wong's approximations *ignored* the already present "barrier modification effects" in Wong expression via its ℓ-summation, which led them [2] to an ℓ-summed extended-Wong model, with ℓ-summation effects included explicitly.

Gupta and collaborators [3]-[10] also introduced the concept of relative pre-formation probability P_0 of various decay products, in their, so-called, dynamical cluster-decay model (DCM), in order to be able to study the relative contributions of various components (ER, ff and qf or capture) of σ_{fus},. Thus, in DCM, in addition to the penetrability P through a *barrier for the decay products*, there is a relative pre-formation factor P_0 associated with them. Thus, the two models (extended-Wong and DCM) differ in their P being calculated, respectively, for the incoming or decay channel, but are identical for the case of $P_0=1$ for each ℓ. Note, $P_0^{\ell}=1$ implies the condition of incoming nuclei keeping their identity, satisfied only for the qf or capture process. In other words, in DCM, $P_0^{\ell}=1$ for qf and then P is calculated for the incoming channel.

The extended-Wong model [2] as well as the DCM [3-10], both of Gupta's group, are applied to various reactions with dominant ER, ff, qf (≡capture), ER+ff, ER+ff+qf. In the following, we illustrate their distinguishing aspects via the reaction $^{64}Ni+^{112}Sn \rightarrow ^{176}Pt^{*}$ with measured total fusion cross-section σ_{fus} built up of the evaporation residue (σ_{ER}) and fission (σ_{fiss}) cross-sections, $\sigma_{fus}=\sigma_{ER}+\sigma_{fiss}$. The important point is that Wong model describes only σ_{fus}, and DCM describes all the individually measurable cross-sections of the decay products (here σ_{ER} and σ_{fiss}), and hence σ_{fus}, *together with the fragment masses of the identified decay processes*.

The Extended Wong Model and the Dynamical Cluster-Decay Model (DCM)

Extended-Wong model: Fusion cross-section due to two deformed and oriented nuclei (with orientation angles θ_i), lying in two different planes (with azimuthal angle Φ between them), and colliding with $E_{c.m.}$, defined by Wong [1] in terms of ℓ partial waves, is

$$\sigma(E_{c.m.},\theta_i,\Phi)=\frac{\pi}{k^2}\sum_{\ell=0}^{\ell_{max}}(2\ell+1)P_\ell(E_{c.m.},\theta_i,\Phi)$$

$$\text{with}\quad k=\sqrt{2\mu E_{c.m.}/\hbar^2}\ . \qquad (2)$$

P_ℓ is the transmission coefficient for each ℓ, calculated in Hill-Wheeler approximation of an inverted harmonic oscillator to interaction potential $V_\ell(R,E_{c.m.},\theta_i,\Phi)$ due to *incoming channel*, as

$$P_\ell=\left[1+\exp\left\{\frac{2\pi(V_B^\ell(E_{c.m.},\theta_i,\Phi)-E_{c.m.})}{\hbar\omega_\ell(E_{c.m.},\theta_i,\Phi)}\right\}\right]. \qquad (3)$$

Here, $V_B{}^\ell$ and $\hbar\omega_\ell$ are the barrier height and curvature at barrier position $R_B{}^\ell$. Wong carried out the summation in Eq. (2) *approximately* by assuming $\hbar\omega_\ell=\hbar\omega_0$, $V_B^\ell\approx V_B^0+\hbar^2\ell(\ell+1)/2\mu R_B^{0^2}$ and $R_B{}^\ell\approx R_B{}^0$, and obtained a formula in terms of the ℓ=0 barrier-based quantities $V_B{}^0$, $R_B{}^0$ and $\hbar\omega_0$, the barrier height, position, and curvature for ℓ=0, as

$$\sigma(E_{c.m.},\theta_i,\Phi)=\frac{R_B^{0^2}\hbar\omega_0}{2E_{c.m.}}\ln\left[1+\exp\left\{\frac{2\pi}{\hbar\omega_0}(E_{c.m.}-V_B^0)\right\}\right] \quad (4)$$

which on integrating over both θ_i and Φ gives the fusion cross-section $\sigma(E_{c.m.})$. Eq. (4) is referred to as the *ℓ=0 barrier-based Wong formula*.

For making an explicit ℓ-summation in Eq. (2) [2], the ℓ-dependent barrier quantities $V_B{}^\ell$, $R_B{}^\ell$, and $\hbar\omega_\ell$ are needed, given by the ℓ-dependent interaction potential

$$V_\ell(R)=V_P(R,A_i,\beta_{\lambda i},T,\theta_i,\Phi)+V_C(R,Z_i,\beta_{\lambda i},T,\theta_i,\Phi)+\frac{\hbar^2\ell(\ell+1)}{2\mu R^2} \qquad (5)$$

where temperature T-dependent Coulomb and proximity potentials, V_C and V_P, for deformed, oriented co-planar ($\Phi=0^0$) or non-coplanar ($\Phi\neq0^0$) nuclei are from [11] or [12]. $\beta_{\lambda i}$, λ=2,3,4 are the static quadrupole, octupole and hexadecapole deformations, and T (in MeV) is related to the incoming $E_{c.m.}$ or the CN excitation energy E^* as $E^*=E_{c.m.}+Q_{in}=(1/a)AT^2-T$, with a=9 or 10, respectively, for intermediate mass or super-heavy nuclei. Q_{in} is the entrance or incident channel Q-value. This is referred to as the *(ℓ-summed) extended-Wong model*.

ℓ_{max} is determined empirically for a best fit to the measured cross-section (see Fig. 1 in [2]). If the ℓ-summation procedure fails to reproduce data, an empirical "modification of the barrier" is introduced either via the barrier height $V_B{}^\ell$, or via the curvature $\hbar\omega_\ell$, defined as

$$V_B^\ell(\text{modified})=V_B^\ell+\Delta V_B^{emp},$$
$$\text{or}\quad \hbar\omega_\ell(\text{modified})=\hbar\omega_\ell+\Delta\hbar\omega^{emp}. \qquad (6)$$

Note that the *"barrier modification"* $\Delta V_B{}^{emp}$ [or $\Delta\hbar\omega^{emp}$], is a fixed quantity, independent of ℓ, added to (or subtracted from) the barrier height $V_B{}^\ell$ [or curvature $\hbar\omega_\ell$] for all ℓ-values.

DCM: Introducing the relative pre-formation factor $P_0{}^\ell$ for all decay products A_i, i=1, 2, Eq. (2) gives the DCM expression for

CN decay/ formation cross-section for each process (LPs, ff), as

$$\sigma(E_{c.m.},\theta_i,\Phi)=\sum_{\ell=0}^{\ell_{max}}\sigma_\ell=\frac{\pi}{k^2}\sum_{\ell=0}^{\ell_{max}}(2\ell+1)P_0^{\ell}P_\ell \quad (7)$$

where P_0^{ℓ} refers to motion in mass asymmetry coordinate $\eta=(A_1-A_2)/(A_1+A_2)$, given as the solution of stationary Schrödinger equation in η at a fixed $R=R_a$, as

$$\left\{-\frac{\hbar^2}{2\sqrt{B_{\eta\eta}}}\frac{\partial}{\partial\eta}\frac{1}{\sqrt{B_{\eta\eta}}}\frac{\partial}{\partial\eta}+V(R,\eta,T)\right\}\psi^{\nu}(\eta)=E^{\nu}\psi^{\nu}(\eta) \quad (8)$$

where $\nu=0,1,2,..$, refers to ground-state ($\nu=0$) and excited-states solutions. Then, the probability $P_0(A_i)=|\psi_R(\eta(A_i))|^2\sqrt{B_{\eta\eta}}\frac{2}{A}$, with a Boltzmann-like function $|\psi|^2=\sum_{\nu=0}^{\infty}|\psi^{\nu}|^2\exp(-E^{\nu}/T)$.

In Eq. (8), the fragmentation potential $V(\eta)$ at fixed $R=R_a$ is

$$V_R(\eta,T)=\sum_{i=1}^{2}[V_{LDM}(T)+\delta U(T)]+V_P+V_C+V_\ell, \quad (9)$$

with V_{LDM} and δU as the liquid drop and shell effect energies.

The penetrability P_ℓ in Eq. (7) of DCM is the WKB integral,

$$P=\exp\left[-\frac{2}{\hbar}\int_{R_a}^{R_b}\sqrt{2\mu[V(R,T)-Q_{eff}]}\,dR\right], \quad (10)$$

solved analytically [13], whose first turning point $R_a=R_1(\alpha_1,T)+R_2(\alpha_2,T)+\Delta R(T)$ is defined through a neck-length parameter ΔR for the best fit to measured cross-section for each process and the second turning point R_b satisfy $V(R_a)=V(R_b)=Q_{eff}=TKE(T)$, which means that $V(R_a)^{\ell}$ acts like an effective Q-value, $Q_{eff}(T,\ell)$, given by the total kinetic energy TKE(T). ℓ_{max} is fixed for the light particles cross-section $\sigma_{ER}(\ell)\to 0$ at $\ell=\ell_{max}$. For the definition of angles α_i in radius vectors R_i, and the orientation θ_i, see Fig. 2 in [3]. Note that the neck-length parameter ΔR also contains the effects of "barrier lowering" in it for each decay channel, defined for each ℓ as the difference between V_B^{ℓ} and $V(R_a)^{\ell}$, $\Delta V_B^{\ell}=-[V_B^{\ell}-V(R_a)^{\ell}]$, the actually calculated and the actually used barriers. Finally, for qf (≡capture), only the incoming channel plays the role, and hence $P_0^{\ell}=1$ in DCM.

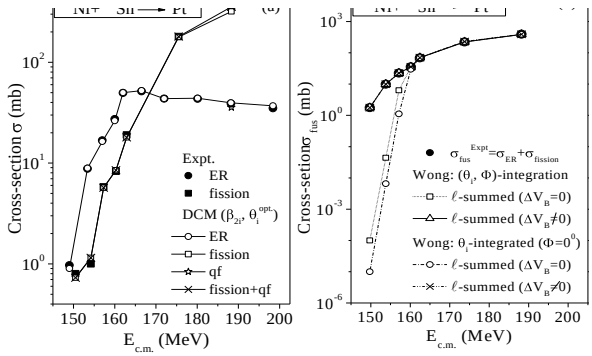

Fig.1: *(a) Calculated DCM σ_{ER}, σ_{fiss}, σ_{qf} [9]; (b) extended-Wong model σ_{fus}[10], compared with experimental data.*

Calculations and Results

We illustrate the distinguishing features of the two model (extended-Wong and DCM) for the reaction $^{64}Ni+^{112}Sn\to^{176}Pt^*$ decaying via ER and fission processes [14]. Fig. 1(a) gives the DCM results, showing (via P_0 calculations) that ER and fission are the only viable decays, and the calculations fit the data nicely for co-planar ($\Phi=0^0$) nuclei, predicting a small qf component at the highest one above-barrier energy [9], which might become zero for, not yet studied, $\Phi\neq 0^0$ case. Note, however, that "barrier modification" at sub-barrier energies is in-built in DCM [9].

Fig. 1(b) gives the extended-Wong model fitted σ_{fus}, for θ alone and (θ, Φ) integrations [10], requiring 'barrier modification" for the best fit at sub-barrier energies in both cases.

Conclusion

We have shown that the DCM is able to describe the detailed compound nucleus decay, like the individual decay processes, together with their fragment masses, whereas the extended-Wong model gives simply the (total) fusion cross-section alone. The non-coplanar degree of freedom Φ
is introduced and the quasi-fission (qf) component, if any, in σ_{fiss} at above-barrier energies, and barrier-modification for σ_{ER} at below-barrier energies are studied.

ACKNOWLEDGEMENTS
Work supported by the Department of Science and Technology (DST), Govt. of India.

References

1. C.Y. Wong, *Phys. Rev. Lett. 31, 766 (1973).*
2. R. Kumar, M. Bansal, S.K. Arun, and R.K. Gupta, *Phys. Rev. C 80, 034618 (2009).*
3. R.K. Gupta, S.K. Arun, R. Kumar, and Niyti, *Intern. Rev. Phys. (I.RE.PHY.) 2, 369 (2008).*
4. B.B. Singh, M.K. Sharma, and R.K. Gupta, *Phys. Rev. C 77, 054613 (2008).*
5. R. Kumar and R.K. Gupta, *Phys. Rev. C 79, 034602 (2009).*
6. S.K. Arun, R. Kumar, and R.K. Gupta, *J. Phys. G: Nucl. Part. Phys. 36, 085105 (2009).*
7. R.K. Gupta, S.K. Arun, R. Kumar, and M. Bansal, *Nucl. Phys. A 834, 176c (2010).*
8. R.K. Gupta, *Lecture Notes in Physics, 818*, "Clusters in Nuclei", ed. C. Beck (Springer-Verlag 2010) Vol. 1, p. 223.
9. M.K. Sharma, *et al. J. Phys. G: Nucl. Part. Phys. 38, 055104 (2011); AIP Conference Proceedings 1265*, edited by R. Alcaron, *et al., (2010) p. 37.*
10. R.K. Gupta and M. Bansal, *Intern. Rev. Phys. (I.RE.PHY.) 5, 74 (2011).*
11. R.K. Gupta, N. Singh, and M. Manhas, *Phys. Rev. C 70, 034608 (2004).*
12. M. Manhas and R.K. Gupta, *Phys. Rev. C 72, 024606 (2005).*
13. S.S. Malik and R.K. Gupta, *Phys. Rev. C 39, 1992 (1989).*
14. W.S. Freeman, *et al. Phys. Rev. Lett. 50, 1563 (1983);* K T. Lesko, *et al. Phys. Rev. C 34, 2155 (1986).*

Experimental Reactor Physics and its role in the Nuclear Reactor Design

Rajeev Kumar

Introduction

The title of the articles sounds somewhat similar to Experimental Nuclear Physics, but that is not the case, in fact it is very much different except one part that is nuclear data which will be described later in the article. Basically Reactor Physics is a field which deals with the neutron transport in the reactor core. This is further divided into two branches viz., (i) the steady state neutron transport and (ii) the neutron kinetics. Theoretical models are used to study the neutron transport in the core. Various computer codes based on deterministic as well as stochastic principles are available.

Though, there is enough experience in construction and operation of nuclear reactors worldwide, yet when we design new type of nuclear reactor system, it is very important to validate its design in the domain of physics as well as in engineering. As far as physics design is concerned, it progresses in two steps, the first is that one has to model the reactor core theoretically and calculations are done to get the various design parameters using the available computer codes and then all these calculations are checked/benchmarked against the experiments carried out in a test reactor facility. This is where experimental reactor physics comes into picture. Various reactor physics experiments are carried out in the test facility to produce the experimental data which are compared with the calculated values. The comparison between the measured and calculated values gives the feedback which helps in designing the new reactor system. Presently, there is worldwide interest in designing the new type of nuclear system like Gen IV Reactors, accelerator driven sub critical reactor etc. Experimental reactor physics is very much required to validate the design of such systems. Research and development to design an Advanced Heavy Water Reactor (AHWR) based on thorium fuel cycle is going on in Bhabha Atomic Research Center (BARC), Mumbai, India. Various experiments are being carried out in test critical facility to validate the design parameters of AHWR.

Experimental Reactor Physics

Let us first understand in brief what is Reactor Physics all about? The core of a nuclear reactor consists of fuel viz. Uranium, moderator (to slow down and thermalise the neutrons in thermal reactor) and coolant to remove the heat produced in the fuel. The fuel channels in the core are arranged in a symmetric and periodic manner. The geometry of this arrangement can be square or triangular/hexagonal depending on the desired core feature. Reactor physics deals with the neutron transport through the materials present in the core in steady state as well as in transients with respect to time. There are several quantities which are required to be defined to study a reactor core; some very basic quantities are discussed here. 1) *Neutron flux*: Number of neutrons traveling through unit area in unit time is called neutron flux and denoted by Φ (neutrons per cm^2 per second). Neutron distribution in energy (energy spectrum) and neutron distribution in space are important quantities which depend on the core condition. One thing should be noted here that in spite of the fact that neutron are fermions, Maxwell distribution is followed in reactor physics. The reason is that for typical neutron flux $\approx 10^{12}$ neutron per cm^2 per second, the neutron density is orders of magnitude less than the same inside a nucleus where it behaves like fermions. In other words the average distance between the neutrons in a reactor is much greater than their de Broglie wavelength (there is no overlapping

of wave functions), therefore quantum effect does not come in to the picture. 2*) Neutron multiplication factor (k*): Nuclear fission is chain reactions which multiply the number of neutrons; this neutron multiplying property is defined by multiplication factor (k) which depends on the core configuration and conditions. It is a ratio of number of neutrons in a particular generation to the same in preceding generation. For self sustaining controlled chain reaction the value of k should be equal to unity and it is called critical condition. Otherwise if the value of k is less or greater than 1, the system is called subcritical or supercritical respectively. 3) *Worth of control system*: It is related to the properties of the neutron absorbing materials (required for controlling the chain reaction) 4) *Burn up*: It deals with the composition of fuel which changes as fuel burns to produce the energy. A number of fission products which keeps on accumulating in the fuel, absorb the neutron in a non fission reaction and hence affect the neutron multiplication factor. 5) *Nuclear data*: It is basically the cross sections for several reactions which may take place when neutrons interact with materials as it moves in the core.

Nuclear data is very important input to the reactor physics calculations. The cross sections of a given reaction and nuclei are measured in various laboratories worldwide with different accuracy and precision. Sometimes it happens that the cross section for a particular isotope in high energy (few hundred MeV) range has relatively high experimental errors. All these facts cause the uncertainty in the reactor physics calculation, since it uses the nuclear data as one of its input. Apart from others, error in nuclear data is a major source of uncertainty in calculated design parameter of a reactor core. The only way to account these uncertainties is to carry out the experiments in test reactor facility and compare the measurements and calculations. This is where experimental reactor physics comes into play. It has further two branches one is in core measurement and the other it out core measurements which is generally carried out in radiation shield design.

In-core measurement is being discussed here in brief. The method used in the in-core measurement is activation technique. It is a well established technique and used in various other fields also. The neutron detectors used are called activation detectors, they are basically small size foils (2 mm x 2mm) of various materials like Gold, Copper, Manganese, Iron , Nickel and Titanium etc. The basic measurable quantity in the neutron environment is the reaction rate i.e., the number of reactions that take place per unit nuclei per unit time defined as;

$$Reaction\ rate = \int \sigma(E)\phi(E)\, dE$$

Here, $\sigma(E)$ is the activation cross section for a given type of reaction (fission, absorption or scattering etc) and $\Phi(E)$ is neutron flux. Both these quantities are function of energy. The cross-section $\sigma(E)$ values are known from nuclear data and hence above mentioned integral can be unfolded to get the neutron flux. Other quantities important to characterize a reactor core also can be derived from the reaction rate and can be used to validate the calculated values.

Now let us see how do the reaction rates are measured using activation technique? When a foil like Gold (^{197}Au) is exposed in a neutron environment, it absorbs a neutron ((n,γ) reaction) and formation of ^{198}Au takes place which is radioactive isotope of gold and undergoes beta decay (Half life=2.7 days) to produce ^{198}Hg* having an exited nuclear state. The Excited ^{198}Hg* nucleus comes down to its ground state by emitting characteristic gamma rays (411 keV). In a simple language we can say that neutron flux information is stored in the gold foil in the form of induced gamma activity. The reaction can be written as equation (1).

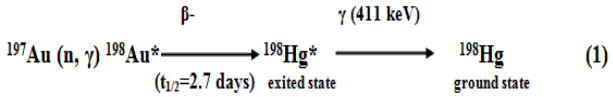

(1)

The gamma activity of $^{198}Hg^{*}$ is counted by high purity Germanium detector (HPGe) and the gamma activity can be related to neutron reaction rate written in equation (2).

$$\int \sigma(E)\phi(E)\,dE = A/(N\,\varepsilon_1\varepsilon_2\,\varepsilon_3 G(\tau)(1-\exp(-\lambda t))\exp.(-\lambda T)) \quad (2)$$

Where,
A = Counted gamma activity using HPGe
N = total number of target atoms
ε_1 = isotopic abundance
ε_2 = yield of gamma ray
ε_3 = photo-peak counting efficiency of HPGe
T = time elapsed between end of irradiation and start of counting
t = duration of irradiation
λ = Decay constant for radioactive isotope
$G(\tau)$ = self shielding factor of activation foil, τ is no of mean free path.
$\sigma(E)$ = Activation cross-section at energy E
$\phi(E)$ = Neutron flux at energy E.

This was a typical example to show, how an activation detector works. However, Gold, Copper, Manganese are thermal activation detectors since they have good activation cross section in the thermal energy region (0.025 eV to 1 eV). For fast energy region, detectors like Titanium, Nickel and Iron are used, these are called threshold detectors because they have finite cross section only after certain energy for example Iron, ^{54}Fe (n, p) ^{54}Mn has about 3 MeV of threshold energy.

The merit of activation detector is that they are very small in size hence flux perturbation inside the core is negligible and at the same time they can be placed any where inside the core; for example flux inside the fuel pin also can be measured using these detector. It is an offline measurement technique and there is no interference of gamma rays which is a matter of concern in other methods. This was all about static neutron flux measurement. For kinetic measurement other technique whose response is a function of time like reactor period measurement is used.

Role of Experimental Reactor Physics

Today, there is an increasing demand of electricity in the society. Per capita electricity consumption also is an index of development in the country. Considering the facts like green house effect and global warming, nuclear energy is the better option. But at the same time there are some problems with issues like nuclear waste management globally and availability of fissile material in Indian context. Research and development are going on to take care of these issues where scientist and engineers are working on alternative fuel cycle and new reactor types, for example Accelerator Driven Subcritical System (ADSS) is one of them. The role of experiment is discussed here briefly. In ADSS, a subcritical reactor core (K<1) is coupled with accelerator based spallation neutron source. Spallation is nuclear reaction in which few GeV proton bean impinges on high Z material target and produces lot of neutrons which will help to sustain the chain reaction in subcritical system. The advantage of ADSS is that being a subcritical system, safety related issues are matter of low concern relative to existing critical reactors. The problem of waste management is also supposed to be taken care of by ADSS.

ADSS is different from the existing critical system in many aspects for example fuel type and neutron energy region. The available nuclear cross-sections of some important isotopes in high energy region need more accurate measurement to minimize the uncertainties in the calculations. Subcritical reactor physics is different from physics of

critical system. Hence, new computational tools are being developed. Considering all these facts, it is very important to carry out the experiments and generate the data so that uncertainties in the theoretical modeling can be accounted for and new computational tool can be benchmarked against the measurements. Experimental reactor physics can help in performing this task and hence it always plays an important role in designing the new reactor system.

Proton Computed Tomography (pCT) for Cancer Therapy

Dr. Naimuddin

Introduction

Proton therapy is a rapidly expanding form of cancer treatment. Because protons have a finite range in matter, this treatment modality allows for a greater degree of conformality than conventional external beam X-ray therapy. To maximize the inherent advantages of proton therapy, the range of protons inside the patient must be able to be predicted with millimetre resolution. In current clinical practice, proton therapy treatment plans are made with pre-treatment X-ray CT scans of the patient. To convert the X-ray CT Hounsfield units to proton relative stopping powers, which are required by the treatment planning software, an empirically derived calibration function is used, which is specific to each X-ray CT machine. However, because of the different dependence on Z and the Z/A ratio of X-ray attenuation and proton energy loss, the relationship between Hounsfield units and relative stopping powers is not unique. This conversion process leads to range uncertainties at treatment time. A preferable scenario is one in which the relative stopping power of each patient is reconstructed directly. This is the goal of proton computed tomography (pCT). Figure 1 shows a typical computed tomography scanner.

Figure 1: *Computed tomography scanner*

History of proton (hadron) therapy

The use of energetic protons for therapeutic means was first proposed by Robert Wilson in 1946[1], while working on the design of the Harvard Cyclotron Laboratory. Wilson proposed that proton beams would be advantageous for the treatment of deep-seated tumours because of the favorable relationship between deposited dose and depth in the absorbing material. This characteristic of heavy charged particles is known as the Bragg peak, a phenomenon whereby the maximum dose along a trajectory is deposited in a peak-like distribution toward the end of the range.

Computed tomography with heavy charged particles, and protons in particular, was first proposed as a possible alternative to X-ray CT by Allan Cormack [2, 3]. Cormack proposed that the variable density of matter with constant chemical composition could be determined by measuring the energy loss of charged particles in the matter. Cormack suggested that the values reconstructed with charged particle CT would be an important tool in the treatment planning process of heavy charged particle therapy, where the depth of the Bragg peak must be determined with a high degree of accuracy.

Though the proton CT was first proposed in 60s but a clinical system is yet to be realized. Difficulties experienced in previous projects included long acquisition times and sub-standard spatial resolution relative to X-ray CT. The current pCT development project makes use of advances in high energy physics detector technology and focuses on generating pCT specific image reconstruction algorithms to counteract the aforementioned issues.

Mimicking the progression of X-ray imaging, the initial heavy charged particle

imaging studies were of radiographic nature (2D projections). Studies showed that by using a stack of parallel sided aluminium plates of a thickness just less than the proton range, radiographs of much greater contrast could be recorded with protons than that obtained with X-rays [4]. Subsequently, it was demonstrated that the high contrast images obtained by proton radiography provided improved imaging of low contrast lesions in human specimens over conventional X-ray techniques [5]. The high contrast obtained in this energy-loss form of radiography is a consequence of the sharpness of the Bragg peak. Figure 2 shows the comparison of energy (dose) deposited by x rays and protons in matter (body).

A tomographical reconstruction with heavy charged particles was firs carried out by Goitein in 1972 [6]. He employed projection data measured by Lyman with alpha particles to demonstrate the utility of his least-squares reconstruction algorithm. Later, in studies by Crowe and colleagues at LBL, it was shown that alpha particle CT had a dose advantage over X-ray CT in human head reconstructions. In this system, stacks of scintillating plates were used to determine the residual energy of the alpha particles.

It was not until 1976 that a prototype proton computed tomography (pCT) system was constructed by Cormack and Koehler and tested at the Harvard Cyclotron Laboratory [7]. Their system was based on scanning a radially symmetric Lucite phantom, containing sugar solution and polystyrene inserts, with a collimated 158 MeV proton beam. The detector system consisted of a scintillator crystal mounted on a photomultiplier to measure the energy of protons after traversing the phantom. The radial density profile was reconstructed with Cormack's line integral theory [2, 3]. With this simple system, it was shown that density differences of 0.5% could easily be distinguished. However, the authors also noted that reconstruction artifacts were present at boundaries between substances of differing density. It was suggested that this was the result of a differing degree of multiple Coulomb scattering (MCS) in the two regions.

Later, Hanson and colleagues achieved the first 2D tomographical images generated with protons [8]. Hanson's system consisted of a hyper-pure germanium detector (HPGe) and a multiwire proportional chamber (MWPC) to measure the residual energy and exit position of each exiting proton, respectively. Collimated 192 and 240 MeV proton beams from the Los Alamos Meson Physics Facility were used to scan 20 and 30 cm cylindrical phantoms submerged in a water bath, respectively. The phantoms contained cylindrical inserts of varying density to quantify contrast resolution. The scanning was achieved by lateral translation of the phantom across the proton pencil beam and phantom rotation following full translation. It was found that the pCT scanner could deliver 9 times less average dose than the contemporary X-ray CT EMI scanner for a given density resolution. The disadvantage of pCT was found in the lack of spatial resolution. Even with the use of the position sensitive single particle tracking MWPC to counteract the effects of MCS, a decrease by a factor of 2−2.5 in comparison to the images generated by the EMI scanner was quoted. Hanson pointed to the possibility of using curved trajectories as opposed to straight lines in the reconstruction to improve spatial resolution.

Hanson and colleagues also went on to carry out pCT scans of biological specimens with a magnetically scanned pencil beam and the same detector system as described above [9]. By rebinning individual proton exit positions and using an iterative peak fitting procedure to assign a mean residual range to each spatial bin, 2D pCT images of a human heart and brain were generated with the filtered backprojection reconstruction algorithm. A comparison with

two contemporary X-ray CT scanners reconfirmed the previous findings that, although a superior dose-density resolution relationship could be achieved with pCT, spatial resolution was degraded.

The development of pCT experienced a hiatus following the work of Hanson and colleagues. It was not until the expansion of proton therapy in the 1990's that renewed interest was placed in proton imaging. Schneider and colleagues at the Paul Scherrer Institute, Switzerland used a proton radiography apparatus to examine the accuracy of proton therapy range prediction with X-ray CT methods [10, 11, 12]. By comparing X-ray CT predicted residual proton ranges with those measured by a proton radiography system, they showed that standard treatment planning procedures in proton therapy could result in range uncertainties of up to 3% of the proton range [13].

In 2000, Zygmanski and colleagues presented results from a cone-beam pCT system with the goal of applying the stopping power tomographs to proton therapy treatment planning. The residual energy detector system consisted of a solid state intensifying screen viewed by a cooled CCD camera. This planar detector configuration allowed for fast acquisition and reconstruction of 3D proton RSP maps.

The Feldkamp-Davis-Kress (FDK) [14] cone-beam reconstruction algorithm was used to obtain the CT voxel data representing proton stopping powers. It was found that the pCT reconstructed values were closer to real phantom stopping powers than the values calculated with X-ray CT followed by conversion. However, due to the significant lack of spatial resolution and large degree of noise, this concept was not pursued further.

Current status of proton (hadron) therapy

Treatment of patients with protons was first carried out in 1955 at the Lawrence Berkeley Laboratory (LBL), California. In 1961 the Harvard Cyclotron Laboratory and Massachusetts General Hospital began collaboration in the pursuit of proton therapy. Over the next 41 years, this program refined and expanded the founding techniques, in particular by introducing Bragg peak treatments. While proton treatments at LBL used high energy "shoot through" style proton treatments, the advantage of stopping the proton beam at the distal edge of the tumour was first realised by the Boston collaboration. During this period patients were also treated at other research facilities in the U.S.A, Sweden and Russia. However, it was not until 1990 that the first hospital based proton treatment facility was installed at Loma Linda University Medical Center (LLUMC), California. Since then, an ever expanding number of hospital based facilities have been established. There are currently 28 proton therapy centers operating throughout the world; 12 in Europe, the UK and Russia, 8 in North America, 7 in Asia, and 1 in South Africa. In addition there are 21 facilities in the planning stage or under construction. By the end of 2008, over 60,000 patients had received proton therapy. The primary factors limiting even further expansion of proton therapy are construction and running costs, and the size of the accelerators and beam delivery systems required to treat with up to 250 MeV protons in a rotating gantry. Unfortunately there is not a single hadron therapy center in India at the moment. Nevertheless, India is seriously considering building one proton therapy center at the Variable Energy Cyclotron Center (VECC) at Kolkata during the next plan. Tata Memorial Hospital at Mumbai is also working on a plan to install one hadron therapy machine.

How it works

To cover an entire tumour volume with a uniform dose, the range of protons must be modulated and the initial pencil beam must be spread laterally. This 3D modulation can be achieved by passive scattering or active scanning means. In a passive scattering system the energy of the proton beam emerging from the accelerator is modulated by a rotating wheel of varying thickness. These modulator wheels can be designed in such a way to produce a plateau high dose region over a specified range. This dose distribution is known as a spread out Bragg peak (SOBP) as shown in Figure 2. Between the nozzle exit and the patient surface, a field-specific collimator is used to shape the field laterally to conform to the target volume and a range compensator is used to correct for patient surface irregularities, density heterogeneities in the beam path, and changes in the shape of the distal target volume surface. The lateral spread of the beam is usually achieved with a double scattering system in which the initial pencil beam is scattered to a Gaussian distribution and then flattened with a second compensating scatterer. Passive scattering systems are the most common method used in current clinical practice.

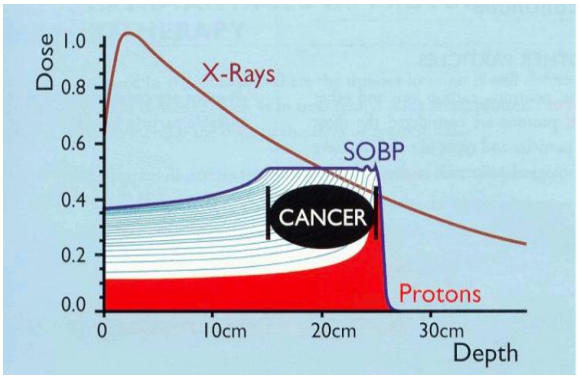

Figure 2: *A comparison of energy deposited by X ray and protons as a function of depth. X ray deposit energy in small packets all along their path through tissue, whereas proton deposit much of their energy at the end of their path (called "**Bragg Peak**") and deposit less energy along the way.*

In the active scanning approach, the energy of the proton beam is altered at the level of the accelerator. The pencil beam is then magnetically guided to cover the target volume laterally and vertically. Although active scanning systems are somewhat more of a technical challenge, a number of advantages over passive scattering systems exist. A significant factor is that the proton beam traverses fewer components in the beam line, resulting in more efficient treatments and a reduction of unwanted neutron dose to the patient. Also, truly 3D intensity modulated proton therapy (IMPT) becomes possible. Here, the intensities of individual pencil beams are optimized, resulting in highly conformal dose distributions. However, more research and development is required before intensity modulated proton therapy becomes common place.

To capitalize on the fundamental properties of proton beams, the distribution of proton stopping powers within the body must be well known prior to treatment. Currently, this information is gained from pre-treatment X-ray computed tomography (CT) scans of the patient. Such a system reconstructs the distribution of photon relative linear attenuation coefficients, values known as Hounsfield units. To obtain the proton relative stopping power (RSP) map, the reconstructed Hounsfield units are converted with an empirically derived calibration curve. The machine dependent calibration function is calculated by taking an X-ray CT scan of a phantom containing inserts of known RSP values. However, because of the different dependence on Z and the Z/A ratio by photon and proton interactions, the relationship between Hounsfield unit and proton RSP is not unique. This conversion process can lead to range uncertainties of up to 3% of the proton range, resulting in a possible under-dose to the tumour volume or an over-dose to the surrounding healthy tissue. While more accurate conversion methods have been proposed, a favorable

solution is to measure and reconstruct the proton RSP distribution directly. This is the primary goal of proton computed tomography (pCT).

What are we doing

We have started construction of a clinically usable pCT detector system for imaging head-size phantoms in a single gantry rotation of 3600. Irradiation times less than 6 minutes are required which in turn require high data acquisition (DAQ) rates for proton tracking and energy loss measurements. We have proposed to use scintillation fiber technology with sub-millimeter resolution to replace the Silicon strip tracking system that is presently being used in prototypes, for example one at Loma Linda University Medical Center (LLUMC) in California, USA. A new proton range detector with stacked scintillator plates will replace the segmented CsI calorimeter used to enhance data rate capability as shown in Figure 3. Second, develop image reconstruction software capable of reconstructing images of head phantoms in less than 10 minutes from approximately 108 proton histories recorded by the pCT detector.

Development of the proton computed tomography is multidisciplinary in nature and hence expertises of many fields are required. With the advances in accelerator physics it has become feasible nowadays to obtain high intensity proton beams for cancer therapy at relatively lower cost. The development of high resolution and precise detectors for the detection of fundamental particles has made it possible to develop the detector system for the proton tomography without much problem. Also, the use of software to simulate the detector and then to reconstruct the real image of the scan is humongous. Since this technology is finally going to be used by the radiation oncologists so their participation is also important. So we can say that in true sense this work is multidisciplinary in nature which includes mathematics, computer science, medical science, accelerator physics and high energy physics.

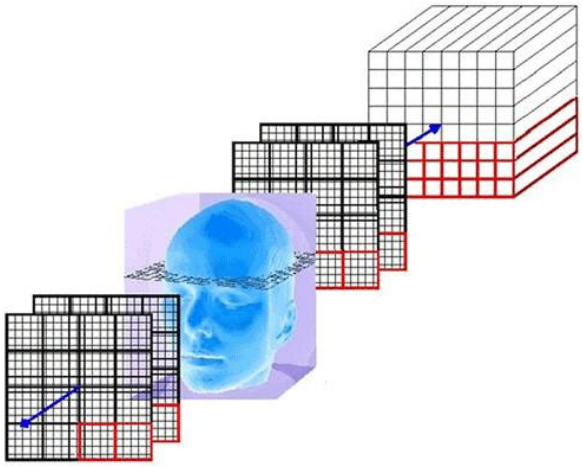

Figure 3: *Conceptual design of proton computed tomography system. Two 2D sensitive proton tracking modules are positioned pre- and post-patient. A segmented crystal calorimeter records residual energy.*

Conclusions

Proton therapy is becoming one of the most effective radiation therapy for cancer treatment. Because of the finite range of protons in matter, this treatment modality allows for a greater degree of conformality than the conventional x-ray therapy. But, in order to maximize the inherent advantages of proton therapy, the range of protons inside the patient must be able to be predicted with millimetre resolution. In current clinical practice, proton therapy treatment plans are made with pre treatment X-ray CT scans of the patient. The use of X-ray CT images for proton treatment planning ignores fundamental differences in physical interaction processes between photons and protons and is therefore inherently inaccurate. X-ray radiographs depict only skeletal structures; they do not show the tumour itself. In view of this, imaging the patient directly with proton CT by measuring the

energy loss of high-energy protons that traverse the patient is highly desirable.

Acknowledgement

Much of the introductory sections of this article has been adopted from Scott Nocholas Penfold Ph.D. Thesis, who worked on the development of second generation of pCT.

[1]. R.R. Wilson, "Radiological use of fast protons," Radiology, 47, 487−491 (1946).
[2]. A.M. Cormack, "Representation of a function by its line integrals, with some radiological applications," Journal of Applied Physics, 34, 2722−2727 (1963).
[3]. A.M. Cormack, "Representation of a function by its line integrals, with some radiological applications. II," Journal of Applied Physics, 35, 2908−2913 (1964).
[4]. A.M. Koehler, "Proton radiography," Science, 160, 303−304 (1968).
[5]. V.W. Steward and A.M. Koehler, "Proton beam radiography in tumor detection," Science, 179, 913−914 (1973).
[6]. M. Goitein, "Three-dimensional density reconstruction from a series of two-dimensional projections," Nuclear Instrumentation and Methods, 101, 509−518 (1972).
[7]. A.M. Cormack and A.M. Koehler, "Quantitative proton tomography: Preliminary experiments," Physics in Medicine and Biology, 4, 560−569 (1976).
[8]. K. M. Hanson, J.N. Bradbury, T.M. Cannon, R.L. Hutson, D.B. Laubacher, R. Macek, M.A. Paciotti, and C.A. Taylor, "The application of protons to computed tomography," IEEE Transactions on Nuclear Science, 25, 657−660 (1978).
[9]. K.M. Hanson, J.N. Bradbury, R.A. Koeppe, R.J. Macek, D.R. Machen, R. Morgado, M.A. Paciotti, S.A. Sandford, and V.W. Steward, "Proton computed tomography of human specimens," Physics in Medicine and Biology, 27, 25−36 (1982).
[10]. U. Schneider and E. Pedroni, "Proton radiography as a tool for quality control in proton therapy," Medical Physics, 22, 353−363 (1995).
[11]. P. Pemler, J. Besserer, J. de Boer, M. Dellert, C. Gahn, M. Moosburger, U. Schneider, E. Pedroni, and H. StÃ¤uble, "A detector system for proton radiography on the gantry of the Paul Scherrer Institute," Nuclear Instruments and Methods in Physics Research A, 432, 483−495 (1999).
[12]. U. Schneider, J. Besserer, P. Pemler, M. Dellert, M. Moosburger, E. Pedroni, and B. Kaser- Hotz, "First proton radiography of an animal patient," Medical Physics, 31, 1046−1051 (2004).
[13]. B. Schaffner and E. Pedroni, "The precision of proton range calculations in proton radiotherapy treatment planning: experimental verification of the relation between CT-HU and proton stopping power," Physics in Medicine and Biology, 43, 1579–1592 (1998).
[14]. L.A. Feldkamp, L.C. Davis, and J.W. Kress, "Practical cone-beam algorithm," Journal of the Optical Society of America A, 6, 612–619 (1984).

Muon and neutron induced background in low-level Gamma-ray spectrometry

*A. J. Khan**

Low-background γ spectrometry using high purity germanium (HPGe) detectors is an important tool for basic and applied projects involving γ-ray measurements and assessments. Low-background γ spectrometry has been originally driven by neutrino physics at deep underground research laboratories; however, emphasis has been given recently to environmental measurements. Latest reviews can be found in Refs. [1,2,3].The principal source of the background in γ spectrometry consists of the terrestrial γ radiation, which can be considerably reduced by passive shielding. However, highly penetrating cosmic-ray muons enters the passive shielding at ground-level locations and produce a characteristic continuum with the maximum around 200 keV and a pronounced annihilation peak in the γ-ray spectrum [4]. Cosmic-ray muons can only be rejected with the active shielding. Cosmic-ray muons are also subjected to muon capture in the Ge-detector crystal and lead shielding resulting in the formation of highly exciting nuclei which emit neutrons [5]. These neutrons either scatter inelastically or cause thermal capture as well as thermal and fast activation in Ge, Pb, and materials surrounding the detector, leading to many γ rays in the background [6,7]. Another source of background is radon and daughters [8]. Further background is caused by β-particle bremsstrahlung from the decay of ^{210}Pb/^{210}Bi present in the lead shielding [9]. Finally, background arises from radioactive impurities in the detector materials and shielding. One of the most detailed backgrounds in γ spectrometry was measured in Ref. [10]. Usually, a distinction is made between ultra-low background and low-background. Ultra-low background pertains to the systems located in deep underground locations, where muons and neutrons are either considerably reduced or absent, making active shields often unnecessary. The low-background systems are located at ground level or at shallow underground locations. In those systems, active shields are necessary. There are significant variations in the detector + shielding + location configurations. Although the physical principles of γ background are understood, it takes a considerable effort to construct a functional low-background γ spectrometer, frequently resulting in new information. At Wadsworth Center, Albany, NY, we have been performing low-background γ spectrometry for two decades, which often involved long-term planning and undergoing upgrades. The applied uses of γ spectrometry at Wadsworth Center involve monitoring of environment, food, air, water, surveillance of nuclear facilities, as well as health physics and homeland security applications. Low-background γ spectrometry is applicable to very low activity matrices, such as water or chemically separated samples. Specific projects include mandated analysis of $^{226,\ 228}$Ra in drinking water and monitoring of ^{134,137}Cs at nuclear facilities. We also actively participate in routine radiological exercises to be prepared for any nuclear emergency. In the present work we describe significant reduction of the γ-ray background at Wadsworth Center. It was achieved by muon rejection with plastic scintillators as well as by employing an ultra-pure shielding lead, outlined in the subsequent sections. Due to the exceptionally efficient muon rejection, some of the most intense peaks in the residual γ spectrum are those from the neutron interactions. Therefore, this work complements previous investigations on the cosmic-neutron interactions. Future planned upgrades are also described.

Experimental

We currently use a 132% efficient (2.584 kg) HPGe detector (Model GC13021 by Canberra Inc., Meriden, CT, USA) in an ultra-low background U-type cryostat configuration (Model 7915-30ULB by Canberra). The detector is inserted into a 3-layer lead shield. The original shield consisted of two layers: an outer 3"-thick layer made of Boliden grade lead (20 Bq kg^{-1} ^{210}Pb content) and an inner 3"-thick layer grade lead (< 3 Bq kg^{-1} ^{210}Pb, < 1 mBq kg^{-1} ^{40}K). This shield was custom designed by Canberra (Model 777S). We have recently added an Alpha-lo grade 2 cm-thick lead insert. This ultrapure lead has α flux of 7×10^{-4} cph cm^{-2} and 0.01 ppm of K impurity. Ge detector chamber is purged with the boil-off nitrogen from the Ge detector Dewar in order to remove radon and daughters. The lead shield is surrounded from the top and the sides by a 6-panel 2"-thick plastic scintillator muon shield (one side is split into two panels for cryostat insertion). The muon shield is made of BC-408 grade plastic scintillator. Each scintillator panel has two embedded hemispherical photomultiplier tubes which allowed for a compact and convenient configuration. The spectrometer is placed in a 6"-thick wall steel room made of pre-World War II steel, which is located under a 47-story building providing 33 m of water equivalent (mwe) shielding from cosmic rays in the vertical direction. However, since the laboratory is located at the ground level, it is much less shielded against cosmic rays streaming from the sides (Fig. 1). There are several known electronics setup methods for rejection of muons event-by-event [11]. In the preliminary tests described here we chose the signals from the plastic-scintillator photomultiplier tubes were matched using high-voltage bias. The signals were then mixed and the sum was preamplified, amplified, and discriminated. The resultant logical TTL gate of 50 μs duration was used to prompt veto the Digital Signal Processor (Model 9660 by Canberra) which processed the energy pulses from the Ge detector.

Results and discussion

The effect of Alpha-lo lead insert was investigated by measuring the total spectrometer background with and without the insert. In this measurement, muon shield was not used. A 12 % reduction of the background was observed with the insert. This appears to be a modest reduction. However, if it was measured with the muon shield on, it would be a major reduction in background (see below). Since the average environmental γ-ray energy is below 2 MeV and the average energy loss by the muon in the plastic scintillator is about 10 MeV, γ rays and muons are, in principle, well separated in the plastic scintillator by the pulse height. However, if the plastic scintillator is not shielded, there is a considerable counting rate from environmental γs in the scintillator resulting in blurred separation. Vetoing Ge detector in such case leads to a very high dead time and the muon shield is less effective in lowering the background. At Wadsworth Center location, plastic scintillators are shielded from much of the environmental radiation by positioning them inside the steel room. Therefore, the total plastic scintillator signal, without the need of γ/muon separation, can be used to veto Ge detector, and this is a key element in excellent rejection of cosmic-ray muons from the background (see below). We performed the measurements of γ intensity loss in the Ge spectrum due to scintillator vetoing, using common radioactive standards. We observed a 3.8 % loss of γ intensity at 60 keV, 2.3 % loss at 1173 keV, and a 4.3 % loss at 1332 keV. The background γ-ray energy spectra obtained under varied shielding configurations are depicted in Fig. 3. The spectrum inside the lead shield (second one from the bottom) is primarily from muons interacting with the Ge crystal and lead. It agrees very well with the spectrum calculated in Ref. [4]. By applying muon-shield veto, that

background is reduced by a factor of 17. Overall, we have achieved background reduction by a factor of 9436 relative to the ambient. Our integrated background rate in the γ energy range of 50-2700 keV was measured as 2.3 counts per min, corresponding to 15 counts ks^{-1} kg^{-1} Ge. This compares well with the IAEA MEL Monaco laboratory, which achieved the value of 10, the lowest among ground-level or shallow-underground located laboratories [12].The lowest background γ-ray spectrum from Fig. 3 is replotted in Fig. 4. The corresponding resolved γ peaks and they assignments are listed in Table 1. The most intense peaks are results of scattering, capture, and activation of Ge by neutrons from muon capture. Due to excellent muon-background reduction, this work offers one of the best measurements of cosmic-neutron interactions in Ge. Many of the Ge metastable states have life-times much longer than the duration of the veto gate (50μs) and, therefore cannot be rejected in the present configuration. However, several prompt peaks are also present, indicating that the electronic system is not fully optimized. There are many natural-radioactivity peaks, most likely from the materials used in the construction of the cryostat. The combined γ-peak intensity is 22 % of the total background intensity. Also a reasonably 511-keV peak is still present. One can conclude that still unrejected muons are recorded by the Ge detector. This offers some more room for further reduction of background.

Conclusions

We have constructed a low-background γ-ray spectroscopy facility. An excellent cosmic-ray muon background rejection has been achieved due to, in part, positioning of the plastic scintillators inside a shielded steel room. Therefore, this work offers one of the best measurements of muon and cosmic-neutron interactions in Ge. We have achieved background level which is among the lowest among ground-level laboratories. Additional advantages of our facility are easy access and a location in the vicinity of several large metropolitan population centers. They enhance our role as a reference laboratory and for emergency response. The γ-ray spectrometer at Wadsworth center, Albany, NY is currently undergoing further upgrade. It will consist of a new 130 % Ge detector in an XtRa configuration with a carbon composite window for detection of low-energy γ rays from bulk samples [3]. Ultrapure materials for cryostat construction will be used to reduce natural radioactivity component. Bottom plastic scintillator will be added to prevent muon leaks through the corners of the scintillation panels and to veto possible scattered muons. A cryogenic radon trap is being constructed to reduce radon and daughters background [8]. Additional measures will be attempted in to possibly further reduce the background by inserting low-Z fillers in the vicinity of the detector, and by electronic tuning.

References

1. M. Laubenstein, M. Hult, J. Gasparro, D. Arnold, S. Neumaier, G. Heusser, M. Köhler, P. Povinec, J.-L. Reyss, M. Schwaiger, P. Theodórsson, Appl. Radiat. Isot. 61 (2004) 167.
2. M. Hult, Metrologia 44 (2007) S87.
3. M. Köhler, D. Degering, M. Laubenstein, P. Quirin, M.-O. Lampert, M. Hult, D. Arnold, S. Neumaier, J.-L. Reyss, Appl. Radiat. Isot. 67 (2009) 736.
4. P. Vojtyla, Nucl. Instr. Meth. Phys. Res. B 100 (1995) 87.
5. S. Charalambus, Nucl. Phys. A 166 (1971) 145.
6. G. Heusser, Nucl. Instr. Meth. Phys. Res. A 369 (1996) 539.
7. J.-H. Chao, Appl. Radiat. Isot. 44 (1993) 605.
8. M. Wójcik, G. Zuzel, Nucl. Instr. Meth. Phys. Res. A 539 (2005) 427.

9. P. Vojtyla, Nucl. Instr. Meth. Phys. Res. B 117 (1996) 189.
10. P. Bossew, Appl. Radiat. Isot. 62 (2005) 635.
11. S. Hurtado, M. García-León, R. García-Tenorio, Appl. Radiat. Isot. 64 (2006) 1006.
12. P.P. Povinec, J.-F. Comanducci, I. Levy-Palomo, Appl. Radiat. Isot. 61 (2004) 85.

Dinosaurs versus Dark Matter

Syed Afsar Abbas

Not too long ago the Hollywood movie "Jurassic Park III" was running to packed houses all over the world. This was a sequel of the earlier movies the "Jurassic Park" and "The Lost World". The main reason for the popularity of these movies is the gigantic and ferocious creatures shown therein. These creatures are called dinosaurs. The movies were fictionalization of a hypothetical scientific technique of gene manipulation which brought these dinosaurs to life in the modern context.

In reality dinosaurs which could be as tall as a several stories high building, ruled the Earth for about 150 Million years. Note that in contrast the mankind at best is perhaps only about 1 Million years old. And let us not forget that already the mankind has created a situation that has the potential of destroying the whole world. Viewed this way, mankind should be perceived as the species that has failed the Universe and the extensive span of the dinosaurs species would attest to their having been highly successful creatures of the Universe.

As such the dinosaurs should have continued to dominate for much longer but then something happened and some 65 Million years ago the reign of the dinosaurs came to an almost abrupt end. That is to say that all the dinosaurs became extinct. Today one of the outstanding mysteries of science is what caused the extinction of the dinosaurs.

The extinction of dinosaurs is significant for the mankind in another way. Mankind never co-existed with the dinosaurs. While the dinosaurs were roaming the Earth as its supreme master, the species of mammals were just evolving. However the domination of the dinosaurs was such that it would not allow any other species, such as mammals to grow. So much so that only some primitive form of mammals such as rodent could survive and that too by scurrying into tiny holes while these gigantic creatures walked the Earth as they felt like. Recently it has also been becoming clear that some of the species of the dinosaurs were developing into intelligent animals. For example Velocitiraptor, the swift dinosaurs that one saw in the "Jurassic Park" were also highly intelligent. Had the dinosaurs not become extinct then the history of the Earth would have been quite different today. In that case, it may not be too bizarre to visualize that today an intelligent dinosaur would have been writing an article for the Physics Bulletin and other intelligent dinosaurs would have been reading it. It would be anyones guess as to how they would be looking like! Well, anyway, it was mainly due to the extinction of the dinosaurs that the mammals were allowed to proliferate, expand and evolve so that at some stage an intelligent Homo Sapiens species came into existence.

Now let us go to another mystery of the Universe. The famous science fiction novel, “The Invisible Man " by H G Wells starts with the arrival of a stranger in a quiet English village. He was wrapped up from head to foot. Bizarre incidents start occurring in the village. Ultimately the villagers broke into his room and demanded that he show his face. With laughter he unwound the bandages. Once the clothes were gone, there was nothing there. They could see right through him. Obviously there was a person there but that his body was invisible.

It is amazing that currently in astrophysics it is turning out that there is an analogous problem of the missing Universe. As sophisticated instruments have allowed us to peel off the 'bandages' of the universe we have become aware of the fact that much of the Universe is invisible. This means that just as in

the above story the body of the universe is there, but it cannot be detected directly by any instruments available to the scientists.

The first one to point out this was Fritz Zwicky of USA in the 1930's. But most of the scientists rejected this proposal.However further observations in the recent years have vindicated Zwicky. It is now generally accepted by scientists that the visible matter in the universe constitutes only a miniscule amount and that the bulk of 'all that is out there' in not visible to us. Amazingly almost 90 percent of matter in our own galaxy may be invisible. The matter which is invisible to us is called the 'Dark Matter' by the scientists. We have very little idea as to what it is. The situation is similar as to the existence and the identity of the invisible man.

The main evidence for the existence of Dark Matter comes from the gravitational pull of one object upon the other. We can determine its mass using simple physics. For example, the knowledge of the distance of moon from Earth and it's speed enables us to calculate the gravitational pull needed to keep its orbit. This is all that is needed to calculate the weight of the Earth. Similarly we can determine the weight of the sun by studying the Earth's motion around it.

We can use the same methodology to study our galaxy - the Milky Way. It consists of about 100,000,000,000 stars with our own sun being a typical star. The force of gravity holds these objects together. The Milky Way is known to rotate around its centre. By studying the rotational motion of stars lying in the outer periphery of the system we can obtain the total mass of the galaxy. But now one encounters a conundrum. One finds that the gravitational force needed to account for the observed velocities is about ten times larger than what would result from all the visible stars and all the gases alone. The same puzzling situation is found to exist in other galaxies also. Hence one is forced to conclude that there is a huge amount of matter which is not visible to us, the so called Dark Matter. Careful calculations reveal that surprisingly as much as ninety percent of the total matter in the universe is made up of the Dark Matter.

Note that there is another mystery of the Universe which we are not tackling here and that is that of the Dark Energy. This is quite different from Dark Matter. At present we believe that of all that is there in our Universe Dark Energy constitutes about seventy percent, Dark Matter twenty five percent and visible matter only five percent. However one should not confuse the numbers, locally as far as our own galaxy is concerned plus other galaxies, the data calls for ninety percent of Dark Matter constitution.

The only thing that we know about the Dark Matter is that it is out there and that it is the predominant form of matter in the universe. We know practically nothing else about it. One would definitely like to know the identity of this mysterious Dark Matter. The only way that one can identify an object unambiguously is to catch it. Hence all over the world a sort of race is on to catch a Dark Matter particle and some twenty detectors at present are active.

In trying to unravel the mystery of the Dark Matter, theoretically too there have been umpteen number of suggestions ranging from brilliant to bizarre (of course what is brilliant for one may be bizarre to another one) have been presented. The number of suggestions abound. One hears terms of the kind MACHOS, WIMPS, strangelets, rungions etc. It would be good if a Dark Matter particle is found through direct detection. However, one may ask if there are any indirect signatures of dark matter. This is the way that Samar Abbas and myself while at the Institute of Physics, Bhubaneswar had approached the problem in 1998. We found that amazingly this way we were able to explain the mystery of the extinction of dinosaurs.

Dark Matter is viewed as occupying a spherical halo surrounding the galaxy. The earth is constantly passing through the dark halo of the Milky Way. As it does so, it will gradually capture Dark Matter particles by elastic scattering, gravitational attraction and orbital capture. The rate at which the Earth shall accumulate Dark Matter can be worked out mathematically. This captured Dark Matter gradually drifts towards the centre of the earth. Here the number of Dark Matter particles continues to increase as this is the stablest least-energy configuration. Once a critical density is reached, however, the Dark Matter particles start to annihilate with one another. This leads to generation of huge amount of heat in the core of the Earth. This excess heat is 1000 - 100,000 times the current heat output of the earth. This heat is produced in the core of the Earth. What exactly would be the geological effects of such an event?

These large quantities of heat would gradually escape from the core, melting its way to the surface in the form of a superplumes. Geothermodynamic theory indicates that superplume formation is one of the most efficient methods by which the Earth's core can rapidly shed excess heat. In addition, the heat is likely to destablize the core, leading to geomagnetic reversals, which also display a positive correlation with volcanism. On the surface this would lead to explosive silicic volcanism, followed by large-scale basalt volcanism. These truly cataclysmic events lead to the formation of the massive flood basalt volcanic provinces such as the Deccan Traps of Central India which has been dated at 65 Million years ago.

Such enormous volcanic provinces were associated with significant atmospheric pollution. It is estimated that the Deccan Traps ejected more than 10 million cubic kilometres of basalt, 200 billion tonnes of hydrochloric acid, 1 trillion tonnes of sulphuric acid and 20,000 tonnes of fine dust. The environmental impact of such an event would be severely debilitating: the quantities of pollutants and dust belched into the atmosphere would be akin to a full-scale nuclear winter, leading to global climate deterioration.

Indeed, the resultant ecological catastrophe would involve the extinction of much life. And as per our suggestion this is exactly what happened 65 Million years ago to wipe out dinosaurs. Another popular suggestion for the extinction of the dinosaurs is due to an asteroid/meteor impact 65 Million years ago. And although an impact crater of similar age has been discovered in the Yucatan peninsula of Mexico, the Deccan flood basalt volcanic episode also coincides with this event. Much controversy surrounds the true cause of the catastrophe, but some investigators believe that the effects of the impact were limited to North America, while the Deccan flood basalt volcanoes were responsible for the extinction worldwide.

The significance of what we have discussed here lies in the fact that it connects two of the most puzzling and outstanding mysteries of modern science viz, the extinction of dinosaurs and the enigmatic Dark Matter of cosmology. Dark Matter was the cause that led to the extinction of dinosaurs. And as dinosaurs departure in a way opened the way for the arrival of mankind, we have reasons to be grateful to our mysterious friend, the Dark Matter.

The Story of Heat and Engines

W. Haider

It was earlier assumed that the relationship of energy and the consequent work done holds only if friction is absent or negligible. If frictional forces are present, work done in moving objects warms up the objects offering friction. As a result that much less work is available to increase the potential/kinetic energy of the objects. Thus it seems possible to modify the laws of conservation of mechanical energy to include the effect of frictional forces.

As an example consider the case of a book that has been given a push such that it slides on a horizontal table. If the surface is even slightly rough the book would stop moving after a while and its kinetic energy (K.E.) would disappear. Further as its Kinetic Energy disappears there is no increase in its potential energy. Thus it appears that the mechanical energy is not conserved. However a close examination reveals that as the moving book stops the book as well as the surface of the table are warmer than before. Thus the disappearance of kinetic energy of the book is accompanied by appearance of heat. This suggests that the kinetic energy of book was converted into heat and that heat is a form of energy just like Kinetic Energy or Potential Energy. That heat is a form of energy was gradually accepted by the middle of nineteenth century. In this small article I would try to bring out this story which was understood as a result of practical knowledge gained in developing the steam engine.

Two hundred years ago most work was done manually. During 1700 A.D. as mines were dug deeper in search of coal the problem of pumping water out from the flooded mines had to be solved. The steam engines were developed initially to solve this problem.

The steam engine is essentially a machine to convert energy of some kind of fuel (eg. Oil, coal, nuclear energy of uranium) into heat energy which is then used to do some mechanical work. Other devices have been constructed now but steam engine is still a good model to understand the process od energy conversion.

Since ancient times it has been known that heat can be used to produce steam which can be used to do mechanical work. The early toys (eg. Aeolipile by Heron at Alexandria in 100 A.D.) worked on Newton's third law enunciated much later. However this was only a toy and not until the late eighteenth century commercially useful steam engines were invented.

We now say that steam engines use heat energy to do mechanical work. However many inventers in the eighteenth and even nineteenth century thought of heat as some kind of thin liquid. Further steam engines were first developed by men more concerned with making money as well as effectiveness of safety of mines. It was later that the involvement of knowledgeable people with curiosity to understand the working of engines led to discoveries in physics.

The first commercial steam engine was invented by an englishman Thomas Savery (1650-1715) to pump water out of the deep coal mines. The serious drawback of the Savery's engine was the use of very high pressure steam which led to serious accidents. This defect was removed by another englishman Thomas Newcomen (1663-1729) and his engine could do other work also. However in both these engines several valves had to be manually closed and opened at proper times but later a method was invented to do this automatically

using the rhythm and some energy of moving parts of the engine to control various sequences of its operation. This idea is called the feedback.

The engine developed by Newcomen was widely used in U.K. and other European countries throughout the 1700's. It used large amount of coal to produce little work. However the engine was used due to the urgent demand of machines to pump out water from the mines.

James Watt and the Industrial Revolution

A much better steam engine was invented by James Watt whose father was a carpenter constructing equipment for ship builders. Due to poor health James Watt could not continue his education and worked at his father's shop. He went to London to learn instrument making trade. After getting some training he come back to Scotland in 1757 and was appointed as instrument maker at Glasgow University.

During the winter break of 176-64 Watt was given the job of repairing Newcomen's engine for demonstration purpose at the University Lectures. While doing this he learnt about the amount of steam required to run the engine. After doing several test runs he realized that the major problem in the wastage of energy was due to the temperature of cylinder walls. He realized that most of the heat energy was being used up in heating the cylinder which was cooled down again to condense the steam. He soon realized that this wastage of energy could be rectified. He modified the engine such that when the steam had done its work of pushing the piston up it was taken to a separate chamber to be condensed. This helped keep the cylinder hot and condenser cool all the time, thus avoiding the loss of steam energy in heating up the cylinder again and again.

It seems that Watt's invention of a separate condenser is a small step. However this small step was crucial in enhancing the efficiency of the engine by more than twice. By saving of fuel, James Watt was able to make a fortune by selling his engine to coal mine owners. The money charged by Watt was dependent on the power of the engine. Power is now defined as the rate of work and now appropriately called as Watt.

1 Watt = 1 Joule/sec.

As engine with a separate condenser by Watt, much superior to Newcomen's engine, led to its application for many kinds of jobs eg. running of machines in factories, railway engines, steam boats etc. It stimulated a big boost to the growth of industry in Europe and USA and a big economic and social transformation of Western civilization: Industrial Revolution. It resulted in raising the living standards of people. However, not all effects of industrialization were positive. The factory structure provided a large number of greedy employers to exploit workers. They made huge profits while keeping the workers and their families on the verge of starvation. The worst excesses had to be eliminated through reform in the early nineteenth century in England through new laws to reform the adhoc system.

Nowadays the steam engines are no longer widely used a source of power to run industry or transportation. However, steam is used still as a major source of power. The invention of steam turbine by Charles Parson in 1884 has replaced all older kinds of steam engines. They are also used at most electric power stations running the wheel of modern civilization. Even in nuclear reactors the nuclear fission energy is used to produce steam to drive turbines and electric generators.

The basic principle of Parsons Turbine is that a jet of high pressure steam hits the blades of a rotor, driving it at high speed.

The Joule's Experiment

The question disturbing to some people was "what happens to heat as it does work through a steam engine?"

The answer given by scientists in the early nineteenth century was that the amount of heat remains constant while it does work when it passes from a high temperature to a lower temperature. Heat was regarded as some thin substance called "Caloric", whose amount in Universe is conserved. It was thought that heat is like water which can be made to do some work as it falls from height. However, some intelligent people disagreed with this explanation and thought that heat is a form of energy. James Prescott Joule conducted a series of experiment in the 1840's to clearly show that heat is just another form of energy. Through verifiable experiments he showed that same expenditure of mechanical energy resulted in a fixed amount of heat energy where there was no heat.

In one experiment he used falling weight to drive an electric generator. The current generated was used to heat a wire immersed in water. The rise in temperature of water can be used to calculate the heat energy produced by falling weights. In another experiment he compressed a given volume of gas in a bottle immersed in water. One can easily calculate amount of work spent to compress the gas and the heat produced by noting down the rise in temperature of water. However, the most famous experiment even now done in laboratories was using the potential energies of falling weights to turn paddles in a container of water. The friction between the paddles and water creates heat to raise the temperature of water.

The results of his experiment published in 1849 are:

1. The amount of heat produced is always proportional to the amount of mechanical energy spent.
2. The amount of heat required by 1 pound of water to raise its temperature by 1˚ F was created by a fall of 772 lb of weight by 1 foot.

The first result shows that heat is a form of energy while the second result gives the exact relationship between a unit of mechanical energy and heat energy. In the MKS system we express this by saying the unit of heat; a Kilocalorie equals 4184 Joules of mechanical energy.

The mechanical equivalent of heat makes it possible to define heat engines in terms of efficiency. Efficiency is defined as the fraction/percentage of input energy appearing as useful output work. The law of conservation of energy implies that the best engine would be 100% efficient, i.e., when all the heat energy is converted into work. However, it turns out that there are theoretical limits on efficiency.

An elementary note on the nuclear forces

B. P. Singh and R. Prasad*

In the year 1911, Rutherford established that every atom has a nucleus at its centre. Later on it was well established that the atomic nucleus consists of neutrons and protons. The nucleus of the atom X is denoted as ${}_{Z}X^{A}$, where A is called the atomic mass number (total number of nucleons), Z the atomic number (number of protons) and (A- Z) = N, is the number of neutrons in the nucleus. Some of the important facts about stable nuclides are;

1. There are about 300 stable nuclides and many more unstable (radioactive) nuclides.
2. All the positive charge and more than 99.9% mass of the atom is contained inside the nucleus of the atom.
3. Most of the nuclides are spherical in shape.
4. A few nuclei are non spherical in shape and are called deformed nuclei. The deformation from spherical shape, which is either prolate (cigar like) or oblate (disc like) is measured in terms of the quadrupole moment Q, which has positive value for the former and the negative value for the later.
5. All the nuclides behave like a spinning top. A quantum number S or J is assigned to the nucleus to represent its spin. For some nuclei it may be zero.
6. Many nuclei behave like a tiny bar magnet. Magnetic dipole moment μ is associated with a nucleus to represent this behaviour.
7. The largest number (≈165) of stable nuclides is of those which have even Z and even N; even-odd (65) or odd-even (60) are next in abundance. Odd-odd stable nuclides are only a few (4).
8. Nuclei having N and/or Z equal to 2, 8, 20, 28, 80 and 126 show special stability. They are either very strongly bound or have many stable isotopes. These nuclides are called magic nuclei and their corresponding nucleon number as magic number.
9. Mirror nuclei (nuclei having same A but interchanged values of N and Z like ${}_{1}H^{3}$ & ${}_{2}He^{3}$;etc.) show similarities in their nuclear structure.

In a nucleus the nucleons are held together in a small volume of, generally, spherical shape (radius $\approx 10^{-12}$ cm or 10 fm) by means of strongly attractive forces called nuclear forces. The nuclear forces are very strong comes from the fact that protons which are positively charged are held together inside the nucleus (by the attractive nuclear forces) overcoming the large repulsive Coulomb forces.

First indication about the existence of nuclear forces was obtained from the hyperfine structure in the atomic spectra. Further evidence about the presence of strongly attractive nuclear forces was gathered from the anomalous scattering of high energy alpha particles by atomic nuclei. Since, the target nuclei and the incident alpha particles are both positively charged, a beam of high energy alpha particles undergo Coulomb scattering (also called Rutherford scattering). Since, Coulomb force is well known the scattering cross-sections for Rutherford scattering can be easily calculated for all values of impact parameters. Experimentally, it has been observed that the measured scattering cross-sections for small impact parameters deviate by a large amount from the values calculated assuming Coulomb interaction. This happens because the nucleons inside the incident α-particle start feeling the presence of the nuclear field of the target nucleus at small impact parameters (i.e., when they pass through closer distance to the target nucleus).

As is well known there are FOUR basic forces or interactions in nature viz., Strong

nuclear, Weak nuclear, Electromagnetic and Gravitational. Just to give a feel of the relative strengths of various interactions they are compared below in TABLE 1. According to the modern theories, every field/interaction is brought about by the quanta of field, which mediates the interaction. The mediating quanta for each interaction are also indicated in this table. Photon, the quanta of electromagnetic field, W-boson the quanta for weak interaction and π-meson the quanta of strong nuclear field have already been discovered. Search for graviton, the assumed quanta of gravitational field is still on. Each of these fields has a specific range. The range of gravitational and electromagnetic fields is infinite. However, the range of strong and weak fields is very small typically of the orders of a few Fermi.

TABLE 1		
Interaction	Strength	Quanta
Strong	1	π-meson
Electromagnetic	10^{-2}	Photon
Weak (beta decay)	10^{-12}	W-boson
Gravitational	10^{-39}	Graviton

In order to appreciate the strength of nuclear forces, let us look at the size of the nucleus. As a matter of fact every nucleus has a distribution of positive charge inside it. Experiments carried out by Hofstadter have revealed that the charge density of the positive charge inside the nucleus varies from the centre of the nucleus as shown in Fig.1. The distance from the centre at which the charge density falls to half of the central value is generally defined as the nuclear charge radius or simply the nuclear radius R. In general, the radii of all stable nuclides have been found to be of the order of Fermi (10^{-15} m). The fact that nucleons are bound in such a small volume indicates that forces responsible for holding the nucleons together are really very strong.

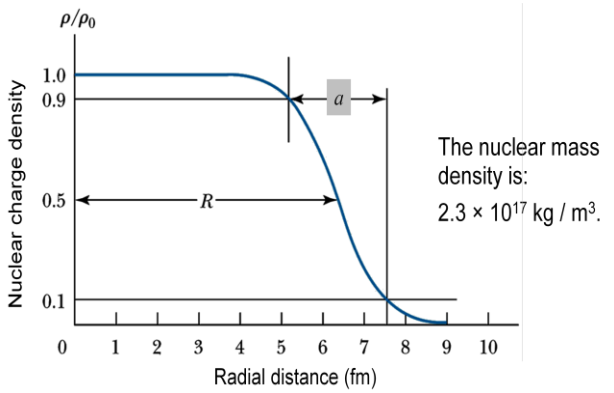

Fig.1: *A typical nuclear charge density distribution as a function of distance from the centre of a nucleus.*

For stable nuclei it has been experimentally found that the radius R of a nucleus having A number of nucleons is related to the atomic mass number A by the relation;

$$R = r_0 A^{1/3}$$

Where, r_0 is a constant. As such, the volume V of a nucleus of A nucleons, assuming it to be spherical is;

$$V = \frac{4}{3}\pi R^3 = \frac{4}{3}\pi r_o^3 A = K A.$$

Here, K is a constant. Further, the mass M of a nucleus having A nucleons is proportional to the number of nucleons A, i.e.,

$$M = K_1 A$$

Here, K_1 being another constant.

From the above two equations one can observe that the density ρ $(M/V = K_1/K =$ constant) of the nucleus is constant. The fact that the density of nuclear matter is constant is reflected in another important property of nuclear forces called the saturation property, and will be discussed later.

What holds the nucleus together?

In the past quarter century physicists have devoted a huge amount of experimentation and mental labour to this problem – probably more man-hours than have been given to any other scientific question in the history of mankind.

----- Hans A. Bethe

Another measure of the strength of the nuclear force is the binding energy with which the constituent particles are held together. Nuclear forces are very strong. This is also evident from the large binding energy of nucleons inside the nuclei i.e., ≈*8 MeV* per nucleon. For comparison, the average binding energy of electrons in the atoms is ≈*eV* to *keV* only. Moreover, there is a very big difference between the binding of nucleons in a nucleus and the binding of electrons in an atom. In an atom the positively charged nucleus at the centre provides the Coulomb field which extends up to infinity with decreasing strength. Negatively charged electrons in an atom are held by this central Coulomb field at different distances from the centre. As such, the valence electrons which are farthest from the centre are held with smaller binding energy (~eV), while inner electrons have binding energies ≈few keV. In the case of nucleus, there is no central force. The nucleons inside the nucleus interact with each other through strong nuclear force and this mutual interaction provides the binding. Later, it will be shown that the range of nuclear force i.e., the distance up to which they affect the other nucleons is very small, only a few Fermi (≈$2x10^{-15}$ *m*). As such, it is evident that the nature and strength of nuclear forces are very much different from the Coulomb force.

Another classical force is Gravitational force. Gravitational force also has infinite range. The attractive force that binds the progressively growing galaxy together is the gravitational force. It is the force that not only holds us to the Earth but also reaches out across the vastness of intergalactic space. The binding energy due to gravitational force between two nucleons at a distance ≈$2x10^{-15}$ *m* inside the nucleus is only ≈ 10^{-37} *MeV*. From the above, it is clear that nuclear forces which are non-central having short range and provides very strong binding to the nucleons are entirely different from the infinite range central classical forces that can provide very weak binding. It may therefore be concluded that classical forces are not adequate to explain the strong binding of nucleons inside the nucleus.

Further, we know from our undergraduate classes that, in order to confine a nucleon within a nucleus of the radius of a few Fermi, its de-Broglie wavelength must be correspondingly small. The de-Broglie wavelength λ is related to the momentum p (= mv) of the particle by the relation:

$$\lambda = \frac{h}{p} = \frac{h}{mv}$$

But the kinetic energy $E = p^2/(2m)$

So, its kinetic energy must be around;

$$p^2/(2m) = h^2/(2m\lambda^2)$$

If one calculates this value of kinetic energy, taking λ equal to the radius of the nucleus and '*m*' equal to the mass of the nucleon (~10^{-27} *Kg*), it comes out to be ≈20 MeV or so. It means that a nucleon inside the nucleus must be moving with a kinetic energy ≈*20 MeV* or more. In order to confine this high kinetic energy nucleon inside the nucleus, the nuclear force must provide a potential well. The depth of this potential well must be equal or larger than the sum of the kinetic energy (≈20 MeV) and the binding energy (≈8 MeV) Therefore, to confine a nucleon of this much

energy, it requires a large average potential well of depth ≈30 MeV.

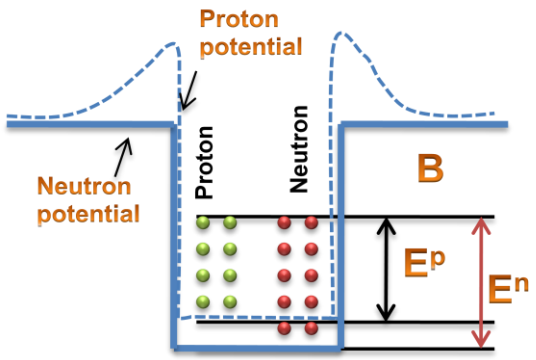

Fig.2: *A typical nuclear potential well for a depth ≈ 30 MeV*

It is now well established that both proton and neutron are not point particles and consist of charge distributions. The typical charge density distributions of proton and neutron are shown in Fig.3.

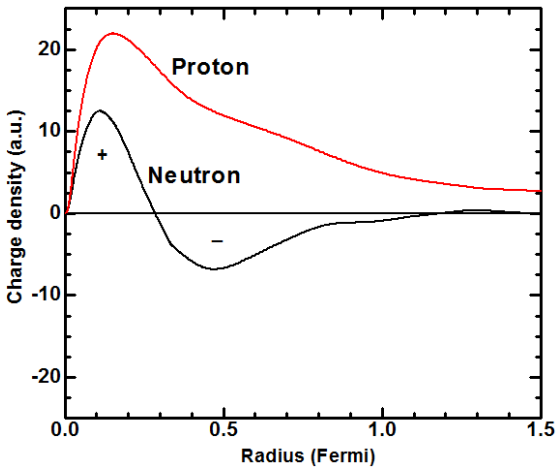

Fig.3: *Charge density distributions of nucleons*

It may be observed that a neutron, though overall electrically neutral, has a positive charge distribution around its centre and a distribution of negative charge towards the surface. However, the total amounts of positive and negative charges inside the neutron are equal. As such, for an external observer the neutron appears electrically neutral. Although, spin is an abstract quantum mechanical concept but for simplicity it may be assumed that both the neutrons and protons undergo spin motion around their axis giving rise to the spin of ½ħ. Spinning positive and negative charges give rise to current elements in nucleon, which in turn may generate intrinsic magnetic dipole moment. The intrinsic magnetic moment of the proton μ_p, is taken as positive, while the intrinsic magnetic moment μ_n of the neutron is negative because of the negative charge towards its surface (see Fig.3). Nucleons inside the nucleus may interact with each other through their intrinsic magnetic moments. The magnetic potential energy due to intrinsic magnetic moments μ_n and μ_p of neutrons and protons is $\approx \mu_n \times \mu_p / r^3$. At the separation $r \approx 2x10^{-13}$ cm, this value comes out to be $\approx 0.03MeV$. The sign of the magnetic force i.e., whether it is attractive or repulsive will depend on the relative orientation of the spins of neutron and proton. It will be of opposite sign for parallel and of negative sign for anti-parallel spins. However, experiments have indicated that nuclear forces are attractive for both the parallel as well as anti-parallel spin orientations. Hence, the nuclear forces cannot be solely of the magnetic origin. We may, therefore, conclude that the electrostatic (Coulomb), gravitational and magnetic forces are qualitatively and quantitatively inadequate to act as anything more than very minor perturbations on the specifically strong nuclear forces.

Some of the important properties of nuclear forces studied on the basis of various observations and empirical facts are; (a) short range (b) state or spin dependence (c) charge symmetry & charge independence (d) saturation (e) tensor nature (f) many body forces etc. In the following an attempt has been made to explain these properties in terms of simple explanations and analogies.

As has already been indicated, that nucleons inside the nucleus are in constant motion having large kinetic energies. Nucleons, similar to the electrons in the atom, move in definite orbits having different values of relative

orbital angular momentum ℓ. Apart from that nucleons also have intrinsic angular momentum called spin S ($=^1/_2\,\hbar$). The total angular momentum of a system of two nucleons having relative orbital angular momentum ℓ is given by the quantum mechanical sum $\ell \pm s_1 \pm s_2$. In the ℓ =0 state (called the *S*-state) the total angular momentum of a two-body system may be zero (singlet state, anti-parallel spins) or 1 (triplet state, parallel spins). The Pauli's exclusion principle does not allow *di*-proton or *di*-neutron as stable systems. However, a neutron and a proton do make a stable system ${}_1H^2$, called deuteron. The binding energy of the deuteron is about 2.2 MeV.

Spin dependence of nuclear forces may be explained with the help of example of the simplest bound system, the deuteron. Experimentally, it is known that spin quantum number of deuteron *J=1*. Now;
$J= \ell$ *(relative motion)* $\pm s_n \pm s_p$
(Quantum mechanical sum)

If we assume that in its ground state deuteron has ℓ =0 or in s-state. The values of intrinsic spins s_n and s_p each are equal to ½. Therefore;
$J= 0 \pm 1/2 \pm 1/2$
J=0 (singlet state) or 1 (triplet state)
J=0 may be obtained if we assume the spins of neutron and proton inside a deuteron to be anti-parallel, while *J=1* is obtained if we assume spins to be parallel.

Had the nuclear forces been spin independent, then the possibility of finding deuteron with *J=1* and *J=0* should have been equal. However, experimentally *J=0* (bound state) of deuteron is not found. This indicates that somehow, nuclear forces prefer parallel spins rather than anti-parallel spins (in s-state) or in other words, nuclear forces are stronger when the spins are parallel. An analogous classical force occurs between two bar magnets as shown in Fig.5.

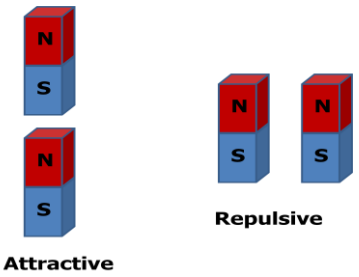

Fig.5: *A typical classical analogue of the spin dependence of forces.*

In 1939, it was found that the deuteron has a finite non-zero quadrupole moment with a value of *Q=0.003* barns. This value of quadrupole moment (QM) indicates that deuteron is not a spherical structure. The positive value of QM indicates prolate deformation with spin axis being the symmetry axis. It indicates that deuteron looks like (Fig.6) the picture on the left than on the right.

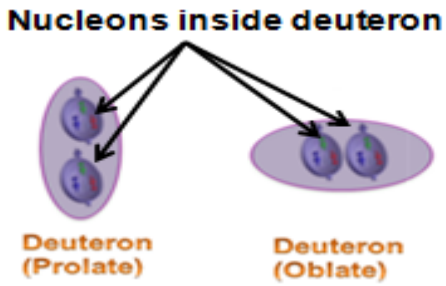

Fig.6: *Parallel spins of neutron and proton indicated in two different orientations.*

It means that probability of finding a neutron and a proton side by side is less than the probability of finding them on top of each other. Positive QM of the deuteron indicates that there is a part of the nuclear force which depends on the spin and spatial position of the nucleons at the same time. In other words, it means that force between a neutron and a proton in deuteron also depends on the angle between spin orientations and the radius vector. (See figure below). This part of the nuclear force is called tensor force.

$F_{np}=f(\theta_1,\theta_2);$

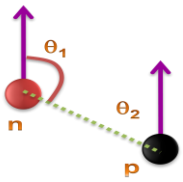

Experimentally, it has been found that the J of deuteron is 1 and it has even parity. Using the quantum mechanical expression for the addition of angular momentum;

$J = \ell \pm s_n \pm s_p$.

To obtain the value of $J=1$, the possible options are *(i) the* $\ell = 0$ and the spins are parallel *(b)* $\ell = 1$ and parallel spins *(iii)* $\ell = 1$ and anti-parallel spins and *(iv)* $\ell = 2$ and parallel spins. Further, the parity of a system depends on the value of the orbital angular momentum ℓ through the following relation;

Parity $\pi = (-1)^{\ell}$.

The positive parity *(+1)* for deuteron may be obtained for two different values of ℓ*(=0* and *2).* So the deuteron may not be a pure *s*-state or in other words the deuteron may be a mixture of various ℓ-states including ℓ=o. Since, parity of deuteron is positive, so the possible ℓ values which may yield the experimental value of $J=1$, may be *0 and 2.*

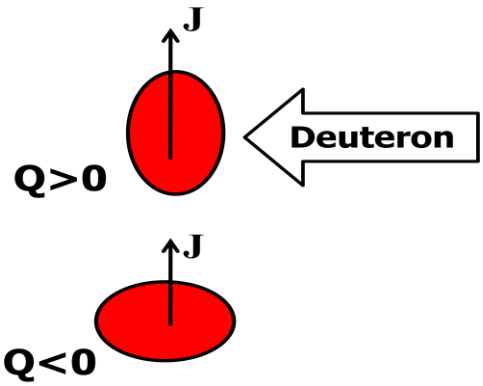

Fig.7: *Prolate and oblate nuclei, with spins pointing in the z-direction. The nuclei are assumed to be axially symmetric; z is the symmetry axis.*

Thus, observed value of $J=1$ for deuteron may be obtained with two possible values of ℓ=0 (*s-state*) and $\ell=2$ *(d-state*). The nuclear force which can mix different ℓ-states is called the tensor force. The first evidence of the non central nature or the tensor nature of nuclear forces came from the experimental information of the quadrupole moment of deuteron. The tensor force in the deuteron is attractive in the cigar shaped configuration and repulsive in the disc shaped one. As has already been said the deuteron in ground state is not a pure s-state but is a mixture of s-state and d-state. Calculations have shown that, when about *96%* of the *s*-state is taken along with about *4%* of the *d*-state, it reproduces the correct value of the quadrupole moment *Q*, as well as the magnetic moment μ for the deuterons. It may however, be pointed out that the role of tensor forces in nuclei is still a somewhat open problem. It certainly plays an important role at large inter particle distance.

The most elementary force is a two body force. For simplicity let us assume that the nuclear forces are two body forces between the pairs of nucleons. These forces may be of three types (i) *Fpp* (ii) *Fpn* and (iii) *Fnn*, respectively between pairs of protons, between proton & neutron and between the pairs of neutrons. These nuclear forces do not include the gravitational force and Coulomb force between nucleons. As has already been pointed out the strong nuclear force F_{pp} between two protons (*p-p*) represents the attractive force between two protons and does not include their purely classical Coulomb force $F_{pp}(Coul)$. Moreover, $F_{pp}\ (Nucl) >> F_{pp}(Coul)$. This follows from the fact that protons (charge density) inside nuclei are uniformly distributed throughout the nuclear volume. This is possible only if *Fpp (Nucl)* is much stronger than *Fpp (Coul)*, otherwise the protons would have been concentrated at the surface of the nuclei.

The nuclear forces *Fpp*, *Fpn* and *Fnn* are all, basically, attractive. Existence of neutrons

and protons in a bound state (in the form of nuclei) is itself an evidence of this. Further, these nuclear forces have short range. If it were not so, all the nucleons in different nuclei will coalesce into one big nucleus and everything will probably turn into a huge nucleus like a super-neutron star, and there will be not be a variety of elements that are found in nature.

The charge symmetry of nuclear force means that *Fpp = Fnn*, while charge independence means that *Fpp= Fnn= Fpn*. These properties of nuclear forces are derived from the binding energies and the structure of excited states of mirror nuclei. As an example let us consider the mirror pair ${}_1H^3$ and ${}_2He^3$. The binding energy for nucleus ${}_1H^3$ which has one proton and two neutrons will come from *2*-pairs of *Fpn* and one *Fnn*. Similarly, the binding energy of ${}_2He^3$ (two protons and one neutron) will come from *2*-pairs of *Fpn* and one pair of *Fpp* minus the Coulomb energy of the repulsion of two protons. Since, the number of *pn* pairs in the two nuclei is equal, any difference in their binding energies will arise due to the difference in the values of binding provided by *Fnn* and *Fpp* and Coulomb energy of the excess proton in ${}_2He^3$. Experimentally determined difference in the binding energy of the two nuclides is *0.76 MeV*, which is just equal to the Coulomb energy of the excess proton in ${}_2He^3$. It means that, *Fpp* is equal to *Fnn*. Detailed studies of the energy spectra of mirror nuclei shows that *Fnn=Fpp=Fpn*, proving the charge independence of two body nuclear forces. The fact that $F_{pp} \approx F_{nn}$ is also indicated by the fact that the pairing energy for protons and for neutrons is almost same.

A look at the chart of stable nuclides shows that light stable nuclides prefer to have equal number of neutrons and protons. However in heavy nuclides the number of neutrons N is always more than the number *Z* of the protons. Looking to the neutron excess *(N-Z)* in nuclides, it may be pointed out that only light nuclei tend to have equal number of neutrons and protons i.e., *N=Z*. However, as *Z* increases the disruptive forces due to Coulomb repulsion would prohibit the formation of stable nuclides, if some extra attractive forces were not brought into nuclear structure. These extra attractive forces are provided by neutrons whose number *N* exceeds *Z*, i.e., *N>Z*, by a larger and larger amount, if *Z* increases further.

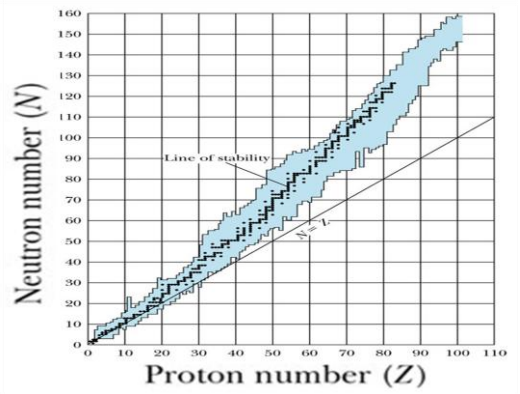

Fig.8: *A typical representation of neutron number verses proton number in the stable nuclides.*

In Fig.8, a plot of neutron number *N, vs* proton number *Z*, for stable nuclides is shown. The deviations from the *N=Z* line indicates the neutron excess i.e., *(N-Z).* In Fig.9, this neutron excess *(N-Z)* is plotted as a function of atomic mass number '*A'*.

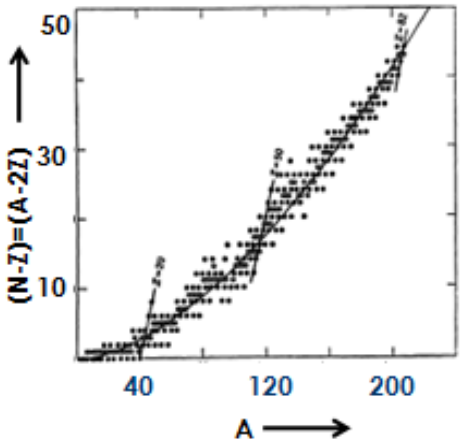

Fig.9: *The excess neutron number (N-Z) as a function of mass number A for the stable nuclides (Fig. from R.D. Evans).*

As can be seen from Fig.9, a good fit to the *(N-Z)* plot is obtained from a simple relationship *(N-Z)* ≈ *Constant x* $A^{5/3}$. This equation is of interest here, because it contains important information about the nuclear forces. To understand this, let us consider the Coulomb disruptive energy E_c of a charge '*Ze*' distributed throughout a volume of radius *R*. It is proportional to $(Ze)^2/R$. Further, it has already been shown that the radius of the nucleus $R \alpha A^{1/3}$. As such E_c becomes proportional to $(Ze)^2/A^{1/3}$. To a first approximation, it may be assumed that *Z* is proportional atomic mass number *A* or Z α *A*. Coulomb repulsive energy E_c would then be proportional to $\approx A^2/A^{1/3} \approx A^{5/3}$. From the forgoing discussion, it follows that the major role of the neutrons excess *(N-Z)* is to neutralise the Coulomb repulsive energy, which also varies with *A* in the same fashion as the neutron excess *(N-Z).*

Another important property of nuclear forces is saturation that leads to the exchange forces. To understand this, let us consider a nucleus having *A* nucleons. If each nucleon exerts the same attractive force on all other nucleons then there would be *A(A-1)/2* attractive bonds. If so, for *A*>>1, the binding energy would increase as $\approx A^2$.

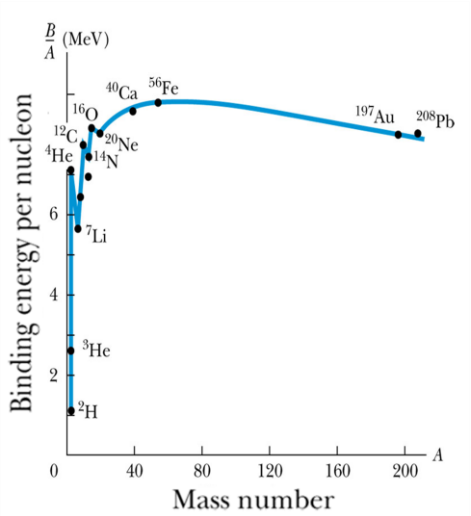

Fig.10: *A typical binding energy per nucleon curve as a function of atomic mass number.*

Experimentally, this square law is not followed. Experimental binding energy per nucleon is shown in *Fig. 10*. As may be observed from this figure, leaving the region of very light nuclei, the average binding energy per nucleon is nearly constant. It means that the total binding energy of the nucleus is, therefore, proportional to *A* and not to A^2. The approximate constancy of *B/A* over most of the range of the mass region is indicative of the saturation property of the nuclear forces. It means that inside the nucleus each nucleon attracts only a few nucleons around it and not all the other nucleons in the nucleus.

This is analogous to the chemical binding energy, between the atoms in a liquid, which is known to be proportional to the total number of atoms. For example, in a drop of water there is a strong homo-polar binding between individual pairs of hydrogen atoms with the formation of H_2 molecule. A third hydrogen atom is not nearly so strongly attracted and hence the H_2 molecule is said to be saturated. The total binding energy of a drop of liquid is approximately equal to the combined energies of the individual pairs of hydrogen atoms i.e., proportional to the total number of atoms present. The successful mathematical representation of the homo-polar bonding is obtained using the concept of exchange forces, which physically corresponds to a continued process of exchanging the electrons of one atom with the other atom in the molecule. The concept of exchange forces has been adopted in nuclear physics principally because such methods are known to give saturation.

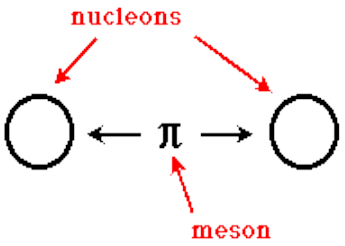

Fig.11: *A typical representation of exchange of π-meson between nucleons.*

The particle which is exchanged between two nucleons is π–meson or pion. A typical representation of this exchange is shown in Fig.11. Symbolically, the exchange force between a proton and a neutron can be described as;

$p + n \rightarrow (n' + \pi^{+}) + n \rightarrow n' + (\pi^{+} + p) \rightarrow n' + p'$

Here, the initial proton has become a neutron by losing a positive pion, which then joins the original neutron and converts it into proton. The original protons and neutrons have now changed their coordinates. Positive, negative and neutral pions are involved in the exchange process according to;

$n + p \rightarrow (p' + \pi^{-}) + p \rightarrow p' + (\pi^{-} + n) \rightarrow p' + n'$

$n + n \rightarrow (n' + \pi^{o}) + n \rightarrow n' + (\pi^{0} + n) \rightarrow n' + n'$

$p + p \rightarrow (p' + \pi^{o}) + p \rightarrow p' + (\pi^{0} + p) \rightarrow p' + p'$

The exchange character of nuclear forces is a purely quantum feature. Two nucleons, when interacting with each other, can exchange their position, spin, and iso-spin, or a combination of these. There are basically three types of exchange forces which have been studied extensively. These are briefly described below;

Heisenberg forces: These forces brings about the exchange of both the position and spin coordinate of two interacting nucleons. The Heisenberg forces are attractive for triplet interaction while repulsive for singlet interaction. The total nuclear forces can not be of Heisenberg type, as the most stable system is alpha particle (binding energy ≈ 28.3 MeV) not the deuteron (binding energy ≈2.2 MeV). Therefore, all the nucleons inside an alpha particle should have same spin orientations, but it is not so.

Majorana forces: These are the forces in which there is exchange of position coordinates but not of spin. These can be visualised physically in terms of exchange of π-mesons. These are attractive for relative angular momentum $\ell = 0, 2, 4...$ while repulsive for odd relative angular momentum.

Bartlett Forces: In these forces there is exchange of spin coordinates.

Thus, using the concept of exchange forces saturation of nuclear forces has been achieved.

Although, the assumed two body forces to describe strong nuclear interaction have been able to explain some basic properties of nuclei, particularly the low lying states, binding energies, spins etc., of light nuclei but they are not adequate to explain the properties and structure of heavier nuclei. It is not unexpected also, as two body force is the most elementary force, which may hold in a system of few nucleons. A real nucleus is a many body system and it appears that more complicated force that may describe the simultaneous interactions between many particles is required. From the point of view of calculations it will be extremely involved to solve such simultaneous equations. Recently, some attempts have been made to invoke three body forces to reproduce the properties of ${}_1H^3$ nucleus.

Researches during the last two decades have indicated that both neutrons and protons are not so much elementary as had been thought. Nucleons are themselves made up of some more elementary particles called Quarks. As a matter of fact it is now established that not only nucleons but all other nuclear particles like π-mesons etc., are made up of different types of quarks. These quarks are very strongly bound in the nucleons and may be released from the nucleons only at very high energy interactions.

TABLE 2		
Quark structure of some particles		
S.No.	*Particles*	*Quark structure*
1.	*Proton*	uud
2.	*Neutron*	udd
3.	$\pi+$	$u\bar{d}$
4.	$\pi 0$	$u\bar{u}$
5.	$\pi-$	$d\bar{u}$

Availability of high energy and heavy-ion accelerators have given a big boost to the research in this direction. Quarks have non-integer charge. There are several types of quarks specified by their quantum numbers denoted by ‘up’; ’down,; ‘colour’, ‘charm’ etc. In table 2, quark structure of some particles is given. The quark field is assumed to be mediated by gluons, the quanta of the field.

Unified View of Physics

Abbas Ali

ABSTRACT

Twentieth century saw the coming of age and maturing of Physics just as nineteenth century saw maturing of Chemistry. What was, by the end of twentieth century, the current view of Physics? In the beginning of twentieth century it was realized that there are four different types of fundamental forces and interactions, namely, gravitational, electromagnetic, weak and strong nuclear interactions. By the end of twentieth century the last three were nearly effectively described by unified theories, called the GUTs or grand unified theories. Of course some problems still remain there but these are not so serious. Then there are proposals for giving a unified description of all four fundamental interactions. An overview of this saga is the subject matter of this article. The description is at popular level but some physics background is still required.

Key Words: *Fundamental Force, Gravitational, Weak, Strong, Electromagnetic Interactions, Special and General Theories of Relativity, Quantum Mechanics, Quantum Field Theory, Quantum Electrodynamics, Quantum Chromodynamics,Glashow-Salam-Weinbeg Model, Grand Unified Theories, Supersymmetry, Supergravity, Superstring Theory.*

The Physics You Already Know

Dear Students,

Today I shall make a long scientific journey with you. It is part of the occupation of a scientist to explain his findings to the public. It is not easy. And it is not going to be easy even if the audience is scientifically literate like the gathering today. Ideally the organization of the material should be such that expertize of the audience disappears in the middle of the lecture. Since I would like to present the very best to my younger brothers and sisters I shall not aim for that ideal. Your expertize should disappear much before the middle of my talk. I hope you can hang on to my presentation till the end and I urge you to strive for that. On my part I shall endeavour my best to make the things easy. We shall begin with electricity and magnetism. Gauss' law for electrostatics, corresponding law for magnetism, Faraday's law of electromagnetic induction and the Ampere's circuital law give you four mathematical equations of electricity and magnetism. You either have studied them or you shall encounter them in your graduate course which has any emphasis on Physics. These equations are written in the integral form to begin with and then we write them in differential form for the rest of the time.

These are as follows:

(i) Gauss' law for electrostatics

$$\nabla \cdot \mathbf{E} = \frac{\rho}{\varepsilon_0}, \tag{1}$$

(ii) Gauss' law for magnetostatics

$$\nabla \cdot \mathbf{B} = 0, \tag{2}$$

(iii) Faraday's Law for electromagnetic Induction

$$\nabla \times \mathbf{E} = -\frac{\partial \mathbf{B}}{\partial t} \tag{3}$$

(iv) Ampere's law

$$\nabla \times \mathbf{B} = \mu_0 \mathbf{J} \tag{4}$$

Here Faraday's law says that changing magnetic field gives electric field. In Ampere's law we get magnetic field from electricity. Here we already get a hint of the type of things we are going to encounter - for general public electricity is different and magnetism is

different. For us they are very closely related to each other.

Maxwell's Electromagnetic Theory

Maxwell modified these equations to the following form:

$$\nabla \cdot \mathbf{E} = \frac{\rho}{\varepsilon_0}, \quad (5)$$

$$\nabla \cdot \mathbf{B} = 0, \quad (6)$$

$$\nabla \times \mathbf{E} = -\frac{\partial \mathbf{B}}{\partial t} \quad (7)$$

$$\nabla \times \mathbf{B} = \mu_0 \mathbf{J} + \mu_0 \varepsilon_0 \frac{\partial \mathbf{E}}{\partial t}. \quad (8)$$

How do they differ from the earlier form? As you see these differ from earlier equations only in the last term in the last equation - that is all. Now these are called Maxwell's equations. None of them is from Maxwell but we still use his name because of his introduction of a term in the Ampere's circuital law. The new term added by Maxwell is called the displacement current. This has the important implication. As a result of this addition we realize that changing electric field will give magnetic field. This can happen even in vacuum. Thus in vacuum a changing electric field will give magnetic field and a changing magnetic field will give electric field and so on. Thus they will sustain each other. We call such a situation an electromagnetic waves. Even light is an electromagnetic wave. A closer look at these results tell us that we have unified several things together. Electricity, magnetism and light. In fact the whole electromagnetic spectrum is included here. We have the usual VIBGYOR spectrum of visible light. Before that we have the radio waves, microwaves and the infra red radiation. After the visible spectrum we have the ultraviolet waves, X-rays and the γ-rays. All of them are described by Maxwell's equations! This is an exciting thing. An single set of equations is sufficient to cover three completely different fields of Physics. These are electricity, magnetism and optics and in fact much more. Can we do more? Can we combine more things together to get a unified description? Answer turns out to be overwhelmingly yes.

Special Theory of Relativity

Let us take the Lorentz force equation.

$$\mathbf{F} = q[\mathbf{E} + \mathbf{v} \times \mathbf{B}]. \quad (9)$$

Now if your friend is moving in a train and there is magnetic field around you shall say that a force will act on him if he has a charge on him. Since he is stationary with respect to himself he has zero velocity and he will say that no force is acting on him. Only one of you can be correct. Who is correct? It turns out that this problem can not be solved unless we do what Einstein did. This is to introduce Special Theory of Relativity. Introduction of special theory of relativity is also like unification. This time mechanics is being unified with electromagnetic theory. For sake of completeness here are the two postulates of special theory of relativity. (1) Laws of Physics are the same in all inertial frames. (2) The maximum possible speed for a signal is the speed of light in vacuum and it is the same for all inertial observers. A frame or a reference frame is just a coordinate system except that now time is also plotted as an additional, that is, fourth axis. In case anybody has still missed - we have reconciled mechanics with electricity and magnetism! It is not much different from unification.

Non-commercial Break

The geographical region to which we belong is somehow deprived of some finer things of life. Poet Surendra Sharma said that in the name of culture we have only agriculture. In this region the development of literature,

including poetry and prose, and other cultural artifacts of a mature and grown up societies are missing near completely. It was my personal feeling that we could not talk about any freedom fighter, a writer or any other figure of national importance. To give you an idea of the discrepancy I'd like to give you an example. The national language of India is defined as the Hindi spoken between Delhi and Meerut. That is exactly where we live! Now if that is the national language then why are the local words of this area completely missing from standard Hindi vocabulary. Just tell me the local word for cow dung cake and the corresponding word used in Hindi. Our cultural refinement stops at Ragini, Kabaddi and Volleyball tournaments. I suppose we should be paying some attention to this aspect of life. In this regard it gives me further pleasure that we are talking about those things here that other much more developed societies talk about.

Quantum Mechanics

More than a century ago we were getting such results in Physics which could not be explained by the laws known at that time. For example if we use electromagnetic theory then we find that any accelerated charged particle will radiate electromagnetic waves and hence will loose its energy. Now electrons in atoms move in circular or elliptical orbits and in both of these cases electrons are accelerated and hence they should loose energy. If that is the case then slowly the electrons will move towards the nucleus and fall into it and any and every atom will be destroyed. People thought that all atoms will destroy themselves but it will take some time. After calculations it was realized that atoms should destroy themselves in the fraction of a second. But that is not happening. So what is happening? Around 80 to 90 years ago it was realized that the rules that we were using to draw above conclusions are applicable to large systems only and the rules for small systems like atoms, molecules and nuclei are quite different. In fact the rules that are applicable to small systems start looking like the usual rules when we look at the larger and larger systems. These rules, the laws of Physics for very small systems, constitute the real laws of Physics and we call the collective knowledge as Quantum Mechanics. Among the most common results of quantum mechanics is the fact that small systems are described by an equation called Schrodinger Equation. It looks like this:

$$i\hbar\frac{\partial\psi(x,t)}{\partial t} = -\frac{\hbar^2}{2m}\nabla^2\psi(x,t)+V(x,t)\psi(x,t). \qquad (10)$$

Here $\psi(x,t)$ is called the wave function of the system that we are trying to describe, for example, an atom, a molecule or a nucleus. Many interesting things are discovered here about the world that are not apparent to us in the common life. Only few of them can be mentioned because we have to cover a long list of developments. For example energy of most of the physical systems can not be continuous. This is what we discover when we study quantum mechanics. In many cases the energy is quantized - it can take only discrete values. This is the case, for example, energy of electron in hydrogen atom. Then there is another result. In hydrogen atom or otherwise if we take an electron then we can not measure both its position and momentum with complete accuracy. If we measure the position very precisely then we have very little knowledge of its momentum and other way round. This is called Heisenberg's uncertainty principle. Mathematically we write it as

$$\Delta x \Delta p_x \approx \frac{1}{2}\hbar. \qquad (11)$$

Here Δx is the uncertainty is the measurement of the x-coordinate of the particle and Δp_x is the uncertainty in the corresponding component of the momentum. Finally I'll

mention another puzzling result of quantum mechanics. At small scales, when we are studying small systems, we realize that particles might behave like waves and waves might behave like particles. This is called wave particle duality. So is an electron a particle or a wave? Experimentally in some cases it behaves like a particle. In some cases it behaves like a wave. Same is true for electromagnetic waves. These are waves as we know but in photo-electric effect these waves really behave like a particle that we call photon. And that is the reality as we see at small scales. Depending upon the situation a physical system will behave like a particle or a wave.

Quantum Field Theory

Now since the theme of the talk is unification we shall again ask the related question - can we combine special theory of relativity and quantum mechanics together? A simple mathematical combination in this case leads us to a theory which we call relativistic quantum mechanics. A little bit of further investigation tells us that this can not be the complete story and something more is required. This lead us to the overarching framework, a generalization of relativistic quantum mechanics, called quantum field theory. It differs from relativistic quantum mechanics, among other things, that there can be creation and destruction of particles. This creation and destruction of particles is not unfamiliar to us. When an electron in an excited atom jumps to a lower level of energy it emits a photon. Before emission the photon did not exist.

Four Fundamental Forces and Interactions

We shall use the words forces and interactions interchangeably. So how many different types of fundamental forces, and hence interactions, are there? When we bring a magnet near a brass object nothing happens. But if we leave a brass object from our hand then it drops on the ground. From these things we realize that there are at least two different types of forces and hence interactions. Number one - the electromagnetic force that we have discussed earlier. The magnet is only one manifestation of that. Then there is gravitational force that is very well known to us. Are there other forces also? Answer is yes because we already know about radio activity - accidentally discovered by Henry Becquerel in 1896. We know radio activity has some thing to do with the nucleus of the atom. It turns out that inside the nucleus there are two more types of forces sitting - weak and strong. Our radioactivity, nuclear power, atom bomb, hydrogen bomb and nuclear medicine are possible because of them only. Thus we have fore fundamental forces or interactions in nature: (i) Gravitational (ii) Electromagnetic (iii) Weak and (iv) Strong. Out of these the gravitational one is the weakest.
Scientist : Gravitational force is the weakest.
TV Host : Have you ever fallen from the second floor? This seems like a puzzle. Basically this is still true because most of the matter is electrically neutral, like atoms, so we do not see the electromagnetic force in the same powerful form as gravitational one except in case of thunders and power lines of thousands of volts. Finally weak and strong interactions are observed inside the nucleus only and hence we do not feel them that much. We get some idea of the strength of the nuclear forces from the fact that radioactivity can not be stopped by means of chemical or physical processes.

Quantum Electrodynamics

This is the quantum field theory that describes electromagnetic interactions. remember that quantum field theory is a generalization of a mixture of special relativity and quantum mechanics. This is amongst most successful theories of physics. When you do your practical in the laboratory you start getting your errors at the first decimal place. In case of Quantum Electrodynamics, or QED, theoretical

and experimental results match with each other upto nine decimal places.

Glashow-Salam-Weinberg Model

Now we have interactions and their fundamental theories. Like QED is the fundamental theory of electromagnetic interactions. So what will be the quantum field theory that describes weak interactions? In 1967 Abdus Salam and Steven Weinberg proposed a theory that is called Quantum Flavourdynamics (QFD) or Glashow-Salam-Weinberg theory of electroweak interactions. This is a theory that not only describes weak interactions but it has eaten up the earlier theory called QED! This is our finest example of unification in Physics. Rather than giving a theory of weak interactions they gave a theory that combines and unifies two interactions together. For this work they got the Nobel Prize for Physics in 1979.

Branches of Physics

The physics of materials is called solid state physics or the condensed matter physics. This is the subject that has interesting phenomena like superconductivity. If we take an atom or a molecule only and then we study them then we are in atomic and molecular physics. There is another name for it - it is called spectroscopy. This is the subject that has interesting phenomena like lasers. If we go further deep into the atom we, of course, find the nucleus there. Study of the nucleus is the nuclear physics. We have already mentioned the interesting things in this case - atom and hydrogen bomb, nuclear power plants and nuclear medicine. The nucleus has the neutron and protons. In fact it is easy to find other animals also there - like pions. If we want to study these things then we are in particle physics. You must have noticed that we are trying to study smaller and smaller things. Basically we are hoping that by understanding the smaller things we can understand the larger things that result as an accumulation of the smaller things. This is called reductionism. From the uncertainty principle quoted above we can argue that we need higher and higher energy to study smaller and smaller systems. This is because

$$\Delta p_x \approx \frac{\hbar}{2\Delta x}. \qquad (12)$$

The conclusion is that to study particle physics, that is smallest things called elementary particles, we need highest energies. Consequently the insider name for particle physics is High Energy Physics. We have already encountered two of the main things in this field - QED and QFD or Glashow-Salam-Weinberg Model.

Quantum Chromodynamics

Quantum Chromodynamics, or QCD, is the quantum field theory that describes strong interactions that we encounter deep inside the nucleus or in particle physics. I do not know whether Lagrangian and Hamiltonian dynamics are taught to you but those are the beginning things if we want mathematical formulation of any field theory. Anyway by now I can only recite the names because any inclusion of technical details is sure to give you headache.

Standard Model of Particle Physics

QCD taken together with QFD is called the Standard Model of Particle Physics.

Grand Unified Theories (GUTs)

The way Abdus Salam and Steven Weinberg combined the weak and electromagnetic interactions together is it possible to combine all three of them together - weak, strong, and electromagnetic? Mathematically people have tried this also and these are called the grand unified theories or the

GUTs. Two most famous models in this class are called the Georgi-Glashow model and the Pati-Salam model. These models demand that the proton should decay after some time - though that time is long. Some experiments were done including the one in Kolar God Mines in Karnataka many years back and there was no indication of proton decay. So at this moment we do not know whether nature really likes to combine the three interactions together.

Supersymmetry

Though we do not know about grand unification - whether nature uses it or not but scientists have gone a few steps further. To talk about those directions in which physicists have exercised their energies we have to talk about bosons and fermions. Bosons are named after our S.N.Bose and Fermions after Enrico Fermi. Bosons have either zero or integral spin in units of $\hbar$ - the Planck constant. Fermions have half integral spins in the same units. Photon is a boson and electron is a fermion. This spin, though like angular momentum, is an intrinsic quantum mechanical property and we can not give a common life comparison of this. (As a side remark we shall add that spin, mostly of electrons, is responsible for all of the magnetic phenomena - para, ferro, ferri, diamagnetism in matter.) Fermions obey the Pauli exclusion principle - two fermions can not have the same quantum numbers. Two or more bosons can have same quantum numbers and that is why we get the things like lasers. Clearly fermions and bosons are quite different from each other. Can we combine fermions and bosons together into a unified description?

Is there some possibility that will take us from fermions to bosons and vice versa?
That is precisely supersymmetry.

We say that a theory has supersymmetry if that theory is invariant, that is it does not change, under supersymmetric transformations. Supersymmetric transformations are the transformations that change bosons to fermions and fermions to bosons.
This is a mathematical framework - a theory.

Science is empirical. This means a theory is right if it confirms with experiments otherwise wrong.

CERN and LHC

So far we have not got any experimental evidence that nature is supersymmetric. But this is one on the actively investigated theory at LHC (Large Hadron Collider) ant CERN (European Center for Nuclear Research) in Geneva, Switzerland. More than ten billion dollars have been spent on the machine where these experiments to verify supersymmetry and to find a particle called the Higgs particle are going on. Ten billion dollars will be equal nearly 500 billion rupees. This is 500 Arab rupees. Governments of many countries in the world have contributed this money including India, the US and many European countries. A research group at this laboratory can have thousands of scientists and there names appear in a research paper! One of the instruments there, the ATLAS detector, is five story high and the main machine is a circular metro like tube with a perimeter of 27 km.

Einstein's General Theory of Relativity

Out of the four fundamental interactions we have not talked about gravitation. But you already know about it. It is described by Newton's law of gravitation! Most of the things related to gravitation can be described by Newton's law.

$$F = G\frac{m_1 m_2}{r^2}. \qquad (13)$$

In spite of the above fact Einstein proposed a new theory of gravity called the

General Theory of Relativity in 1915 - just ten years after his theory of special relativity. There was no experimental requirement for this theory at the time of its proposal but Einstein said that this can be verified at the time of an eclipse by observing whether the sun bends the light coming from distant stars. This was experimentally observed in 1919 and thus this theory was verified to be true. Newton's law of gravitation comes out of this theory.

Supergravity Theory

We have talked about supersymmetry and we have talked about general theory of relativity.

What will happen if we combine two of them together?

Well people have already done that. In fact when we try to play with supersymmetry, when we try to make it local, we automatically get general theory of relativity! This new thing is called supergravity theory.

Superstring Theory

Can there be something beyond supergravity also. The answer is yes. There is a theory called superstring theory or simply the string theory that incorporated supergravity inside it and many other things. According to superstring theory all the particles of nature are just very small strings. In fact all of them are the same string but it is vibrating with different frequencies and hence we see different particles. This theory combines, unifies and incorporates all of the diverse theories that we have enumerated in this long winding discussion - and in fact more.

Apology

This lecture was supposed to be about string theory. And what we have ended up with? The moment the name of superstring thoery came up the lecture is over. Rather than ending the lecture should have begun here. My apologies for the disappointment. I am sure you understand that if I would have talked about the technicalities of string theory then it would have been of very little use. And thank you very much for your patient hearing of this presentation.

References

There are many books at various levels on these topic in the market but the best thing is the Internet where incredible amount of informations is available for free.

(*This article is based on a talk delivered to undergraduate students at Mihir Bhoj P.G. College, Dadri, Gautam Budha Nagar, U.P..)*

Design and Fabrication of Bulk Heterojunction Solar Cells, utilizing graphene and transparent conducting oxides based electrodes

Firoz Alam

Organic/Polymer solar cells have attracted attention in recent years, because of its advantage of being inexpensive, light weight, flexible, large area feasibility and continuous manufacturing ability. Organic photovoltaic solar cells (OPVs) are based on layers of solution processed bulk-heterojunctions (BHJs) of semiconducting polymers, sandwiched between two electrodes. At present, these solar cells have shown power conversion efficiency of ~10%, which needs to be scaled up to be commercially feasible.

The major future challenges in development of Organic solar cells are:

1. Significant improvement in efficiency of OPV cells.
2. Replacement of transparent ITO electrodes.
3. Stability and Reliability.
4. Development of low cost processing methodology.

A target improvement of >15% is to be achieved to make OPV cells commercially feasible. To overcome above challenges, extensive research in the area of material development, optimization of device parameters, modification in device architecture needs to be done.

A promising approach for making solar cells that are inexpensive, lightweight and flexible is to use organic (that is, carbon-containing) compounds instead of expensive, highly purified silicon. But one stubborn problem has slowed the development of such cells. Researchers have a hard time coming up with appropriate materials for the electrodes to carry the current to and from the cells. Specifically, it has been hard to make electrodes using materials that can match the organic cell's flexibility, transparency and low cost.

The standard material used so far for these electrodes is Indium tin oxide (ITO). ITO has been widely used in optoelectronic devices as transparent conducting electrodes. However, ITO adds to the cost because of the limited availability of Indium on earth, furthermore the issues like Indium ion diffusion into organic layers, and mechanical brittleness of ITO makes it less ideally suitable for OPV device. Graphene, because of it's high electrical conductivity, flexibility and transparency, is being envisioned as a promising material for the replacement of ITO. However, various processing difficulties lies ahead to use atomic layer graphene as an electrode material in Organic solar cells.

Graphene

Graphene is a 2-D carbon material with single atomic layer thickness made of sp^2 carbon atoms and has a large specific area with high mobility of 10, 000 $cm^2V^{-1}s^{-1}$, and tunable band gap. Graphene is also a promising electron acceptor in photovoltaic devices. Graphene, has been the focus of much research since its isolation because of the unique transport properties. Because of graphene's high optical transmittance and conductivity it is also being considered as a transparent conductive electrode. In comparison to traditional transparent conductive electrodes such as indium tin oxide (ITO), graphene films have high mechanical strength, are flexible, and are chemically stable. Production of large-area and high-quality graphene films is necessary for device applications such as Organic field effect

transistors (OFETs), Organic solar cells (OSCs) and Organic light emitting devices (OLEDs).
The biggest problem with getting graphene to work as an electrode for organic solar cells has been getting the material to adhere to the panel. Graphene repels water, so typical procedures for producing an electrode on the surface by depositing the material from a solution won't work.

However, the flexibility and light weight of organic solar cells with graphene electrodes could open up a variety of different applications that would not be possible with today's conventional silicon based solar panels. Organic solar cells, being transparent could be applied directly to windows without blocking the view, and also could be applied to irregular wall or rooftop surfaces. In addition, they could be stacked on top of other solar panels, increasing the amount of power generated from a given area. And they could even be folded or rolled up for easy transportation.

Transparent Conducting Oxides

The transparent conductive oxide (TCO), such as indium-tin-oxide (ITO), Al-doped zinc oxide (AZO) and Zn-doped indium oxide (IZO) have attracted much interest in the application of optoelectronic devices such as solar cells and liquid crystal displays due to their high conductivity and high transparence in visible region.

ITO (Indium Tin Oxide, 80-90% Indian oxide with a minor amount of tin oxide has been very popular for LCD flat panel displays. They generally have a slightly yellowed appearance and have also been used as infrared-reflecting coatings on windows. Fluorine-doped tin oxide (SnO_2:F) is becoming more popular in research based sensitized photovoltaics. Although the conductivity performance can be slighter than ITO, (SnO_2:F) is generally less expensive in material cost and manufacturing.

Conjugated Polymer

Organic polymer having extended π-conjugated system are special class material which on doping with specific charge carrier behaves like a semiconductor and this novel characteristic make them synthetic metal. The electronic conductivity of these conducting polymers can be varied from 10^{-10} - 10^{5} S/cm. chemically doping and undoping can reversibly control the electrical properties of the polymer and that is the reason of extensive use of these polymers as sensors.

Importance of the present Work

Graphene is transparent, so that electrodes made from it can be applied to the transparent organic solar cells without blocking any of the incoming light. The proposed work will be focussed on researching unique methodology to prepare high quality single layer graphene sheets. These graphene sheets will be processed further and employed in device fabrication as a substitute for ITO, thus providing us a cheaper, flexible and efficient device. Prototype development of graphene based organic solar cell module will also be attempted. This work could also lead to flexible organic light emitting devices (OLEDs) and organic thin film transistors (OTFTs).

Quantum Computer: A Big Technological Challenge

Azharuddin

Introduction

There are many complex problems such as finding prime factor of a large number, searching an entry in a big unsorted database in real time, molecular simulation etc. that are thought to be intractable and cannot be solved and simulated even on the latest supercomputer. These problems are not practically feasible because of the speed limitation and lack of good efficiency of algorithms of today's classical computers. Downsizing the size of the electronic components, e.g., transistors, on ICs we can enhance the speed of classical silicon computers. But how much can we reduce the size? Is there any lower limit of this? Yes, there is a lower limit. If we keep on reducing the size, we shall reach the barrier of quantum world below which the things are no more classical. One can be fool enough to fabricate an IC having component size lying in the range of quantum world and to apply classical laws to its circuitry operation.

Is the practical limitation of classical computer's speed weakening our interests in research in those fields where problem complexity is increasing day by day? In fact, when a usual trend in science and technology reaches its limitation, a new trend comes into existence for the continuation of the developments and advancements of scientific researches and practical implementation of theories. Then, one can guess that there would be a nice gift of science and technology which is able to overcome all the limitations of classical computation. Yes, there is something which is being expected to solve all the practically intractable problems in real time. This "something" is "quantum computer".

A quantum computer is a strange exploitation of quantum mechanics. Such a machine will be far more efficient at factoring a big number or searching database compared to its classical counterparts. Quantum computers promise to exceed the computational efficiency of ordinary classical computers because quantum computing algorithms allow to perform tasks in fewer steps.

What is a Quantum Computer?

A quantum computer resembles a classical one. It processes quantum information. Quantum information can be implemented by utilising any property (of course one must have enough external control on that property to be utilised) of a particle or an atom or a molecule or a cluster of atoms or molecules. For example, spin of a particle can be treated as to hold quantum information. Similarly, magnetic moments of molecules, polarizations of photons, energy states of ions etc. can also be the other candidates. A quantum computer makes direct use of quantum mechanical phenomena, such as superposition and entanglement, to perform operations on quantum data.

A quantum computer can process vast amounts of information in a very little span of time. This weird potential is very useful for cryptography, searching data, factoring large numbers quickly and the simulation of quantum-mechanical systems as these processes demand very large amount of data processing.

The reversible feature of a quantum computer makes it capable of functioning with no net energy consumption (theoretically). To elaborate quantum reversibility, it drives itself forward in infinitesimal (reversible) steps. In contrast to "run" terminology of classical computer programs, quantum computer programs "evolve" during the processing of quantum data. Incidentally, reversibility also

means that the inputs of a quantum computer can be regenerated from the outputs, provided the program should run backwards.

Quantum Computing Candidates

Massachusetts Institute of Technology, Oxford University, IBM and Los Alamos National Laboratory are the most successful in development of quantum computers.

Nuclear Magnetic Resonance (NMR) technology is the most popular today, because of some successful experiments. MIT and Los Alamos National Laboratory have constructed a simple quantum computer using NMR technology. Some other designs are based on ion trap and quantum electrodynamics (QED). Scientists are utilizing many quantum properties of materials for the implementation of quantum computers. There are a number of quantum computing candidates. A partial list is given below:

- Nuclear magnetic resonance on molecules in solution (liquid NMR)
- Trapped ion quantum computer
- Superconductor-based quantum computers
- Spin-based quantum computer
- Electrons on helium quantum computers
- Topological quantum computer
- Quantum dot (a single electron trapped inside a cage of atoms)
- Optical lattices
- Solid state NMR Kane quantum computers
- Molecular magnet
- Fullerene-based ESR quantum computer
- Optic-based quantum computers (Quantum optics)
- Transistor-based quantum computer

In 2009, researchers at Yale University made the first simple solid-state quantum processor. The two-qubit superconducting chip was able to run elementary algorithms. Each qubit consisted of a billion aluminum atoms but they acted like a single one that could occupy two different energy states.

In 2010, researchers at the California Institute of Technology (Caltech) have demonstrated quantum entanglement for a quantum state stored in four spatially separate atomic memories.

In 2011, scientists from Oxford University have made a significant step towards an ultrafast quantum computer by successfully generating 10 billion qubits of quantum entanglement in silicon for the first time.

People have also succeeded to run Shor's algorithm on a silicon-based quantum computing chip, based on quantum optics.

Qubit: Unit of Quantum Information

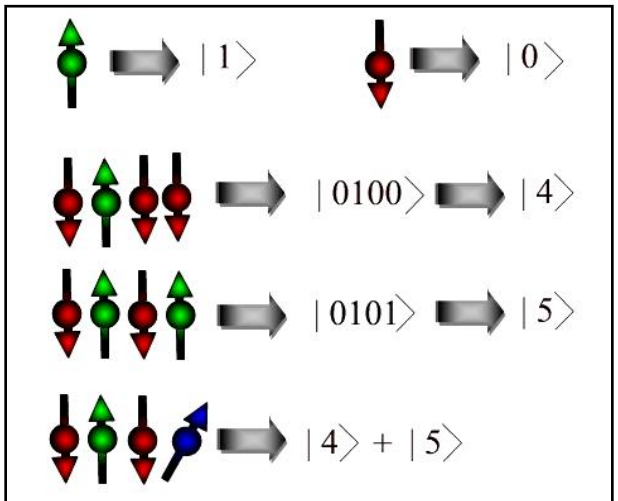

Figure 1: Qubits can be in quantum superposition of all allowed states

A quantum system having two distinct quantum states (e.g., spin-up and spin- down states of a particle) can help implement 0 and 1 qubit states. 0 corresponds to one quantum state and 1 corresponds to another quantum state of the quantum system. For example, if |1> represents 1 state and |0> represents 0 state, then

pure qubit state would be a linear combination of these two states:

$|\psi> = \alpha |1> + \beta |0>$

where $|\alpha|^2$ is the probability of outcome |1> and $|\beta|^2$ is the probability of outcome |0> and $|\alpha|^2 + |\beta|^2 = 1$. Now depending upon the values of α and β the qubit value of the quantum system can be either 1 or 0 or any quantum superposition of them. Similarly, a string of qubits can be in any superposition of its bit-string configurations. This quantum superposition property greatly enriches the kind of information that can be represented by qubits.

A quantum computer maintains a set of qubits and operates by manipulating those qubits, i.e. by transporting these qubits from memory to quantum logic gates and back. A pair of qubits can have four discrete combinations i.e., 00, 01, 10, 11. If a datum is represented by two qubits, then it can have any discrete state of the above four, or a state of quantum superposition of these four discrete states. In general a quantum computer with *n* qubits can be in an arbitrary superposition of up to 2^n different states simultaneously (this compares to a classical computer that can only be in *one* of these 2^n states at any one time). A quantum computer operates by manipulating those qubits with a fixed sequence of quantum logic gates. This sequence of gates is called a quantum algorithm.

Is there any restriction of choosing quantum properties for the implementation of qubits? In fact any system possessing an observable quantity A which is conserved under time evolution and such that A has at least two discrete and sufficiently spaced consecutive eigenvalues, is a suitable candidate for implementing a qubit.

Speed and Power of a Quantum Computer

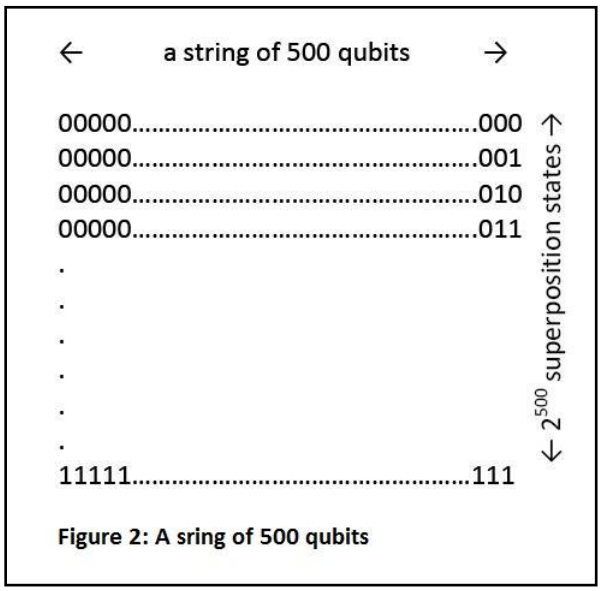

Figure 2: A sring of 500 qubits

Chuang stated, "A supercomputer needs about a month to find a phone number from the database consisting of world's phone books, whereas a quantum computer is able to solve this task in 27 minutes".

Quantum computer with 500 qubits (assuming that each qubit has only two distinguishable states) gives 2^{500} independent superposition states as shown in fig (2). Each superposition state is a string of five hundred 1's and 0's. Such computer can operate on 2^{500} states simultaneously.

During the measurement of quantum data, the string of five hundred qubits collapses into a single superposition state out of 2^{500} possible states giving a single answer. To praise the potential of such a quantum computer, it can defeat a classical one with approximately 10^{150} processors.

According to Moore's Law, the number of transistors of a microprocessor continues to double in every 18 months. This law predicts a classical computer in year 2020 with 40 GHz CPU speed and 160 GB RAM. An analogue of Moor's law for quantum computers states that

the number of quantum bits would be double in every 18 months. But adding just one qubit is quite enough to double the speed.

Quantum Entanglement

Quantum entanglement is a typical property of a quantum system. Components of a quantum system are linked together through quantum entanglement. Classical physics undoubtedly fails to explain this strange quantum mechanical feature. Description of one object among many entangled objects requires full mention of its counterparts. Even though the objects are spatially separated this requirement is essential. Quantum entanglement helps entangled objects share information among them. This interconnection is purely a quantum phenomenon and it cannot be explained by classical physics.

Spin property of a system of two entangled particles can be correlated. Both the particles can have the same spin or the opposite spins. Measurement of one's spin gives the spin of the other. Distance between the two particles is irrelevant.

In pair production, the system of two particles produced in the process can also be termed as entangled system. One particle has many physical properties such as charge, spin etc. opposite to the other one. So, knowledge of one's properties tells the other's.

A quantum computer would have to entangle the qubits over a significant distance. A classical computer uses electrical signal to transmit information from one device to another. Analogously, a quantum computer exploits entanglement property of the qubits for information transmission. A credit goes to Andrew Berkley and colleagues for their successful implementation of entanglement between two qubits inside a silicon chip over a distance of 0.7 millimetres. This distance, though it does not sound like the opposite ends of the universe, is very significant to the scale to build quantum computer components.

Quantum mechanically, information can be sent from one particle to another faster than the speed of light. Although this sounds incredible it has been proven. If we have a system of two particles, let's say electrons, that are entangled and we change the spin of one of them, the other will automatically change its own spin at a speed faster than light even though they are kept at opposite ends of the universe. This property, if fully controlled, would make quantum computers run at infinite speed.

Quantum Decoherence

Quantum system being extremely sensitive to interaction with the surroundings, a quantum computer is very difficult to maintain its quantum state during probing the system from the outside. Any interaction (or measurement) leads to a collapse of the wave function of the quantum system. This wave function collapse is called decoherence. Quantum decoherence is one of the major obstacles in the quantum computer implementation. It is extremely difficult to isolate a quantum system from the environment. The larger the number of qubits the harder is it to maintain the coherence.

Decoherence arises when a system interacts with its environment in a thermodynamically irreversible way. One can consider quantum decoherence as the loss of information from a system into the environment.

In order to make quantum computers powerful, many operations must be performed before quantum coherence is lost. It can be impossible to construct a quantum computer that will make calculations before decoherence time (about 10^{-27} seconds!). But if one makes a

quantum computer, where the number of errors is low enough, then it is possible to use an error-correcting code for preventing data losses even when qubits in the computer decohere.

Quantum Logic Gates and Circuits

Ordinary computers deal with data processing on electronic circuits mainly containing logic gates such as AND, OR, NOT etc. Likewise, in a quantum computer, information is passed through quantum circuits containing quantum gates. A quantum gate is a unitary operator U.

Not all the classical logic gates are reversible. For example, if the output of AND is 0, there are three possible values for the input i.e., 00, 01, and 10. All quantum gates, on the other hand, are reversible. Reversibility means inputs can be restored from outputs.

A quantum logic gate must perform its operation faster than decoherence time. Otherwise, quantum information may get altered due to decoherence and there will be errors in the output of the logic gate.

Quantum Error Correction

A quantum computer will certainly interact with its surroundings, resulting in decoherence and hence quantum information stored in the device will decay. Quantum gates are unitary transformations and cannot be implemented with perfect accuracy. A small imperfection in the gates will cause a serious failure in the computation. Any effective scheme to prevent errors in a quantum computer must protect against small unitary errors in a quantum gates, as well as against decoherence.

There are a lot of error-correcting codes. The simplest one is called repetition code. 0 is encoded as 000 and 1 as 111. Then if only one bit is flipped, one gets a state, for example 011, which can be corrected to its original state 111.

Quantum Software

A quantum software or program is a particular quantum state of a system of thousand or million or billion qubits fabricated on a quantum chip that enables a quantum computer to perform a specific task. Such quantum software is very difficult to prepare specially for non-professional users. A user can acquire the quantum software from a vendor rather than prepare it himself. Quantum software is a consumable product and it is damaged after a single use. So, if a user wants to perform the same job many times, then he will have to purchase the same quantum software each time. This can be a misfortune for users but a good fortune for the vendors. Thus we can foresee a flourishing of a quantum software industry. A company can design valuable quantum software and use a special-purpose device to make and store multiple copies of it. A user can download the quantum software for a fee from the company through quantum internet.

Quantum Algorithms

A quantum computer performs a job following a sequence of some pre-defined steps. This sequence of steps is called an algorithm. Superiority of a quantum computer over a classical computer comes due to a perfect quantum algorithm that exploits quantum parallelism. Without a proper quantum algorithm a quantum computer will not necessarily outperform classical computer at all computational tasks. A quantum algorithm is very difficult to formulate. Among many, Shor’s and Grover’s algorithms are the most significant. These algorithms are extremely efficient to reduce computational complexity and enable a quantum computer to defeat a conventional computer by a significant margin. For example, Shor's algorithm allows extremely

quick factoring of big numbers. A classical computer can be estimated at taking millions of years to factor a 1000 digit number, where as a quantum computer would take only few minutes. On the other hand, Grover's algorithm empowers a quantum computer to search an unsorted database incredibly faster than a conventional computer. Normally a classical computer would take N/2 number of searches to find a specific entry in a database with N entries. Grover's algorithm makes it possible to perform the same search in √N searches.

Difficulties in the implementation of Quantum Computers

Quantum decoherence is the major obstacle in a process of producing of a quantum computer. If decoherence problem cannot be solved, a quantum computer will be no better than a silicon one.

A practical working quantum computer requires a well-defined array of qubits for stable memory, feasible state preparation for the initial state, long decoherence time, a universal set of gate operations and capability for single-quantum measurement. Not all these requirements are currently unconditionally achievable.

Future benefits of quantum computers

- Shor's algorithm and cryptography:

Factoring is one of the most important problems in cryptography. For instance, the security of RSA (electronic banking security system) - public key cryptography - depends on factoring and it is a big problem. However, breaking any kind of current encryption that takes almost centuries on existing classical computers, may just take a few moments on quantum computer.

- Ultra-secure and super-dense communications:

It is possible to transmit information without a signal path by using quantum teleportation. There is no way to interrupt the path and extract information. Ultra-secure communication is also possible by super-dense information coding. Qubits can be used to allow more information to be communicated per bit than the same number of classical bits.

- Molecular simulations:

A classical computer cannot simulate quantum effects without slowing down exponentially. A quantum computer, on the other hand, can do the same job in real time. Molecular simulations of chemical interactions will allow chemists and pharmacists to learn more about how their products interact with each other and with a person's metabolism or disease.

- True randomness:

Classical computers can generate only pseudo-random. Pseudo-random generators cannot simulate natural random processes accurately for some applications, and cannot reproduce certain random effects. Quantum computers can generate true random numbers. This potential can play a significant part of applications on statistical approaches of some natural phenomena, for simulations, code making, randomized algorithms for problems solving, stock market predictions etc.

Conclusion

It is obvious that making a practical quantum computer is still far in the future. In practice, quantum hardware is in its infancy. Programming style for a quantum computer will also be quite different. Development of quantum computer needs a lot of money. Even the best

scientists can't answer a lot of questions about quantum physics. Building a practical quantum computer is just a matter of time. Perhaps someday, as suggested by Daniel Gottesman of Microsoft Research and Isaac Chuang of the IBM Almaden Research Center, the capabilities of quantum computers will be significantly extended by 'quantum software' that can be prepared offline and shipped to users over the 'quantum Internet'. Realization of a working quantum computer will be one of the biggest steps in science and will undoubtedly revolutionize the practical computing world.

Further Reading

- Preskill, J. *Quantum Computation* (lecture notes) (www.theory.caltech.edu/people/preskill/ph219/#lecture)
- Preskill, J. *Quantum Computing: Pro and Con* (arXiv:quant-ph/9705032v3 26 Aug 1997)
- Vedral, V. *Quantifying entanglement inmacroscopic systems* (NATURE|Vol 453|19 June 2008)
- Preskill, J. *Plug-in quantum software* (NATURE|VOL 402 | 25 NOVEMBER 1999)
- Aaronson, *S. The Limits of Quantum Computers* (20 08 SCIENTIFIC AMERICAN, INC.)
- Chirolli, L and Burkard, G. *Decoherence in Solid State Qubits* (Advances in Physics Vol. 57, No. 3, May-June 2008, 225-285)
- Boghosian, B. M. *Simulating Quantum Mechanics on a Quantum Computer* (arXiv:quant-ph/9701019v2 8 Mar 1997)
- Kane, B. E. *A silicon-based nuclear spin quantum computer* (NATURE |VOL 393 | 14 MAY 1998)
- Hughes, R. J. *Cryptography, Quantum Computation and Trapped Ions*
- P. Walther, K. J. Resch, T. Rudolph, E. Schenck, H. Weinfurter, V. Vedral, M. Aspelmeyer & A. Zeilinger. *Experimental one-way quantum computing* (NATURE |VOL 434 | 10 MARCH 2005)
- DiVincenzo, D. P. *Quantum Gates and Circuits* (arXiv:quant-ph/9705009v1 7 May 1997)
- Knill, E. *Quantum computing* (NATURE|VOL 463 | PAGE 441-443 | 28 January 2010)

An Introduction to Complex Spectra

Swapnil and Tauheed Ahmad

Introduction

Complex spectra are not just those that are particularly rich in lines or that call for especially intense intellectual efforts to unravel them. The feature of the complex spectra is the appearance of multiplets or groups of lines with characteristic spacings and strengths. For heavy atoms, the multiplets often overlap one another, and the resulting morass of lines may be responsible for the common misconception that the word 'complex' refers to the intricacy of the spectrum. From a theoretical standpoint, the lines of a complex spectrum correspond to transitions between comparatively low-lying configurations that each comprises several active (i.e. valence) electrons. The reality of atoms as they exist in discharges or in plasmas attracts the attention of the experimentalist. For the theorist, there is the challenge of studying a particular aspect of the many-body problem. Two-electron configurations can give rise to complex spectra, but our interest here is limited to those features that are susceptible of generalization to many-electron configurations. The most difficult thing in studying complex spectra is the reliable predictions of the terms and levels.

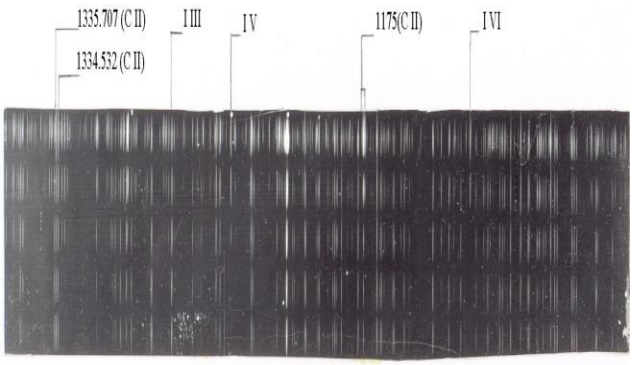

Iodine spectra

Recent progress in the study of complex spectra

The Relativistic Hartree-Fock calculations are not very easy and even doing single configuration calculation doesn't help. Large numbers of interacting configurations, perturb the position of the levels significantly. This was one of the main reasons for complex spectra being left behind. With the availability of the fast computers and various computer codes like those of R.D. Cowan[1] ,C.F. Fischer[2], MCDF [3,4] and the recent version of the MCDF program GRASP [5] etc and high resolution spectrographs, it is now possible to compute the structure of the complex system and can record high quality dense spectra. The next problem lies ahead is the technicalities involved to handle such complex spectra. A comparison of such calculations with the parameters that emerge from the least-squares fitting of the atomic data yields vital information on the validity of the Hartree-Fock method and its various elaborations.

It would be appropriate to introduce some basic terms which are often used to describe the spectrum. The multiplicity (M) of the terms is defines as 2S+1. This can explain that for a single electron in an atom with total spin S =1/2, M = 2S+1 = 2; means doublet term system will be formed while for two electron system with total spin S=1 & 0, multiplicity can be 1 and 3 that will give singlet and triplet terms and the same way, a three and four electron system will produce doublet and quartet, triplet and quintet respectively. This is thus obvious that as the number of active electrons increases in the open shell, the term system becomes more and more complex. For instance the number of levels observed as under:

Configuration	**Number of energy levels**
closed shell (s^2, p^6, d^{10} etc)	1
one electron (p,d,f,g,h, etc)	2
Two d electrons (d^2)	9
Three- d electrons (d^3)	19
Four d electrons (d^4)	34
Five pd electrons (d^4p)	180

Thus, it is clear that a system starts getting complex when there are three or more active electrons involved. A large number of levels will be involved in the emission of a large number of spectral lines. The only large number of lines does not necessarily make system that difficult to study but the interactions among the levels make things worse. The one electron and even two electron systems could be spotted with high accuracy with isoelectronic extrapolations and the levels can be found easily. This was the reason that such systems have been studied long back. However, for interacting systems these techniques fail and they could be only predicted through sophisticated multi configuration interaction Hartree-Fock calculations including relativistic effects. The detailed background about the theoretical approach can be found some elsewhere [6,7]. Only a brief account of methodology can be mentioned here to give an idea about the approaches for complex spectra.

Normally, one electron wave function is written as

$$U_{nlm_l}(r,\theta,\phi) = \frac{(-1)^{\frac{(m_l+|m_l|)}{2}}}{\sqrt{4\Pi}} \sqrt{\frac{(2l+1)(l-|m_l|)!}{(l+|m_l|)!}}\, R_{nl}(r)\, P_l^{|m_l|}(\cos\theta)\exp(m_l\phi)$$

For N electron atoms the wave function can be constructed by taking the product of wave function of its entire electron as:

$$\Psi(r_1,\theta_1,\phi_1.....r_N,\theta_N,\phi_N) = U_{n_1l_1m_{l_1}}(r_1,\theta_1,\phi_1).....U_{n_Nl_Nm_{l_N}}(r_N,\theta_N,\phi_N)$$

The Hamiiltonian for an atom can be written in general

$$H = -\frac{\hbar^2}{2m}\sum_{j=1}\nabla_j^2 - \hbar^2\sum_k\frac{1}{2M_K}\nabla_k^2 - e^2\sum_K\sum_J\frac{Z_K}{r_{Kj}} + e^2\sum_{K>L}\frac{Z_KZ_L}{r_{KL}} + e^2\sum_i\sum_{j>i}\frac{1}{r_{ij}} + H_{SS} + H_{SO} + H_{hfs} + H_{etc}....$$

Schrodinger's wave equation cannot be solved for such a complicated Hamiltonian. Therefore, certain approximations are used to solve them like Central Field approximation. The best wavefunction could be estimated through self consistent field method. To obey the Pauli's exclusion principle, this wavefunction for N electrons can be represented in the form of a determinant which satisfies the condition of anti-symmetric wavefuntion. This could be solved in parts only and these various parts are named as Slater energy parameters (E_{av}, F^k, ζ_{nl}, G^k and R^k et) as explained under:

Para-meter	Name	Description	Scaling of the parameter
E_{av}	Average configuration energy	represents the average energy of the configuration or centre of gravity of the configuration concerned.	100 % of the HFR
F^k	Slater direct radial integral	represents that part of the electrostatic energy, which depends on the orientation of the ℓ vectors and is responsible for the separation of the terms with different L values but same S value in LS coupling, for instance the separation of the terms like ^3P, ^3D	85% of HFR

		,^{3}F etc.	
G^k	Slater exchange radial integral	G^k gives the energies due to the exchange forces, which depend on the spin orientations. They cause the splitting of terms with same L but different total spin S.	80% of HFR
$\zeta_{n\ell}$	Spin orbit interaction integral	$\zeta_{n\ell}$ causes the splitting of the terms with same L and S values i.e. it is responsible for the fine structure splitting.	100-110% HFR
R^k	Configuration interaction integral	R^k parameters are the configuration interaction integrals.	80 -85% HFR

Ab Initio Calculations

In the complex spectra, the levels of one configuration is perturbing the levels of other configuration provided they should belong to the same parity configurations and have same J value. Thus energy of these levels shifted because of perturbation from calculated results. To overcome this problem configuration interaction (CI) code is used. CI effect tends to be largest between configurations when centre of gravity energies E_{av} are not greatly different and/or for cases in which the coulomb matrix element are large in magnitude. Large values of R^K tend to occur particularly when the two configurations belong to the same complex.

Dr. R.D. Cowan [1] of Loss Alamos Scientific Laboratory developed a computer code involving the basic theory behind the structure of the atoms and incorporating the some of his own suggestions to solve these complicated equations. Cowan's approach was essentially to solve the Slater parameters (E_{av}, F^k, ζnl, G^k and R^k). He ran four sets of programs as named by himself follow the sequence as under:

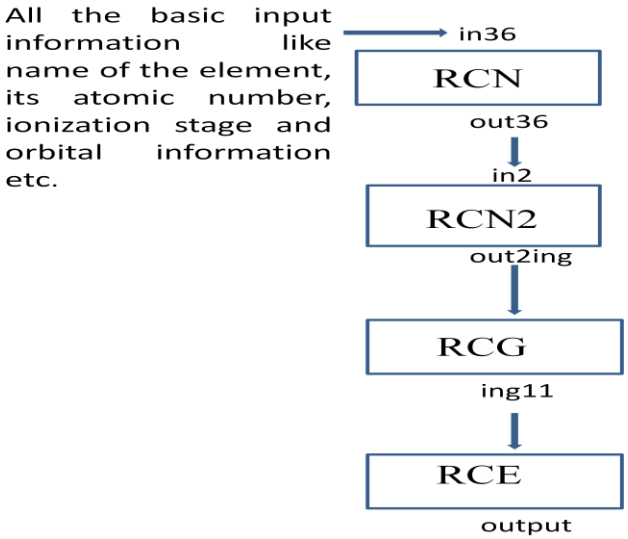

With above-mentioned parameter's scaling, the initial calculations are performed in HFR (Relativistic Hartree-Fock) mode. If all the possibly interacting configurations are included in both even and odd parity systems, the predicted energy levels should be quite close (500- 1000 cm^{-1}). However, this shift is very critical to establish. In some cases, the experimentally observed levels are found below predicted levels and in some cases above the predicted one.

The Spectrum Analysis

Once above requirements are complete, the identification of the lines may start. This is the most important part of the work to pick up the first right line with right ionization characteristic. The first identification determines the shift from the predictions therefore; it must be the right choice. Once the relative shift from the calculated value is known, the establishment of the further energy levels rather becomes a bit

easier. When sufficient number of levels (more than 50% of the total number) usually based on the better predicted transition probabilities are established, least squares fitted (LSF) parametric calculations are performed ignoring the unknown levels. The program adjusts the energy parameters according to the experimentally observed levels and hence calculating the unknown levels more precisely. This way more unknown levels are established. Finally these LSF parameters are used to recalculate the transition probabilities to locate the levels based on the weaker transitions. Those levels, which are permitted by electric dipole selection rules to give only single transitions, are established only after the completion of the analysis with the help of lines of right character which are left over in the required region of wavelength.

Running least squares fitted calculations also require due attention to monitor the variation of the energy parameters. A fit is only acceptable if the scaling factor is in accordance as mentioned earlier, and the standard deviation of the fit is less than 250 cm^{-1}. A beautiful example of the analysis based on this approach can be seen in Ba VII [8]. In complex spectra, sometime the purity of the leading components for some levels has been observed as low as 13%. Naming a level in these circumstances is meaningless. Therefore, they are designated by their energy and J values along with their percentage composition but in many other cases still possible designation can be assigned when level's purity is more than 50%.

Since the entire analysis is based on the correctness of the ionization assignment, extreme care has to be taken in deciding the ionization of each individual line. There are many cases where single transition is used to establish the energy level; the ionization assignment in that case needs to be 100% accurate. This task is achieved by varying experimental condition during the recording of the spectrograms. Charging potential of the source is varied as well as series inductance coil is introduced in the discharge circuit for successive exposure of the recordings. High inductance coil eliminates lines of higher ionization but the lines from lower ionization do appear on that track. This is very effective method of ionization separation.

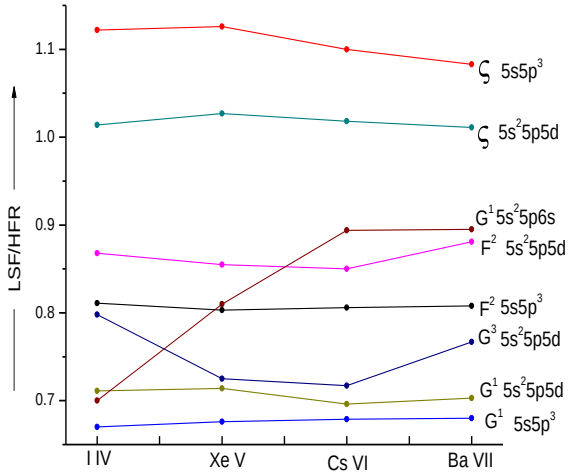

fig: The scaling factors of F^K,$G^K$and ζ parameters of $5s5p^3$,$5s^25p5d$ and $5s^25p6s$ configuration of I IV to Ba VII sequence.

Finally a close comparison on the variation of the energy parameters along the isoelectronic sequence is made as see in above figure and if all looks satisfactory, the analysis is accepted.

References

1. R.D. Cowan, J. Opt. Soc. Am, **58**, 808 (1968).
2. C.F. Fisher "The Hartree-Fock method for atoms" J. Willey and sons (1977).
3. I.P.Grant, B.J.Mckenzie, P.H.Norrington, D.F Myers and N.C. Pyqer.Comput. Phys. Commun **21**, 207 (1980).
4. K.G.Dyal, I.P. Grant, C.I. Johnson, F.A. Parpiya and E.H. Plummer. Comput Phys. Commun **55,** 425 (1989).

5. N.C. Pyper and I.P. Grant J.Chem Soc. Faraday Trans **274**, 1885 (1978).
6. E.U. Condon and H.G. Shortley. 'The theory of Atomic Spectra" Cambridge
7. J.C. Slater "Quantum Theory of Atomic Structure"vol. **I** and vol. **II**; Mc Graw- Hill book Co. 2nd Edition (1960) University Press (1953.
8. A.Tauheed, Y.N. Joshi Phys. Scr. **47**, 555 (1993).

Energy Perspective of Physics

Abbas Ali and Shafeeq Rahman Thottoli

In this article we are giving an overview of energy prespective of different branches of physics. We will first briefly explain the electromagnetic spectrum and its relevances in different areas of physical science. Then we will describe energies involved in thermal physics, solid state physics, spectroscopy, nuclear physics, particle physics and string theory. There is a nice linear organization of these different fields in increasing order of energy.

Introduction

All of us are familiar with the electromagnetic spectrum. In the increasing order of energy and decreasing order of wavelength it is organised as follows:

Radio Waves
Micro Waves
Infrared Radiation
Visible Light
Ultraviolet Radiation
X – Rays
Gamma Rays

The energies corresponding to these parts of electromagnetic spectum are relevant for different braches of physics. For example radio waves are used for communication and hence that is the most relevant energy scale for communication. The radio waves range in wavelength is taken to be from 1mm to km. This corresponds to the energy range that spreads from feV(femto electron volts) to meV (milli electron volts).

Here we are using eV as a unit of energy . One eV is the amount of energy gained by the charge of a single electron moved across an electric potential difference of one volt.

1 volt = 1 joule/Coulomb (J/C)× electron charge(e)

1electron charge = $1.602176565\times10^{-19}$ *coulomb*

1 eV = $1.602176565\times10^{-19}$ *joule*

Micro waves are in the wave length range from mm to meter. In terms of energy the corresponding range is from μeV (micro electron volts)to meV. These two are used for communication.

Infrared radiation has the wavelength range microns to mm. The corresponding energy range is meV to eV. These energies are relevant for thermal phenomenum. Thus these radiations are called thermal radiation also. Energies involved in electronics related physics as well as condensed matter physics also lie around this range.

Visible spectrum of light extends from $4500A^0$ to $7500A^0$. Corresponding energy range is few electron volts. This is the range of wavelengths are relevant for optics and spectroscopic studies.

Ultraviolet spectrum extends from $100A^0$ to 4000 A^0. Corresponding energy range spreads from a few electron vols to 124eV. This range of wavelengths are relevant for spectroscopic studies.

X- ray spectrum has the wavelength range 0.1 A^0 to $100A^0$. Corresponding energy range is eV to keV. These energies are relevant in spectroscopy and nuclear physics.

Gamma ray spectrum has the wavenlength less than 0.1 A^0. The corresponding enegy range is keV to MeV and are relevant in nuclear physics.

Energies beginning with these and beyond are relevant for particle physics and hence particle physics is also called high energy physics.

The actual energy figures for above mentioned branches of physics may not be the same as mentioned above but there is a reason for that. Accumulation of energy may take place because of large number of particles involved or some energy figures might be smaller than above mentioned because of energy attenuation. Inspite of this the most relevant energies are the ones that have been enumerated in the beginning of the section.

In the following sections we summarise actual energies involved in various branches of physics. These energies are spread out around above energies. It will be nice excersice to analyse the physical mechanisms giving rise to this spread.

Thermal physics

Thermal physics is essentially the study of heat, temperature and heat transfer. Thermal energy is due to chaotic molecular motion. There are three factors affecting thermal energy the temperature ,sample size and composition. Anything that changes temperature, sample size or composition of an object can change its thermal energy. In all most every energy transformation some thermal energy is produced in the form of heat. Heat is a transfer of thermal energy due to temperature difference. thermal energy is not measurable but heat is measurable.

The Boltzmann constant is the physical constant relating energy at the individual particle level with temperature.

Value of Boltzmann constant
$k_B = 1.3806488 \times 10^{23} J/K$

The temperature can also be expressed in the eV.
One degree Kelvin = $8.6173324 \times 10^{-5} eV$
I eV =11604. 505 ^{o}K

Some thermodynamical energies are listed below.

States	Temperature in Kelvin(K)	In unit of eV
Triple point of hydrogen	13.81	1.19×10^{-3}
Boiling point of neon	27.102	2.34×10^{-3}
Triple point of oxygen	54.361	4.68×10^{-3}
Triple point of water	273.16	2.35×10^{-2}
Boiling point of water	373.15	3.22×10^{-2}
Freezing point of Zinc	692.73	5.97×10^{-2}
Freezing point of silver	1235.08	0.11
Freezing point of gold	1337.58	0.12

Specific heat is the heat required to raise the temperature of 1 gram of material by 1 degree Kelvin . Different materials have different specific heats. Following table have enlisted specific heats of some common elements.

Material(at 298K, 1atm)	Specific heat(J/g K)	in eV Unit
Ice	2.09	1.80×10^{-4}
Water	4.11	3.54×10^{-4}
Sodium	1.86	1.60×10^{-4}
Aluminium	0.9	7.76×10^{-5}
Iron	0.45	3.88×10^{-5}

The theorem of equipartition of energy states that molecules in thermal equilibrium have the same average energy associated with each independent degree of freedom of their motion and that the energy is 3/2 k_BT per molecule or 3/2 RT per mole for three degrees of freedom. Where k_B is the Boltzmann constant, T is the temperature and R is the universal gas constant. The average translation energy possessed by free particle given by equipartition of energy is sometimes called the thermal energy per particle.

The average kinetic energy of a gas molecule at room temperature is 0.026eV.

Solid State Physics and Electronics

We can see the energy scale involved in solid stated physics and electronics. There are different types of bonds. The bonds and their corresponding energies are listed below.

Bond	**Energy in eV**
Van Der Waal bonds	0.044
Hydrogen bonds	0.2
Ionic bonds	0.17-0.3
Single covalent bond	2-5

Every solid has its own characteristic energy band structure. This variation in band structure is responsible for the wide range of electric characteristics observed in various materials, the band gap generally refers to the energy difference (in electron volts) between the top of the valence band and the bottom of the conduction band in insulators and semiconductors. This is equivalent to the energy required to free an outer shell electron from its orbit about the nucleus to become a mobile charge carrier, able to move freely within the solid material. So the band gap is a major factor determining electric properties of a solid. Substances with large band gaps are generally insulators, those with smaller band gaps are semiconductors, while conductors either have very small band gaps or none, because the valence and conduction bands overlap. The following list shows band gap of some common semiconductors.

Material	**Band gap(in eV)**
Silicon(Si)	1.11
Selenium(Se)	1.74
Germanium(Ge)	0.67
Silicon carbide(SiC)	2.86
Aluminium phosphide(AlP)	2.45
Aluminium arsenide(AlAs)	2.16
Diamond(C)	5.5
Gallium(III) arsenide(GaAs)	1.43
Zinc oxide(ZnO)	3.37
Zinc sulfide(ZnS)	3.6

Spectroscopy

Spectroscopy is the study of the interaction between matter and radiated energy. Spectroscopy is a very spacious field and is divided according to nature of material(e.g. atom, molecule, etc) and that emit or absorb the spectrum. The both spectroscopy have their own characteristics and limits. Atomic spectrum is a spectrum of radiation caused by electron transitions within an atom. These radiations lie from radio to X-ray. The molecule emits the radiation basically in three ways, due to transitions from electronic, vibrational, rotation levels.The different regions of spectra are listed in table below.

We are analyzing some spectroscopic process and we can see the energy range which is involved. The ionization energy of an atom or molecule, is the energy required to remove electrons from gaseous atoms or ions. The first ionization energy of some metals are listed below.

Region of spectra	Frequency	Energy range involved in eV
Infra-red region	3×10^{12} – 3×10^{14}	1.24×10^{-2} – 1.24
Visible region	4.23×10^{14} – 7.5×10^{14}	1.74 – 3.10
Ultraviolet region	7.5×10^{14} – 3×10^{16}	3.10 – 1.2×10^{2}
X-ray region	10^{17} – 10^{19}	4.12×10^{2} – 4.14×10^{4}

Element	First Ionization energy (in eV)
Hydrogen(H)	13.6
Lithium(Li)	5.39
Berillum	9.32
Boron(B)	8.30
Carbon(C)	11.3
Oxygen(O)	13.6
Flurin(F)	17.4
Neon (Ne)	21.6
Helium (He)	24.6

Nuclear Physics

Nuclear physics is the field of physics that studies the building blocks and interactions of atomic nucleus. An important property of the nucleus is that the mass of an atom's nucleus is always less than the sum of the individual masses of the constituent protons and neutrons when separated, this is called the mass defect and the amount of energy that this mass is converted into is called the binding energy.This is the energy required to split a nucleus of an atom into its component parts. The binding energies of nucleons are in the range of millions of electron volts(MeV). Three types of radioactive emission are identified as *alpha*, *beta* and *gamma* rays. These are helium nuclei electron and photon respectively. Nuclear transitions can emit gamma-rays with quantum energies in the MeV range. The binding energy is responsible for the energy produced in nuclear fission and fusion reaction. Some of the binding energies per nucleon for some common elements are shown in the following table.

Element	Binding Energy(MeV)
Deuterium	1.12
Helium 4	7.07
Lithium 7	5.74
Beryllium 9	6.46
Iron 56	8.79
Silver 107 1	8.55
Iodine 127	8.45
Lead 206	7.88
Polonium 210	7.83
Uranium 235	7.59
Uranium 238	7.57

The gamma rays involved in the decay of Cobalt-60 is of the energy 1.17MeV and 1.33MeV and in Sodium-24 decay involves the energies 1.368Mev and 2.753MeV

Particle Physics

As we have seen that another name for particle physics is high energy physics. The typical energies that are relevant for particle physics are of the order of GeV(10^9 eV). High energy physics deals basically with the study of the ultimate constituents of matter and the nature of interaction between them. The experimental studies in this field of science are carried out with giant particle accelerators. High energies are necessary for two reason first is that we are probing at very small scales of distances and one requires radiation of smallest possible wavelength and highest possible energy. Secondly many of the fundamental constituents have larger masses and require correspondingly high energies for their creation.

The major accelerator facilities make use of several types of devices to build up the energy of the particles. Some of the types of apparatus used and maximum available energy are listed below.

Type	**Maximum achieved energy**
Cockroft-Walton Accelerators	proton upto 2MeV
van de Graff Accelerators	protons upto 10 MeV
Tandem van de Graaf Accelerators	protons upto 20MeV
cyclotron	protons up to 25 MeV
electron linac	100 MeV to 50 GeV
proton linac	up to 70 MeV
Synchrocyclotron	700MeV
Betatron	Few hundred MeV
Linear accelerators	50GeV
synchrocyclotron	protons up to 750 MeV
proton synchrotron	protons up to 900 GeV
electron synchrotron	electrons from 50 MeV to 90 GeV

Particle with energy about 1 GeV (10^9 eV) is required to probe the structure inside proton. Higher energy is required for smaller system - about 1000 GeV is needed to probe into the quarks. The same amount of energy is required to create many of the hypothetical particles. Below summarizes some features of the major accelerators in the world (all of them are colliders). A collider is a type of a particle accelerator involving directed beams of particles. Colliders may either be ring accelerators or linear accelerators, and may collide a single beam of particles against a stationary target or two beams head-on.Colliders are used as a research tool in particle physics by accelerating elementary particles to very high kinetic energies and letting them impact other particles.

Accelerator	**Total Energy**
Stanford Linear Accelerator Collider (SLAC) in Palo Alto	100 GeV
Large Electron Positron Collider(CERN-LEP)in Geneva	200 GeV
Relativistic Heavy Ion Collider(BNL-RHIC)in Brookhaven	200 GeV
Tevatron (FNAL) in Chicago	2 TeV
Large-Hadron Collider(CERN-LHC) in Geneva	14 TeV

We are curious about to know what is the world made of? Ordinary matter is made of atoms, which are in turn made of just three basic components electrons whirling around a nucleus composed of neutrons and protons. The electron is a truly fundamental particle, but neutrons and protons are made of smaller particles, known as quarks. Quarks are, as far as we know, truly elementary.

Our current knowledge about the subatomic composition of the universe is summarized in what is known as the Standard Model of particle physics. It describes both the fundamental building blocks out of which the world is made, and the forces through which these blocks interact.There are twelve basic building blocks. Six of these are quarks(up, down, charm, strange, bottom and top). The other six are leptons,these include the electron, muon and the tauon, as well as three neutrinos.

There are four fundamental forces in the universe: gravity, electromagnetism, and the weak and strong nuclear forces. Each of these is

produced by fundamental particles that act as carriers of the force. The most familiar of these is the photon, a particle of light, which is the mediator of electromagnetic forces.The graviton is the particle associated with gravity. The strong force is carried by eight particles known as gluons. Finally, the weak force is transmitted by three particles, the W^+, W^-, and the Z^0.

What is String Theory

The behavior of all of the above mentioned particles and forces is described with impeccable precision by the Standard Model, with one notable exception gravity. For technical reasons, the gravitational force, the most familiar in our every day lives, has proven very difficult to describe microscopically. This is one of the most important problems in theoretical physics to formulate a quantum theory of gravity. In the last few decades, string theory has emerged as the most promising candidate for a microscopic theory of gravity. It attempts to provide a complete, unified, and consistent description of the fundamental structure of our universe('Theory of Everything'). The quantum effect of gravity become strong at planck energy scale which is an energy scale around $10^{19} GeV$.

We have discussed in this article about energy prespectives of different areas of physics. We have seen that typical energy involved in thermal and solid states physics is upto a few electron volts and that in spectroscopy reaches upto keV. The energy range relevant for nuclear physics is kev to MeV. Typical energy of particle physics is in Gev range whereas the enegy relevant for string theory is 10^{19} GeV. Thus various branches of physics are organized linearly with increasing energy.